NOTE TO USERS

Page(s) missing in number only; text follows. Page(s) were scanned as received.

68-73

This reproduction is the best copy available.

UMI®

DISSERTATION

INCREASED CONTAMINANT MOBILITY THROUGH WIND EROSION FOLLOWING FOREST DISTURBANCE

Submitted by

Jeffrey Jay Whicker

Department of Environmental and Radiological Health Sciences

In partial fulfillment of the requirements

for the Degree of Doctor of Philosophy

Colorado State University

Fort Collins, Colorado

Spring 2005

COLORADO STATE UNIVERISITY

March 7, 2005

WE HEREBY RECOMMEND THAT THE DISSERTATION PREPARED UNDER OUR SUPERVISION BY JEFFREY JAY WHICKER ENTITLED INCREASED CONTAMINANT MOBILITY THROUGH WIND EROSION FOLLOWING FOREST DISTURBANCE BE ACCEPTED AS FULFILLING IN PART REQUIREMENTS FOR THE DEGREE OF DOCTOR OF PHILOSOPHY.

Committee on Graduate Work

(*please print name under signature*)

John D Zimbrick
JOHN D ZIMBRICK

Jeffrey Collett

David D Breshears
David D Breshears

Ted M Zobeck
Ted M Zobeck

John E. Pinder III
Co-Advisor JOHN E. PINDER III

Shawki Ibrahim
Co-Advisor Shawki Ibrahim

John D. Zimbrick
Department Head JOHN D. ZIMBRICK

ABSTRACT OF DISSERTATION

INCREASED CONTAMINANT MOBILITY THROUGH WIND EROSION FOLLOWING FOREST DISTURBANCE

In May of 2000, the Cerro Grande fire burned roughly 30% of Los Alamos National Laboratory (LANL), including areas containing a variety of soil-bound radioactive and chemical contaminants. Post-fire tree thinning caused additional reductions in vegetation and disturbed surface soils. The dramatic loss of vegetation and litter cover, coupled with significant disturbances to surface soils, prompted concerns for the safety of the public and LANL workers. The unknown effects of these forest disturbances on wind-driven resuspension of these contaminated soils were of particular concern because of potential for increased inhalation exposures. This study used a variety of aerosol measurements in burned and tree-thinned areas to assess dust flux and associated inhalation doses to LANL workers. Results show that wind-driven dust flux was significantly greater in severely and moderately burned areas relative to unburned areas, by more than one order-of-magnitude initially and by 2-3 times a year after the fire. Unexpectedly, the elevated dust fluxes did not decrease during the second and third years in burned areas, apparently because ongoing drought delayed post-fire

recovery. In the thinned areas, wind erosion was significantly elevated, but there were indications of reduced dust flux during the second year after thinning. Regarding the special concern for burned sites containing depleted uranium (DU), we measured 7-day partition coefficients (K_d) values that ranged from 276-508 mL g^{-1}, which suggests that the DU would generally remain in surface soils being available for wind erosion, if exposed. Finally, we estimate a relative increase of about 1-4% in PM-10 dust emission across the entire LANL resulting from the fire. Calculations of relative inhalation dose from DU suggest a high-end estimate of a 26% increase for LANL workers on severely burned areas. Despite the potential increased doses, the estimated annual dose was < 1 μSv, which is far below the dose limits for occupational or public exposures. Beyond implications of exposure to contaminated soils, our results highlight the importance of considering wind- as well as water-driven transport and erosion, particularly following disturbance, for ecosystem biogeochemistry in general and human and ecological risk assessment in particular.

Jeffrey Jay Whicker
Department of Environmental and
Radiological Health Sciences
Colorado State University
Fort Collins, CO 80523
Spring 2005

ACKNOWLEDGEMENTS

This study and dissertation was prepared under the guidance of my graduate committee that included co-advisors Drs. Shawki Ibrahim and John Pinder III, along with other committee members Drs. David D. Breshears, Jeffrey Collett, John Zimbrick and Ted Zobeck. I especially want to recognize Dr. John Pinder for his mountainous efforts throughout the study. Working with Dr. Pinder was not only a valuable learning experience but also a great joy. I am also very appreciative of the encouragement and support from Dr. David Breshears, with whom I am proud to have as a colleague and as a friend. I would also like to thank Dr. Zobeck who took a chance to help someone he didn't know. Each member of my committee has brought unique and valuable insights to the studies and collectively they made this work much better. I was blessed with a great committee. Finally, this work was funded by Los Alamos National Laboratory through the Technology Development, Enhancement, and Application program, and I am grateful for the support and confidence of numerous managers and coworkers.

On a personal note, I am very humbled by the support of my family. They endured my absences and preoccupations and supported me throughout. To Pat, Matthew and Laura, this accomplishment is not mine alone, but belongs to us. A big thank you and all my love to each of you. You're the best!

TABLE OF CONTENTS

Chapter 1

Increased Contaminant Mobility through Wind Erosion Following Forest Disturbance

1.0 Introduction

The Cerro Grande fire burned over 40,000 acres of ponderosa pine forest, including about 7000 acres within the boundaries of Los Alamos National Laboratory (LANL 2000). Beyond the immediate effects of the fire, there were significant concerns regarding the impact of the fire on increased mobility of radioactive and chemical contaminated soils. The rapid removal of vegetation by fire has been shown to increase water and wind erosion of soils at other DOE semiarid sites (Johansen et al. 2001, Whicker et al. 2002). While effects of forest fire on water erosion is more studied (Johansen et al. 2001) relative with wind erosion, wind erosion can be a dominant mechanism for transport of soils and associated contaminants in semiarid ecosystems, including ponderosa pine ecosystems at Los Alamos National Laboratory LANL where wind erosion was found to transport ~90 times more mass compared to water erosion (Breshears et al. 2003). Further, wind-driven resuspension of LANL soils can result in the long-distance transport and potential inhalation of contaminated soil particles. Consequently, understanding wind transport of contaminated soils is critically important for predicting human and ecological risk in surrounding areas due to: 1) direct

inhalation of contaminated soil, and 2) from redistributing of contaminant soil particles onto lands where they can ultimately enter food pathways.

Despite likely increase in wind-driven transport of LANL soils resulting from the dramatic reductions in vegetation cover from the fire, continuing drought, disease, and thinning operations, there are few, if any, studies on what the magnitudes of these effects on resuspension rates might be. For example, despite the critical role fire could have on wind erosion and contaminant transport, there have been only a couple of studies of the effects of fire on wind erosion. Moreover, these studies have been focused on ecosystems that are very different from that found at LANL. Zobeck et al. (1989) studied the effects of fire on wind erosion in Texas rangeland and Whicker et al. (2002) studied fire effects in shrublands in Southern New Mexico. Both of these studies showed that fire, through its effects on vegetation, significantly increased wind erosion, but the specific results of these studies may underestimate effects for ecosystems at LANL where the mass and vertical structure of the forest vegetation is greater than that in rangeland and shrubland. It is also important to consider the possible moderating effect of the remediation done on LANL severely burned and thinned areas, but the level of effectiveness of these efforts to stabilize the soil remains unknown. Thus, knowledge and consideration of the effects of fire, drought, disease, forest thinning, and follow-up remediation efforts on wind erosion is essential for more accurate human and ecological risk assessment. Therefore, investigation of the effects of the fire and other disturbances to vegetation cover on resuspension of LANL soils is important to assessing risk to both onsite personal (who are typically closer to the source) and to offsite populations (Kraig et al. 2002).

This study was initiated within a year following the Cerro Grande fire to quantify the effects of the fire on potential increases in wind-driven resuspension of LANL soils. The general goal of the study initially was to measure and compare wind-driven dust fluxes in burned and unburned areas and to continue these measurements over time to assess the relationship between resuspension and ecosystem recovery. By the second year of the study, it was becoming apparent that the fire likely increased resuspension, and further compounding the concern, tree-thinning operations were begun to reduce fuel loads at LANL. These operations involved a variety of machines and tracked vehicles. The combined effect of reducing tree structure, removing ground cover, and disrupting the soil surface had the potential to further increase resuspension. Therefore, a new set of measurements was begun in the third year of the study to measure and compare the effects of the tree thinning operations on wind-driven dust fluxes.

The comparative measurements of dust fluxes in burned and unburned, thinned and unthinned forests were not meant to be specific to any particular contaminant, rather the dust fluxes could be used for any contaminant of concern. However, increases in depleted uranium air concentrations were measured at onsite and offsite locations in the years following the Cerro Grande fire (LANL 2002). These findings suggested the possibility that the fire could have increased resuspension of DU contaminated soils within LANL and these soils were transported by the wind to the neighboring communities. Therefore, an additional study to investigate the specific kinetics of DU in LANL surface soils, including the resuspendable fine soil fraction.

This dissertation describes the results of each of the studies. Each chapter represents a single, stand-alone paper that is to be submitted to different journals for peer-review. Each chapter then has the structure of a scientific paper with sections including the Introduction, Methods, Results and Discussion. Because of this organization, the reader can expect some redundant text in background materials in parts of the chapters, but the data used and analyses for each chapter are unique. The second chapter focuses solely on the response of wind-driven dust flux across a gradient of burn severities. This paper will likely be submitted to the Journal of Environmental Quality. The third chapter is focused on the effects of tree thinning in forests on wind erosion. Because of the important implications to biogeochemical processes, as well as contaminant transport, for management of DOE forested lands, this paper will be submitted to Ecological Applications. The fourth chapter describes the results from the measurements of partition coefficients of uranium in LANL soils and is likely to be submitted to Health Physics. Estimates quantifying potential increases in DU radiation dose as a result of the Cerro Grande fire are provided in the fifth chapter, along with a methodology that can be used for other contaminants as well. The sixth chapter summarizes and integrates the findings of all the studies. Finally, Appendix A outlines details on the measurement techniques used throughout this study.

The Cerro Grande fire, despite many tragic consequences, has provided a rare opportunity to study the effects of wildfire on environmental transport of contaminated soils specifically, and more generally, to learn more about the response of the ponderosa pine ecosystem to wildfire and to other environmental disturbances.

1.1 References

Breshears, D.D., J.J. Whicker, M.P. Johansen, and J.E. Pinder III. 2003. Wind and water erosion and transport in semiarid shrubland, grassland, and forest ecosystems: quantifying dominance of horizontal wind-driven transport. Earth Surface Processes and Landforms 28:1189-1209.

Johansen, M.P., T.E. Hakonson, and D.D. Breshears. 2001. Post-fire runoff and erosion from rainfall simulation: contrasting forests with shrublands and grasslands. Hydrological Processes 15:2953-2965.

Kraig, D., R. Randall, D. Katzman, T. Buhl, B. Gallaher, and P. Fresquez. 2002. Radiological and nonradiological effects after the Cerro Grande fire. Los Alamos National Laboratory Report LA-13914.

LANL (Los Alamos National Laboratory). 2000. A special edition of the SWEIS yearbook: wildfire 2000. Los Alamos National Laboratory Report LA-UR-00-3471.

Whicker, J.J., D.D. Breshears, P.T. Wasiolek, T.B. Kirchner, R.A. Tavani, D.A. Schoep, and J.C. Rodgers. 2002. Temporal and spatial variation of episodic wind erosion in unburned and burned semiarid shrubland. J. Environmental Quality 31(2): 599-612.

Zobeck, T.M., D.W. Fryrear, and Pettit, R.D. 1989. Management effects on wind-eroded sediment and plant nutrients. Journal of Soil and Water Conservation, March-April:160-163.

Chapter 2

Increased Wind Erosion from Forest Wildfire: Implications for Contaminant-Related Risks

2.0 Abstract

Assessments of contaminant-related human and ecological risk require estimation of transport rates, but relative to water transport, data for estimating wind-driven transport rates in non-agricultural settings are few and responses to ecosystem disturbances such as forest wildfire are almost entirely lacking. Forest wildfire threatens much of the western United States, due to historic grazing and fire suppression, and can be triggered by drought, which is expected to increase in intensity and frequency from global climate change. We measured wind-driven horizontal dust flux, a metric of transport related to wind erosion, in ponderosa pine forest within Los Alamos National Laboratory in northern New Mexico, where contaminant transport and associated risks are of concern. We compared fluxes over three years for sites differentially affected by the 2000 Cerro Grande Wildfire: unburned, moderately burned (fire mostly confined to ground vegetation), and severely burned (crown fire). Wind-driven dust flux was significantly greater in both types of burned areas relative to unburned areas, by more than one order-of-magnitude initially and by 2-3 times a year after the fire. Unexpectedly, the elevated dust fluxes did not decrease during the second and third years in burned areas, apparently because ongoing drought delayed post-fire recovery.

Our results highlight the importance of considering wind- as well as water-driven transport and erosion, particularly following disturbance, for ecosystem biogeochemistry in general and human and ecological risk assessment in particular.

2.1 Introduction

Processes driving erosion and transport of soil and associated nutrients and/or contaminants are of central concern for a diverse set of issues related to ecosystem management and risk assessment. Soil loss and redistribution through erosion can result in significant short- and long-term effects on human and ecosystem health (Whicker and Schultz 1982; Schlesinger and Pilmanis 1998, Toy et al. 2002, Saxton 1995, Griffin et al. 2001; Whitford 2002, Kaiser 2004). Accelerated soil loss is considered to be one of the most pressing current environmental problems, particularly in parts of Africa, South Asia, and Latin America (Toy et al. 2002, Kaiser 2004) prompting some to refer to soil as an endangered ecosystem (Pimental 2000). Increased rates of soil erosion are largely the direct and indirect results of anthropogenic land use practices, especially practices that cause intense, large-scale disturbances to vegetation communities (McNeill and Winiwarter 2004). Accelerated soil erosion can be associated with high rates of nutrient loss from and redistribution within ecosystems and watersheds that lower soil quality (Baker and Jemison 1991, Tongway and Ludwig 1997, Schlesinger and Pilmanis 1998, Whitford et al. 1998, Aguiar and Sala 1999, Okin et al. 2001, Ludwig et al. 2002, Toy et al. 2002, Selmants et al. 2003, Miller 2004, Wardle et al. 2004).

Soil erosion is driven by both water and wind, but most studies of soil erosion in non-agricultural settings have focused on water-driven processes rather than wind-driven processes. However, recent data estimating the relative rates of water- and wind-driven erosion and transport suggest that wind-driven process have similar, and in many cases greater, impact on loss and local redistribution of soil in semiarid grassland, shrubland, and forest ecosystems (Breshears et al. 2003). Wind erosion is also important at regional to global scales, where dust-storms impact human and environmental health and could provide important feedbacks to climate variability and change (Tegen et al. 1996, Griffin et al. 2001).

Wind erosion can also be important in determining risk levels associated with contaminant transport due potential inhalation of airborne contaminated soils (Whicker and Schultz 1982, Larney et al. 1999). This inhalation of radioactive contaminants from the transport of soils contaminated with low-levels of radionuclides, such as for ^{137}Cs and ^{239}Pu, has been the focus of risk assessments at many Department of Energy and Department of Defense facilities across the U. S. (Anspaugh et al. 1975, NAS 1989).

Soil erosion can increase greatly following an environmental disturbance due to the non-linear relationship between ground cover and erosion rate for both wind and water erosion (Fryrear 1985, Johansen et al. 2001). However, there are limited studies quantifying changes in erosion rates following environmental disturbance, particularly for wind erosion (Zobeck et al. 1989, Whicker et al. 2002). Yet those studies suggest that wind erosion rates can increase by more that an order-of-magnitude following disturbance. Disturbances in semiarid ecosystems are common and result from phenomenon such as drought, insect breakouts, disease, fire, or through anthropogenic

activities such as tree harvesting (Freedman 1995, Rodgers 1996). Among the many types of disturbance that can reduce ground cover, wildfire stands out as perhaps having the greatest potential for rapidly reducing ground cover and thereby increasing erosion rates (Whicker et al. 2002, Nyhan et al. 2001, Johansen et al. 2003). While there are numerous studies on the response of water erosion to wildfire (Nyhan et al. 2001, Johansen et al. 2001), there are few data on wind erosion rates in semiarid forests (Breshears et al. 2003) and even less data evaluating post-fire changes in wind-driven erosion and transport in this important ecosystem. In the case of wildfire, post-fire climate or treatments such as seeding and mulch cover should alter the rates of recovery in ground cover (Veenis 2000), but studies evaluating such post-fire recovery effects on wind erosion are lacking.

The effects of wildfire on soil erosion are of increasing concern in the ponderosa pine forests of the semiarid west because a combination of overgrazing and fire suppression has led to overgrown tree stands with high fuel loads that are vulnerable to catastrophic wildfires (Friederici 2003). The forests are particularly susceptible during periods of extended drought (Swetnam and Betancourt 1998, McCabe et al. 2004). In summary, there are few data that allow assessment of how wind erosion might increase in fire-vulnerable, semiarid forests following wildfire, nor on how persistent possible post-fire increases in wind erosion might be.

The objective of this study was to compare the relative rates of wind-driven dust flux in burned and unburned ponderosa pine forest, as related to characteristics of local vegetation, soil, and micrometeorology. Specifically, we 1) compare horizontal dust flux across a gradient of burn severities as a function of sampling height, 2) show that

horizontal dust flux measures are correlates of direct wind erosion as measured by vertical dust flux, 3) analyze trends in horizontal dust flux for a period from 1 to 3 years following the fire, 4) relate temporal patterns in dust flux to the recovery of forest floor vegetation and litter cover, and 5) highlight implications of our findings for soil quality, biogeochemistry, ecosystem health, and risks associated with contaminant transport.

2.2 Methods

2.2.1 Study sites

Our study was conducted on the Pajarito Plateau in northern New Mexico, USA, near Los Alamos. In May of 2000, the Cerro Grande fire burned over 19,000 hectares of mostly dense Ponderosa Pine forest in the Jemez Mountains of Northern New Mexico. This fire also burned over approximately 3000 hectares of the Los Alamos National Laboratory, hearafter LANL (LANL 2000). Numerous locations on LANL property with the potential to be contaminated with either radioactive (e.g., depleted uranium and plutonium) or chemical materials (Fresquez et al 1998; Veenis 2000) were burned (Kraig et al. 2002), and because the fire dramatically removed live tree density and ground cover (vegetation and litter) it exposed these sites to water and wind erosion (Fryrear 1985, Johansen et al. 2001, Pinder et al. 2004). Wind transport in burned areas could be an especially important mechanism for redistribution, concentration, and off-site transport of these contaminated soils (Anspaugh et al. 1975, Whicker and Shultz 1982, Gonzales et al. 2001, Breshears et al. 2003). While the initial levels of public intakes of these contaminants during the Cerro Grande fire has been evaluated and considered to have presented little health risk (LANL 2000, Kraig et al. 2002), there is

still concern about the long-term effects of the fire and continued dust emissions from LANL.

The study was conducted at six sites along the western edge of LANL south of the city of Los Alamos, NM, USA (35° 52' N and 106° 21' W) at an elevation of about 2400 m. Measurements of wind-driven dust were made from May 2001 through July 2003. The sites are on the Parajito Plateau on relatively flat mesa tops with slopes less than 10% (Breshears et al. 2003). Vegetation was dominated by *Pinus Ponderosa* Douglas ex P.&C. Lawson var. *scopulorum* Englem (ponderosa pine) before the fire. The sampling sites were centrally located within a relatively homogeneous area and at least 100 m downwind along the dominant wind direction (from the west, southwest, or northwest), in locations that were at least 100 m from any road or new disturbance. The criteria for the 100 m distance was based on data from Baldocchi (1997) that suggest that most of the eroding soil in a thick forest is collected at a fetch distance of 10 m, and the fetch should be less than 100 m found for treeless areas (Stout 1990, Zobeck et al. 2003). A line transect was established in the center of each sampling sites along which dust sampling stations were positioned every 30 m.

Three categories of burn severity were employed to assess post-fire dust flux at several levels along a burn gradient (Pinder et al. 2004). The severely burned site was characterized as having most of the ground vegetation and litter cover burned and all portions of the pine trees burned, including the crown (tree top). Typical remediation practices of seeding with annual and biennial forbs and mulching with straw were applied to the severely burned sites (Veenis 2000). The moderately burned site included areas where the fire was primarily a ground fire that scorched but did not

consume the needles. The third forest areas were unburned and used as comparison sites. Within each burn category, two sites were selected to assess variability within burn categories. Because of equipment limitations, one site was termed the Primary site and had greater sampling intensities than the other site, which is termed the Secondary site.

2.2.2 Site characterization

To document the magnitude of fire effects and measure the rate of system recovery for important variables impacting dust flux, measurements were made of vegetation cover, litter cover, tree canopy cover, and soil texture were made at each site (Pinder et al. 2004). Fire effects on individual trees were measured as mortality and canopy scorching (i.e., the percent of the tree's canopy with scorched needles). Fire recovery was measured as the development of litter and vegetation cover on the soil. Micrometeorological measurements were made in the Primary severely burned and unburned plots, and also at the nearby TA-6 meteorological station operated by LANL.

Fire effects on forest structure

Tree structure in the burned and unburned sections of forest was characterized by measuring tree density and tree heights in 100-m^2 plots. There were five randomly selected plots at each Primary site, and four plots at each Secondary site. Tree heights were measured using a forester's altimeter. The percent of live *tree canopy cover* was measured in June 2001 using a concave, mirror spherical densiometer that reflects a vertical view of the tree canopy (Lemmon 1956). The spherical densiometer

measurements were made at 15 and 12 locations in Primary and Secondary sampling sites, respectively.

Recovery of ground vegetation and litter cover was assessed using digital photographs of 1-m2 plots taken at early spring, mid-summer and late summer over the length of the project (June 2001 to August 2003)(Pinder et al. 2004). These pictures were taken from a height of about 2 m and at an angle from the vertical of approximately 25°. The 3.5 megapixel images were magnified (≥ 2x), and the percent cover for each of the vegetation/cover plots determined by visual estimation of the percent of cover of live vegetation and litter within 25 subplots. Vegetation and litter cover were separately evaluated within each subplot. A separate measure of the total cover was estimated from 81 points dispersed throughout the 1-m^2 plot (Pinder et al. 2004).

Soil sampling

Separate soil samples were collected in July 2003 from five random locations within each Primary site and three random locations in each Secondary site. Twenty 20-mm deep and 38-mm diameter cores were collected around a 1-m^2 frame at each soil sampling location and composited. Litter cover was carefully scraped aside to collect only the upper horizon of soil. The soil was then air-dried and submitted to the Colorado State University's Soil, Water, and Plant testing laboratory for measures of 1) percent of sand, silt and clay by mass, and 2) and fraction of particles less than 10 μm in diameter (respirable sizes) using the pipette method (Black et al. 1965).

Meteorological conditions

Meteorological data collection stations (Davis Instruments Corp., 3465 Diablo Avenue, Hayward, CA 94545); which measured wind velocities at 1 m, precipitation, and temperature in 15-minute averages; were installed at the Primary Severely burned and the Primary unburned site. Additional meteorological data were taken from a LANL operated 46-meter tall meteorological tower located within a few km of all the sampling sites. The LANL TA-6 meteorological station provided 15-minute averaged data on a number of meteorological conditions such as precipitation amounts and wind velocities at 11.5 m, 23 m, 46 m, and 92 m (Rishel et al. 2003).

2.2.3 Horizontal dust flux measurements

Horizontal dust flux (HDF) is a metric of material transport associated with wind erosion (Breshears et al. 2003) and was measured using Big Spring Number Eight (BSNE) samplers (Fryrear 1986). A tail fin attached to each BSNE sampler orients their 10-cm^2 opening into the wind where airborne dust enters and is deposited onto a collection pan as winds decelerated through wider portions of the sampler. BSNE field dust collectors have been extensively tested and have good sampling efficiency for soils with higher fractions of sand and silt (Fryrear 1986; Goossens and Offer 2000) such as those that are abundant at LANL (Nyhan et al. 1978). The HDF was calculated by using the mass of the dust collected and dividing the area of the sampler opening (10 cm^2) and the sampling period. The units of HDF were then expressed as g m^{-2} d^{-1}. This value represents a measure of the wind-driven mass of dust flowing horizontally along the earth surface at a particular height. Multiple samplers may be mounted at different

heights to measure gradients in HDF with increasing distance above the soil surface. Lack of time time-resolved data on particle size wind velocity in all the sampling areas precluded corrections for collection efficiency, so a collection efficiency of 100% was assumed and will bias the absolute HDF estimates high.

Three dust sampling stations were used in the Primary sampling sites and two were used in the Secondary sampling sites. A BSNE sampling station consisted of at least three BSNE samplers at heights of 0.25 m, 0.5 m, and 1 m. About 99% of the wind-driven dust mass occurs with 0-1 m interval (Stout and Zobeck 1996). A nonlinear least-squares method was used to determine the parameters for an exponential relationship between height and mean HDF which was then integrated to determine the total horizontal mass passing through a 1-m wide length of ground surface (Stout and Zobeck 1996, Gillette et al. 1997). These self-orienting samplers also integrate horizontal flux over all wind directions, so the integrated horizontal flux represents the horizontal flux passing through a rotating 1-m wide gate up to a height of 1 m (Breshears et al. 2003). The BSNE samplers thus provide measures of integrated wind erosion collected over sampling intervals of normally one to two weeks at multiple heights above the ground.

Dust samples were washed into plastic bags with distilled water, transferred into 22 mL glass vials, dried at 50° to a constant mass, and weighed with a sensitivity of 0.001 g. Horizontal mass flux was calculated as the mass of the dust deposited in the sampler and divided by the product of the sampling period and the area of the opening (10 cm^2). Tap water was used for sample washings for some of the initial samples, and these data corrected for the residual mineral mass.

Measurements of HDF were collected beginning in May of 2001 and extended through July of 2003. Samples were collected generally at intervals of weekly to biweekly in 2001 from June through November, in 2002 from January through November, and from March through July in 2003. Many of these collections were obtained from the same or overlapping intervals in different years. Constraints of resources imposed the mid-year to mid-year sampling program, and the complicating effects that seasonal weather patterns of precipitation and wind speeds would have on HDF data were not immediately appreciated. The effects of these seasonal influences on HDF and the complications imposed upon comparing data among years will be discussed below.

Relationships between the HDF and meteorological conditions were established using 1-m wind and precipitation data from the Davis meteorological station and HDF measurements from 3 nearby BSNE sampling stations. These HDF measurements were made from May 2001 to September 2002 in an open, unforested area. The BSNE, Davis and TA-6 measuring points were arranged in a triangular pattern with approximately 200 m per side.

Finally, vertical flux was measured at the TA-6 meteorological tower using the vertical flux gradient method as reported in Whicker et al. (2002). The vertical flux is the product of the eddy diffusivity coefficient (K_z) and the concentration gradient in the vertical direction (Blackadar 1997), with K_z is equal to the product of the von Karmon constant (0.4), the sampling height of the wind (11.5 m), and the friction velocity (u_*). Friction velocities were measured by a sonic anemometer at the TA-6 tower (Rishel et al. 2003) and the aerosol concentrations were made at 1-m and 3-m sampling heights as

described in Whicker et al. (2002). Friction velocity measurements used were made between August 2000 and August 2001, and a subset of friction velocity measurements, those made at night (more likely to be neutral atmospheric stability), was used in these calculations.

The vertical flux measurements were correlated to HDF measurement made from the BSNE samplers also located near the TA-6 meteorological tower over 15 overlapping time periods. Investigation of potential links between HDF (saltating particles that are locally redistributed) and vertical flux is important for many reasons, but importantly because the vertically transported aerosol is mostly smaller dust particles that are transport longer distances and present a potential inhalation risk if contaminated.

2.2.4 Statistical analyses

Statistical comparisons of HDF among burned and unburned areas were performed using a mixed-model Analysis of Variance (ANOVA) where burn severity, sampling periods and the interaction of burn severity and sampling dates were fixed-effects and sites and specific BSNE locations within sites were random-effects (Milliken and Johnson, 1984). Statistical computations were performed using the Type 3 option of PROC MIXED of the SAS System (Littell et al., 1996). Hypotheses of specific effects, such as 1) the effects of specific burn severities and 2) changes in the effects of burn severities among years, were tested using F ratios computed for Linear Contrasts of Means, hearafter LCM (Littell et al., 1996). Due to the differential effects of precipitation and wind speeds on HDF at different elevations, separate analyses were

performed for the 0.25, 0.5 and 1.0 m elevations, and separately for wet and dry sampling periods. The relationship between the horizontal flux measurement during dry sampling periods and sampling height was determined using a simple exponential function and integrated to obtain estimates of total horizontal flux through a 1-m wide vertical plane. This analysis also allowed for relative comparisons with other wind and water erosion measurements reported in similar studies.

2.3 Results

2.3.1 Impact of fire on tree and ground cover

Measurements show large decreases in *tree canopy cover* along the burn severity gradient with almost no live tree cover in the severely burned area, and tree cover in the moderately burned was about 50% of that found in the unburned location (Table 2.1). Our sampling locations also captured some of the heterogeneity of tree density and tree cover typically found in ponderosa pine forests as we found significant differences in tree cover within burned and unburned types.

Statistical comparisons for *vegetation cover* showed significantly greater vegetation in the severely burned areas relative to the moderately burned and unburned areas, which was due to both viable biological residual and the extensive remediation efforts in the severely burned areas. While the remediation effort likely increased the initial surge in vegetation cover following the fire, we found that the vegetation cover in the severely burned sites decreased each year from 2001 to 2003, which is likely the

result of ongoing drought which persisted throughout the study period (Pinder et al. 2004).

Statistical comparisons for *litter cover* showed that there was significantly greater litter cover in the unburned sites (mostly dead pine needles) than that found in either the moderately or severely burned sites. Litter cover in both the moderately and severely burned sites increased from 2001 to 2002, with no further increase from 2002 to 2003 (Pinder et al. 2004). Litter cover on moderately burned sites was composed of recently shed, scorched pine needles over bare earth that was exposed by the fire.

Trends in *total cover* (vegetation plus litter) showed greater total cover in the unburned sites, next was the moderately burned sites, and finally, the lowest total cover was found in the severely burned sites (Table 2.1). Total cover increased from 2001 to 2002 in both the severely and moderately burned locations mostly from additional litter accumulation. There was no change in total cover over time in the unburned location (Pinder et al. 2004).

Soils were predominantly sands and silts and were generally classified as silt loam soils (Table 2.1). A statistical comparison of soil texture showed no significant differences in soil composition between the different burn locations and there was more variation within burn types than among burn types (Pinder et al. 2004).

2.3.2 Impact of fire on horizontal dust flux

The HDF varied across time and among burn categories (Figure 2.1), with a generally increasing trend in HDF with burn severity (Table 2.2). The magnitude of the differences in HDF among burned sites declined with sampling height (Figure 2.2a).

The ANOVA showed that the HDF measured on severe burn areas were significantly (LCM Fs > 4.5; df =1, > 465; $P < 0.05$) greater than those on unburned areas in all years and at all elevations. The profile of HDF with elevation showed greater increases at the 0.25 m elevation than at the 1.0 m elevation for all three years. For example, mean ($\pm$ standard error of mean) increases in HDF in 2003 were 7.79 $\pm$ 0.74, 2.52 $\pm$ 0.19 and 2.04 $\pm$ 0.19 at 0.25, 0.50 and 1.0 m elevations, respectively.

The response of HDF to the moderate burn was less distinct than that for the severe burn, but the mean HDF on the moderate burns was always greater than that on the unburned areas. Mixed-model ANOVAs based on these data did not indicate any significant difference between moderate and unburned areas, but ANOVAs and linear contrasts on logarithmic transformations of HDF, which are suggested by the standard deviation to mean ratios being > 0.3, indicated significantly ($P < 0.05$ or less) greater HDF on moderate burn sites at all time periods. HDF measurements < 0 were arbitrarily redefined as 0.03 before logarithmic transformations. Mean HDF on severe burn areas were significantly greater than those on moderate burn areas at all elevations (LCM Fs > 19; df =1, 4; $P < 0.05$). The major difference between the response of HDF on severe and moderate areas was the greater increase on severe areas at the 0.25 m elevation. For example, the mean ($\pm$ SE) differences between severe and moderate burn areas in 2003 were 6.56 $\pm$ 0.68, 1.58 $\pm$ 0.18 and 0.94 $\pm$ 0.19 at 0.25, 0.50 and 1.0 m, respectively.

Analysis of fire effects on HDF during dry periods

Measurements of HDF with BSNE samplers located adjacent to the TA-6 meteorological tower showed that with increasing total precipitation in the sampling interval there were statistically significant increases in HDF at 0.25 m ($F = 17.3$; $df = 1, 46$; $P < 0.01$) and 0.5 m ($F = 15.9$; $df = 1, 45$; $P < 0.01$) as shown in Figure 2.3. There was no statistically significant ($F = 0.32$; $df = 1, 46$; $P \geq 0.05$) increase in HDF at 1.0 m with increasing precipitation. There was a statistically significant ($F = 6.1$; $df = 1, 46$; $P < 0.05$) increase in HDF at 1.0 m with increasing mean daily maximum wind speed in the interval. Wind speeds had no statistically significant ($P > 0.10$) effects on HDF at 0.25 and 0.5 m.

Because of the effect that precipitation had on HDF measurements, the HDFs were additionally compared among burned and unburned areas during dry periods. For this analysis, we selected sampling periods where precipitation was < 1.3 mm (0.05 inches). This precipitation threshold was considered to be low enough to have very little effect on the HDF (Figure 2.3), yet contain enough sampling periods for robust statistical analysis. Although fewer sampling periods are available for statistical comparisons, the data indicate greater HDF on burned areas during dry periods than on unburned areas (Figure 2.2b), consistent with the analysis using all data as a shown in Fig. 2a. At 0.25 m, the HDF measures across all three years were significantly greater on severe burn (LCM $F = 368.2$; $df = 1, 3$; $P \leq 0.01$) and moderate burn areas (LCM $F = 56.5$; $df = 1,3$; $P \leq 0.01$). At 0.5 m, the HDF was significantly greater on severe burn areas (LCM $F = 24.8$; $df = 1, 3$; $P \leq 0.05$) but not significantly greater on moderate burn

areas ($P > 0.10$). At 1.0 m, the HDF were statistically significantly greater on both severe areas (LCM $F = 703.6$; $df = 1, 3$; $P \leq 0.01$) and moderate areas (LCM $F = 84.5$; $df = 1, 3$; $P \leq 0.01$).

The mean HDF for dry periods did not dramatically decrease with sampling height as seen in the means from all sampling periods (Fig. 2.2b). However, a very limited set of HDF measurements at height of 7 and 18 cm were made in each of the Primary sites allowed us to determine a best-fit exponential relationship between sampling height (h) and mean horizontal mass flux using data from the dry periods. Integrating these functions provided the total mass flux per unit width (m). A simple exponential model of the form $Y = ae^{bh}$ was used to describe this relationship with a and b being estimated using an iterative least squares method (StatSoft 1994). The values for a and b and the standard errors were 2.64 ± 1.19 and -0.87 ± 0.29 for the severely burned area, 1.36 ± 1.21 and -0.65 ± 0.32 for the moderately burned location. The relationships were statistically significant ($P < 0.05$), but the correlation coefficients for these models were generally low 0.14 and 0.07 for the severely and moderately burned areas, respectively. Integrating these functions to a 1-m height gave an estimated total mass passing through a 1-m wide length of 1.76 g m^{-1} d^{-1} and 1.00 g m^{-1} d^{-1} for the severely burned and moderately burned areas, respectively. The height profile of HDF in the unburned area did not vary significantly with sampling height, so a comparable estimate of HDF is simply the flux averaged over all three heights multiplied by the range of sampling heights (1 m). This gives an estimated mean of 0.74 g m^{-1} d^{-1} passing through the similar 1-m wide length in the unburned areas.

2.3.3 Relationship between horizontal and vertical dust flux

A significant linear relationship was found between the HDF measurements (dependent variable) and the vertical flux measurements ($P < 0.05$; $r^2 = 0.37$). The intercept and the slope with standard errors were 0.02 ± 0.02 and 0.05 ± 0.02, respectively. A plot of this relationship is shown in Figure 2.4. The correlation coefficient suggests that there are other environmental factors to consider in the relationship between HDF and vertical flux. However, this relationship does imply direct links between increases in HDF with vertical flux, and vertical flux is associated with suspension of soil and associated materials, which then are available for long-distance transport.

2.3.4 Forest recovery and horizontal dust flux

There was little indication of declining HDF with time since the fire. Measures of HDF were similar among years or showed trends of increasing HDF. Linear contrasts of means comparing overlapping sampling intervals in the severely burned areas indicated no increase in HDF from 2001 to 2002 at any elevation ($P > 0.05$) but significant increases in HDF between 2002 and 2003 at 0.25 m (LCM $F = 7.06$; $df = 1, 470$; $P < 0.01$) and 0.50 m (LCM $F = 18.1$; $df = 1, 470$; $P < 0.01$). There was no significant increase from 2002 to 2003 at 1.0 m ($P \geq 0.05$). Linear contrasts of means using logarithmically transformed data from the moderately burned plots indicated no increase in HDF from 2001 to 2002 at any elevation ($P \geq 0.05$) but significant increases

in HDF between 2002 and 2003 at 0.50 m and 1.0 m (LCM Fs > 7; df = 1, 470; P < 0.01).

2.4 Discussion

There have been numerous studies on the effects of forest fires on water erosion and runoff, but this study is among the first to document wildfire effects on wind erosion, and in a forest ecosystem that is particularly vulnerable to wildfire (Covington 2003, Friederici 2003). As with water erosion, our results suggest that wildfire increases wind erosion. Specifically, HDF was significantly increased in burned areas, especially in the severely burned areas. The likely causes of increased HDF in the burned areas are higher surface wind velocities (Whicker et al. 2002) and decreased vegetation, litter, and tree cover.

Increases in HDF were most pronounced at the lower sampling heights though this relationship was probably affected by rainsplash at the 0.25 m and 0.5 m sampling heights, and future studies should consider rainsplash. Despite the effects of rainsplash on HDF, the statistical conclusion of increased HDF in burned areas held during dry periods, but the effect of forest burning was less. Greater levels of rainsplash in the burned areas were likely the result of more unprotected bare soil and to some extent the moderating effects tree canopies on raindrop sizes and velocities in the unburned areas. Regarding contaminated soils, increased rainsplash and post-fire vegetation in burned areas suggests higher transfer rates of the contaminant to plant surfaces and subsequent ingestion by grazing animals (Dreicer et al. 1984). The lack of a pronounced decrease in HDF at the higher sampling heights during the dry periods was unexpected (Stout

and Zobeck 1996) and may be explained if a large fraction of the collected dust is not made up of saltating particles, but rather "background" atmospheric dust filtering through the forest and maybe being shaken off tree canopies above the samplers.

We were not able to begin measurements for this study until about a year after the fire, and we may have missed important information on the relationship. Specifically, one would expect that the effects of the fire on soil erosion would be greatest immediately following the fire because of significant loss of vegetation and litter cover. For the time period studied, however, we found that increased HDF in the burned areas persisted through July of 2003, three years post-fire despite extensive remediation (Veenis 2000). Comparisons of burn severities on tree and ground cover indicated that the effects of the Cerro Grande fire was similar to that for other fires in ponderosa pine forests, but the rates of recovery of ground vegetation and litter were slower than those for other fires (Pinder et al. 2004). The slower recoveries, which occurred even on those areas that were seeded and mulched, are likely due to the effects of ongoing drought.

2.4.1 Ecological implications

Airborne dust is constantly being transported through environments (Pye 1987), and this study found that disturbances such as wildfire can significantly increase dust flux, and the increase can persist for many years. This study reports estimates of 1-m integrated dust flux values of slightly more than a kg of dust passing through each meter in a burned forest per year, about 2.4 times that found in unburned forests and about 5 times that found for water erosion on shallow slopes (Johansen et al. 2001; Breshears et

al. 2003). This could be a significant amount of increased dust mass when integrated over large tracts of forested land and over multiple years. The soil particle sizes and chemical constituents of the dust were not measured in this study, but the dust may be expected to be enriched in soil fines containing important soil organic materials and associated soil nutrients. Future work should consider the chemical makeup of the dust to more fully understand the ecological impact of this enhanced redistribution of soil.

Soil is a key-integrating factor in forest ecosystems because of the strong coupling between soil quality and the biotic components in the ecosystem that it supports. Loss of soil and associated nutrients is considered an important indicator of ecosystem function (Tongway and Ludwig 1997, Whitford et al. 1998). Given the response of wind erosion to wildfire suggests that it would also respond to other disturbances. Therefore, wind erosion may be an important metric to include in assessing the impacts of ecosystem disturbance, forest management, and the trajectory of the recovery (Miller 2004; Whicker et al. 2004).

2.4.2 Comparing fire effects on water and wind erosion

Wildfire increases both wind and water erosion, but there are few, if any, comparisons of the relative effects. Johansen et al. (2001) studied water erosion on mild slopes (4-8%) using rainfall simulation on unburned plots and plots burned over by the Cerro Grande fire (in the same Primary Severely burned plot in this study). Using the data from the Johansen et al (2001) water erosion study and this wind erosion study, comparisons of the effects of forest fire are made for severely burned areas.

Estimates of the amount of increased wind erosion are be made using the mean HDF values measured during the study at 1.0 (1-m averages of 0.73 g m^{-2} d^{-1}, 1.18 g m^{-2} d^{-1}, and 1.76 g m^{-2} d^{-1} at the unburned, moderate burn and severe burn areas, respectively), and extrapolating the relationship between HDF and the measured vertical flux (Figure 4). Extrapolated vertical fluxes are of 21 g m^{-2} yr^{1} [e.g., = 365 d yr^{-1} *(0.020 + 0.73 * 0.053)] for unburned forests, 30 g m^{-2} yr^{-1} for moderately burned forests and 41 g m^{-2} yr^{-1} for severely burned forests. These estimates of upward net vertical fluxes are most applicable to the moderately and severely burned locations because of similar ground and tree cover to the TA-6 location where they were made, translate to potential loss of top soil at rates of 2.4 x 10^{-3} cm yr^{-1} in the moderately burned forest and 3.3 x 10^{-3} cm yr^{-1} in the severely burned forest, assuming a soil density of 1.25 g cm^{-3}. The vertical flux estimates suggests an approximate 90% relative increase in vertical flux and an absolute increase of 20 g m^{-2} yr^{-1} in the severely burned area.

The 90% increase in wind-driven erosion rates appears small when compared to the > 20X increase observed by Johansen et al. (2001). Breshears et al. (2003) used 1) the frequency and magnitude of precipitation events for the LANL site and 2) the rainfall simulation plot data of Johansen et al. (2001) on an unburned forest plot to estimate water-driven erosion rates of approximately 1 g m^{-2} y^{-1} before the fire. Assuming a 20-fold increase in water erosion in severely burned areas gives an estimated water erosion rate of 20 g m^{-2} y^{-1} after the fire. This would suggest an increase of 19 g m^{-2} y^{-1} due to water erosion following a fire.

The previous assessment of the impacts of fire on wind erosion rates is based on two assumptions concerning the HDF measures in the unburned forest. The first of these is that the relationship between HDF and vertical flux observed for the TA-6 location is also valid for the forest. It is reasonable to challenge this assumption. The levels of canopy coverage and the tree heights (Table 2.1) would suggest less vertical air movement and mixing. Thus, the ratio of vertical flux to HDF may be less for the forest. The application of Figure 2.4 to Severe burn areas is more plausible because of the loss of the effects of canopy coverage and foliage mass on wind mixing following the fire. The second assumption is that the all the material being measured as HDF in the forest is erosion. It may not be. It may be partly or mostly deposition of airborne particulates entrained by the canopy. Failure of either of these assumptions to be correct results in overestimation of vertical flux for the forest and a corresponding underestimation of the increased rate of wind erosion. Thus, the similarity of the increases in water and wind erosion rates following fire as presented above may be biased and underestimate the relative importance of wind erosion. This underestimation may be by as much as 200 % (= 100 % [41 - 0] / [41 - 21]).

2.4.3 Implications for transport of soil-bound contaminants

Regarding contaminant transport, wildfires likely increase local redistribution of contaminated soils through wind, and the effects can last for years depending on the recovery of the vegetation and litter cover. This local redistribution may concentrate contaminants in vegetation and in areas of aeolian deposition such as in areas of higher canopy cover or leeward sides of topographic objects such as hills and canyons where

the wind velocity is lower (Whicker and Shultz 1982, Ritchie and McHenry 1990, Coppinger et al. 1991, Sutherland et al. 1991, Gonzales et al. 2001, Toy et al. 2002). Importantly, forest fires may also increase long-range (several km) transport of contaminants and increase exposures to the public, as shown in the relationship found in this study between the vertical flux and the HDF. As an example, LANL (2002) shows that depleted uranium air concentrations at the LANL boundaries have significantly increased following the Cerro Grande fire, though the levels remain low and within regulated safety standards.

2.5 Conclusions

Wildfire was shown to increase horizontal dust flux, especially in severely burned locations, and to a lesser degree, in moderately burned locations. The increased dust fluxes have continued over the several years following the fire probably because of continuing drought, which has slowed the recovery of ground vegetation. The finding of increased dust flux implies that wind-driven mobility of soil-bound contaminants may have also increased. This potential increase in contaminant mobility at LANL following the Cerro Grande fire is confirmed by increased air concentrations of depleted uranium, which has been distributed in the local environment through explosive testing (LANL 2002).

2.6 References

Aguiar, M.R., and O.E. Sala. 1999. Patch structure, dynamics and implications for the functioning of arid ecosystems. TREE 14(7): 273-277.

Anspaugh, L.R., J.H. Shinn, P.L. Phelps, and N.C. Kennedy. 1975. Resuspension and redistribution of plutonium in soils. Health Phys. 29:571-582.

Baker Jr., M.B., and R.L. Jemison. 1991. Soil loss- key to understanding site productivity. In: Proceedings of the 36th annual meeting of the Agencies and Science Working Together for the Future, New Mexico Water Research Institute, pp 71-76.

Baldocchi, D. 1997. Flux footprints within and over forest canopies. Boundary-layer Meteorology 85:273-292.

Black, C.A., D.D. Evans, J.L. White, L.E. Ensminger, F.E. Clark, and R.C. Dinauer. 1965. Methods of soil analysis. Part 1. Physical and mineralogical properties, including statistics of measurement and sampling. Agron. Monogr. 9. ASA, Madison WI.

Blackadar, A.K. 1997. Turbulence and diffusion in the atmosphere. New York: Springer.

Breshears, D.D., J.J. Whicker, M.P. Johansen, and J.E. Pinder III. 2003. Wind and water erosion and transport in semiarid shrubland, grassland, and forest ecosystems: quantifying dominance of horizontal wind-driven transport. Earth Surface Processes and Landforms 28:1189-1209.

Coppinger, K.D., W.A. Reiners, and R.K. Olson. 1991. Net erosion on a sagebrush steepe landscape as determined by cesium-137 distribution. Soil Sci. Soc. Am. J. 55:254-258.

Covington, W.W. 2003. The evolutionary and historical context. In: Friederici P. (ed), Ecological Restoration of Southwestern Ponderosa Pine Forests, Island Press: Washington, D.C., pp 26-47.

Dreicer, M., T.E. Hakonson, G.C. White, and F.W. Whicker. 1984. Rainsplash as a mechanism for soil contamination of plant surfaces. Health Physics 46:177-188.

Johansen, M.P., T.E. Hakonson, and D.D. Breshears. 2001. Post-fire runoff and erosion from rainfall simulation: contrasting forests with shrublands and grasslands. Hydrological Processes 15:2953-2965.

Kraig, D., R. Randall, D. Katzman, T. Buhl, B. Gallaher, and P. Fresquez. 2002. Radiological and nonradiological effects after the Cerro Grande fire. Los Alamos National Laboratory Report LA-13914.

Freedman, B. 1995. Environmental ecology: the ecological effects of pollution, disturbance, and other stresses. Academic Press, San Diego.

Fresquez, P.R., D.R. Armstrong, and M.A. Mullen. 1998. Radionuclides in soils collected from within and around Los Alamos National Laboratory. J. Environ. Sci. Health A33(2):263-278.

Friederici, P (ed). 2003. Ecological restoration of Southwestern Ponderosa Pine forests. Island Press, Washington, D.C.

Fryrear, D.W. 1986. A field dust sampler. Journal Soil and Water Conservation 41:117-120.

Fryrear, D.W. 1985. Soil cover and wind erosion. Transactions of the ASAE 28:781-784.

Gillette, D.A., D.W. Fryrear, J.B. Xiao, P. Stockton, D. Ono, P.J. Helm, T.E. Gill, and T. Lee. 1997. Large-scale variability of wind erosion mass flux rates at Owens Lake: 1. Vertical profiles of horizontal mass fluxes of wind-eroded particles with diameter greater than 50 μm. Journal of Geophysical Research 102{D22):25,977-25,987.

Griffin, D.W., C.A. Kellogg, and E.A. Shinn. 2001. Dust in the wind: long range transport of dust in the atmosphere and its implications for global public and ecosystem health. Global Change & Human Health 2(1):20-33.

Goossens, D., and Z.Y. Offer. 2000. Wind tunnel and field calibration of six aeolian dust samplers. Atmospheric Environment 34:1043-1057.

Gonzales, G.J., P.R. Fresquez, and C.M. Bare. 2001. Contaminant concentrations in conifer tree bark and wood following the Cerro Grande fire. Los Alamos National Laboratory Report LA-UR-01-6157.

Kaiser, J. 2004. Wounding earth's fragile skin. Science 304:1616-1618.

Kimmins, J.P. 2003. Forest ecology: a foundation for sustainable forest management and environmental ethics in forestry. Prentice Hall, New Jersey.

Kraig, D., R. Ryti, D. Katzman, T. Buhl, B. Gallaher, and P. Fresquez. 2002. Radiological and nonradiological effects after the Cerro Grande fire. Los Alamos National Laboratory Report LA-13914.

LANL (Los Alamos National Laboratory). 2000. A special edition of the SWEIS yearbook: wildfire 2000. Los Alamos National Laboratory Report LA-UR-00-3471.

LANL (Los Alamos National Laboratory). 2002. Environmental surveillance at Los Alamos during 2002. Los Alamos National Laboratory Report LA-14086-ENV.

Larney F.J., Cessna, A.J., and M.S. Bullock. 1999. Herbicide transport on wind-eroded sediment. J. Environ. Qual. 28:1412-1421.

Lemmon, P.E. 1956. A spherical densitometer for estimating overstory density. Forest Science 2:314-320.

Littell, R. C., G. A. Milliken, W. W. Stroup, and R. D. Wolfinger. 1996. SAS System for Mixed Models. SAS Institute Inc., North Carolina.

Ludwig, J.A., R.W. Eager, G.N. Bastin, V.H. Chewings, and A.C. Liedloff. 2002. A leakiness index for assessing landscape function using remote sensing. Landscape Ecology 17:157-171.

McCabe, G.J., M.A. Palecki, and J.L. Betancourt. 2004. Pacific and Atlantic Ocean influences on multidecadal drought frequency in the United States. Proc. National Academy of Sciences 101:4136-4141.

McNeill, J.R., and V. Winiwarter. 2004. Breaking the sod: humankind, history, and soil. Science 304:1627-1629.

Miller, M.E. 2004. The structure and functioning of dryland ecosystems- conceptual models to inform the vital-sign selection process. United States Geological Survey report, February Draft report.

Milliken, G. A., and D. E. Johnson. 1984. The Analysis of Messy Data. Volume I: Designed Experiments. Van Nostrand Reinhold Company, New York.

NAS (Committee to Provide Interim Oversight of the DOE Nuclear Weapons Complex). 1989. Nuclear weapons complex: management for health, safety and the environment. National Academies Press, Washington, D.C..

Nyhan, J.W., L.W. Hacker, T.E. Calhoun, D.L. Young. 1978. Soil survey of Los Alamos County, New Mexico. Los Alamos Scientific Laboratory Report LA-6779-MS.

Nyhan, J.W., S.W. Koch, R.G. Balice, and S.R. Loftin. 2001. Estimation of soil erosion in burnt forest areas of the Cerro Grande fire in Los Alamos, New Mexico. Los Alamos National Laboratory Report LA-UR-01-4658.

Okin, G.S., B. Murray, and W.H. Schlesinger. 2001. Degradation of sandy arid shrubland environments: observations, process modeling, and management implications. J. Arid Environments 47:123-144.

Pimental D. 2000. Soil as an endangered ecosystem. Bioscience 50(11):947.

Pinder, J.E., J.J. Whicker, and D.D. Breshears. 2004. Effects of the Cerro Grande fire on ponderosa pine forests and recovery of the forest floor at LANL. Los Alamos National Laboratory Report LA-UR-04-2495.

Pye, K. 1987. Aeolian dust and dust deposits. Academic Press: Orlando, FL.

Rishel, J.; S. Johnson, and D. Holt. 2003. Meteorological monitoring at Los Alamos. Los Alamos National Laboratory Report LA-UR-03-8097.

Ritchie J.C., and J.R. McHenry. 1990. Application of radioactive fallout cesium-137 for measuring soil erosion and sediment accumulation rates and patterns: a review. J. Env. Qual. 19: 215-233.

Rodgers, P. 1996. Disturbance ecology and forest management: a review of the literature. United States Department of Agriculture, Forest Service, Intermountain Research Station, General Technical Report INT-GTR-336.

Saxton, K.E. 1995. Wind erosion impacts on off-site air quality in the Columbia Plateau-an integrated research plan. Transactions of the ASAE 38:1031-1038.

Schlesinger, W.H., and A.M. Pilmanis. 1998. Plant-soil interactions in deserts. Biogeochemistry 42:169-187.

Selmants, P.C., A. Elseroad, and S.C. Hart. 2003. Soil and nutrients. In: Friederici P. (ed), Ecological Restoration of Southwestern Ponderosa Pine Forests. Island Press, Washington D.C..

Statsoft. 1994. Statistica for Windows Volume I: general conventions and statistics I. StatSoft release 5.0. StatSoft, Tulsa, OK.

Stout, J.E. 1990. Wind erosion in a simple field. Transactions of the ASAE 33:1597-1600.

Stout, J.E., and T.M. Zobeck. 1996. The Wolfforth field experiment: a wind erosion study. Soil Science 161:616-632.

Sutherland, R.A., T. Kowalchuk, and E. De Jong. 1991. Cesium-137 estimates of sediment redistribution by wind. Soil Science 151:387-396.

Swetnam, T.W., and J.L. Betancourt. 1998. Mesoscale disturbance and ecological response to decadal climatic variability in the American Southwest. J. Climate 11:3128-3147.

Tegen, I., A.A. Lacis, and I. Fung. 1996. The influence of climate forcing of mineral aerosols from disturbed soils. Nature 380:419-380.

Tongway, D.J., and J.A. Ludwig. 1997. The conservation of water and nutrients within landscapes, Chapter 2 In: Ludwig, J., Tongway, D., Freudenberger, D., Noble J. and Hodgkinson K. (eds), Landscape Function and Management: Principles from Austrailia's Rangelands. CSIRO Publishing, Melbourne, Austrailia, pp. 13-22.

Toy, T.J., G.R. Foster, and K.G. Renard. 2002. Soil erosion: processes, prediction, measurement and control. John Wiley & Sons, Inc.: New York, New York.

Veenis, S. 2000. After the fire. Erosion Control, Nov-Dec: http://forester.net/ec_0011_fire.html [Feb. 2005].

Wardle, D.A., R.D. Bardgett, J.N. Klironomos, H. Setälä, W.H. van der Putten, and D.H. Wall. 2004. Ecological linkages between aboveground and belowground biota. Science 304: 1629-1633.

Whicker, J.J., D.D. Breshears, P.T. Wasiolek, T.B. Kirchner, R.A. Tavani, D.A. Schoep, and J.C. Rodgers. 2002. Temporal and spatial variation of episodic wind erosion in unburned and burned semiarid shrubland. J. Env. Qual. 31(2): 599-612.

Whicker, J.J., J.E. Pinder III, D.D. Breshears, and Baker, K.N. 2004b. Secondary effects of thinning in ponderosa pine forests: wind erosion as an ecosystem health metric. Proceedings of the 8th Symposium of Biological Research in the Jemez Mountains, New Mexico.

Whicker, F.W., and V. Shultz. 1982. Radioecology: nuclear energy and the environment. CRC Press, Boca Raton.

Whitford, W.G. 2002. Ecology of desert systems. Academic Press: London, UK.

Whitford, W.G., A.G. DeSoyza, J.W. Van Zee, J.E. Herrick, and K.M. Havstad. 1998. Vegetation, soil, and animal indicators of rangeland health. Environmental Monitoring and Assessment 51: 179-200.

Zobeck, T.M., D.W. Fryrear, and Pettit, R.D. 1989. Management effects on wind-eroded sediment and plant nutrients. Journal of Soil and Water Conservation, March-April:160-163.

Zobeck, T.M., G. Sterk, R. Funk, J.L. Rajot, J.E. Stout, and R.S. Van Pelt. 2003. Measurement and data analysis for field-scale wind erosion studies and model validation. Earth Surface Processes and Landforms 28:1163-1188.

Table 2.1. Site characterization data for the burned and unburned plots. Values provided are means ± one standard deviation.

Site	Ground Cover			Tree cover			Soil Characteristics		
	% Veg. cover	% Litter cover	% Total cover	Trees per hectare	% Live canopy	Average tree height (m)	% Sand	% Silt	% Clay
Unburned									
Primary	5 ± 6	98 ± 4	97 ± 4	1280 ± 450	78 ± 14	9.4 ± 4.6	39 ± 9	49 ± 5	12 ± 4
Secondary	3 ± 3	98 ± 5	96 ± 7	50 ± 60	46 ± 28	12.3 ± 4.6	45 ± 15	41 ± 14	14 ± 3
Moderate burn									
Primary	5 ± 7	79 ± 19	78 ± 16	560 ± 440	38 ± 30	9.6 ± 4.1	46 ± 7	45 ± 7	9 ± 1
Secondary	13 ± 12	83 ± 20	83 ± 16	1180 ± 350	35 ± 18	9.4 ± 4.0	36 ± 3	52 ± 2	13 ± 2
Severe Burn									
Primary	24 ± 16	38 ± 18	51 ± 11	240 ± 190	0 ± 0	11.8 ± 4.8	34 ± 2	54 ± 2	12 ± 1
Secondary	26 ± 17	39 ± 18	52 ± 16	800 ± 670	1 ± 2	13.8 ± 2.7	51± 5	39 ± 7	9 ± 3

Table 2.2. Horizontal dust flux (HDF) on burned and unburned areas in 2001, 2002 and 2003. Data are shown as means ± one standard deviation and are computed for data from both Primary and Secondary sites from all sampling periods. Sample sizes are occasionally less than the expected values due to damage to field samplers and problems in sample processing. Data in parentheses are derived from dry sampling periods (< 1.5 mm precipitation).

Sampling height (m)	n	HDF at unburned site ($g\ m^{-2}\ d^{-1}$)	n	HDF at moderate burned Site ($g\ m^{-2}\ d^{-1}$)	n	HDF at severely burned site ($g\ m^{-2}\ d^{-1}$)
			----2001----			
0.25	60	0.45 ± 0.48	59	0.95 ± 1.26	60	5.53 ± 8.18
	(15)	(0.25 ± 0.18)	(14)	(0.47 ± 0.49)	(15)	(0.76 ± 0.33)
0.5	59	0.45 ± 0.48	60	0.49± 0.64	60	1.23 ± 0.41
	(15)	(0.28 ± 0.23)	(15)	(0.31 ± 0.27)	(15)	(0.5 ± 0.4)
1.0	59	0.42 ± 0.44	59	0.46 ± 0.55	60	0.76 ± 0.41
	(15)	(0.72 ± 0.43)	(14)	(0.33 ± 0.32)	(15)	(0.43 ± 0.22)
			----2002----			
0.25	79	0.69 ± 0.44	79	1.31 ± 1.34	80	4.47 ± 5.43
	(35)	(0.72 ± 0.43)	(35)	(0.82 ± 0.53)	(35)	(1.58 ± 0.66)
0.5	80	0.7 ± 0.41	80	0.93 ± 0.54	80	1.71 ± 0.99
	(35)	(0.79 ± 0.44)	(35)	(0.78 ± 0.32)	(35)	(1.68 ± 0.76)
1.0	80	0.7 ± 0.43	80	0.93 ± 0.56	80	1.43 ± 1.67
	(35)	(0.83 ± 0.49)	(35)	(0.83 ± 0.25)	(35)	(1.60 ± 0.58)
			----2003----			
0.25	60	1.05 ± 0.97	60	2.10 ± 2.15	60	8.72 ± 15.59
	(35)	(0.59 ± 0.28)	(35)	(1.17 ± 0.61)	(35)	(2.14 ± 1.20)
0.5	59	1.09 ± 0.96	60	1.96 ± 1.35	59	3.60 ± 3.94
	(35)	(0.57 ± 0.24)	(35)	(1.44 ± 0.74)	(34)	(1.93 ± 0.97)
1.0	60	1.09 ± 0.94	57	2.15 ± 1.33	58	3.09 ± 2.95
	(35)	(0.59 ± 0.26)	(35)	(1.65 ± 0.92)	(33)	(1.92 ± 0.87)

Figure 2.1. Mean horizontal dust flux (HDF) at 1-m sampling heights categorized by burn type.

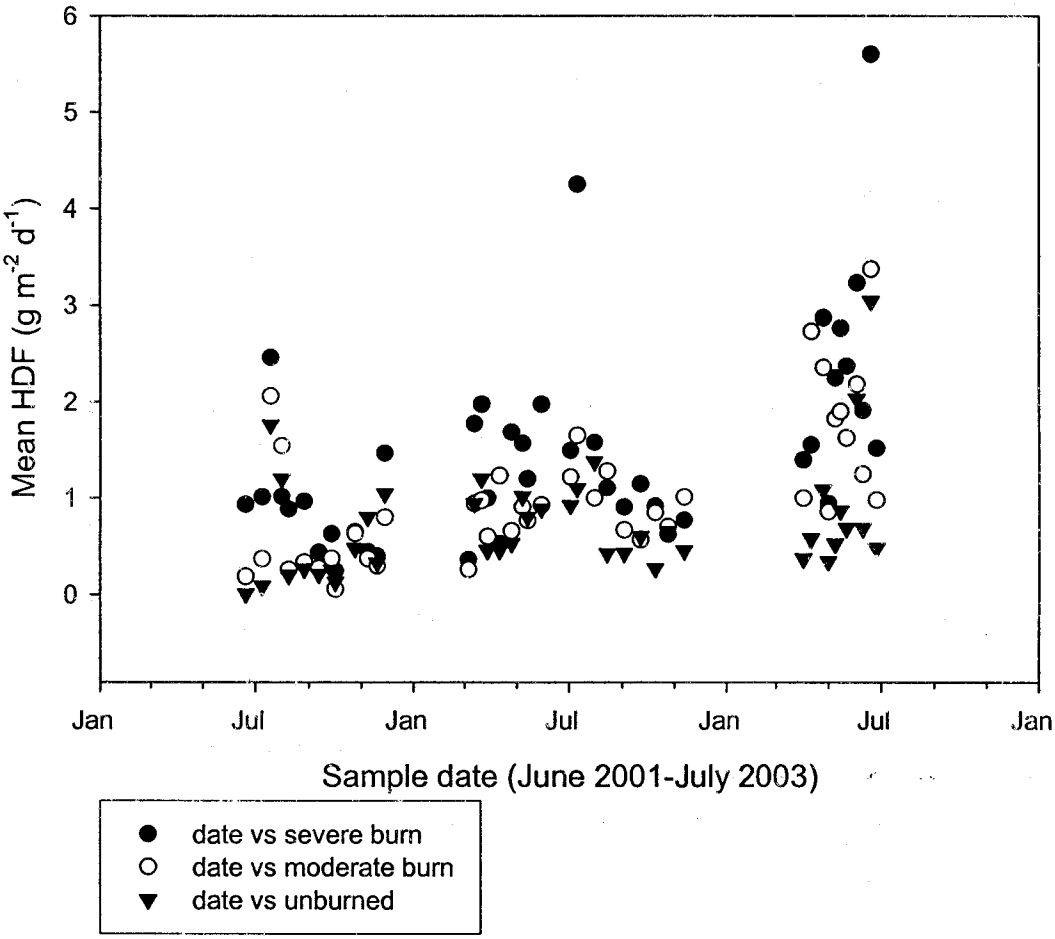

Figure 2.2. Mean and one standard error of the mean for horizontal dust flux (HDF) categorized by sampling heights and averaged over all sampling periods (a) and for horizontal dust fluxes that were averaged over dry sampling periods with precipitation < 1.3 mm (b).

(a)

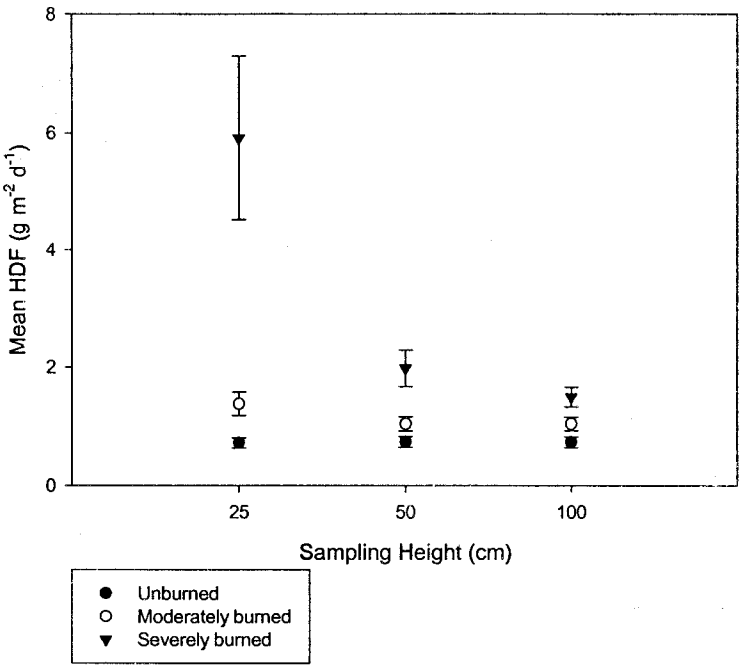

(b)

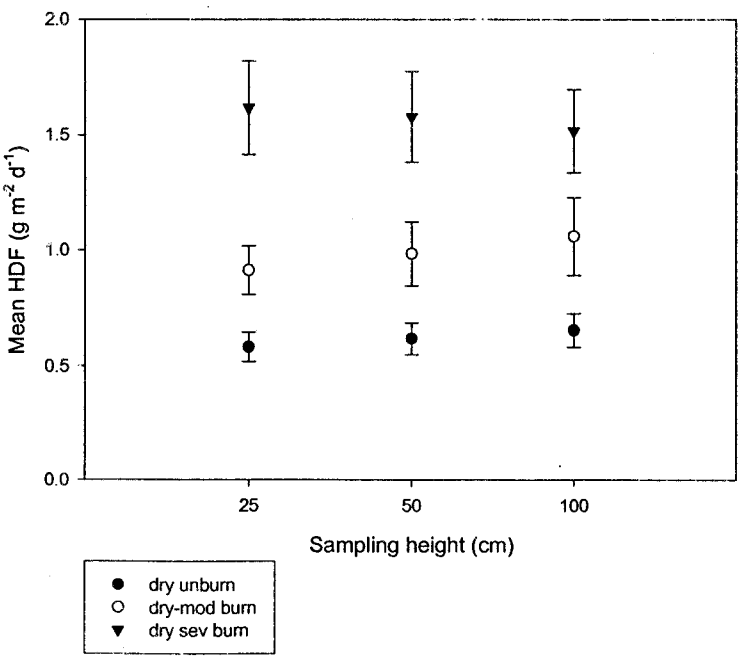

Figure 2.3. Relationship between mean horizontal dust flux, precipitation (column a), and wind velocity (column b) categorized by sampling height.

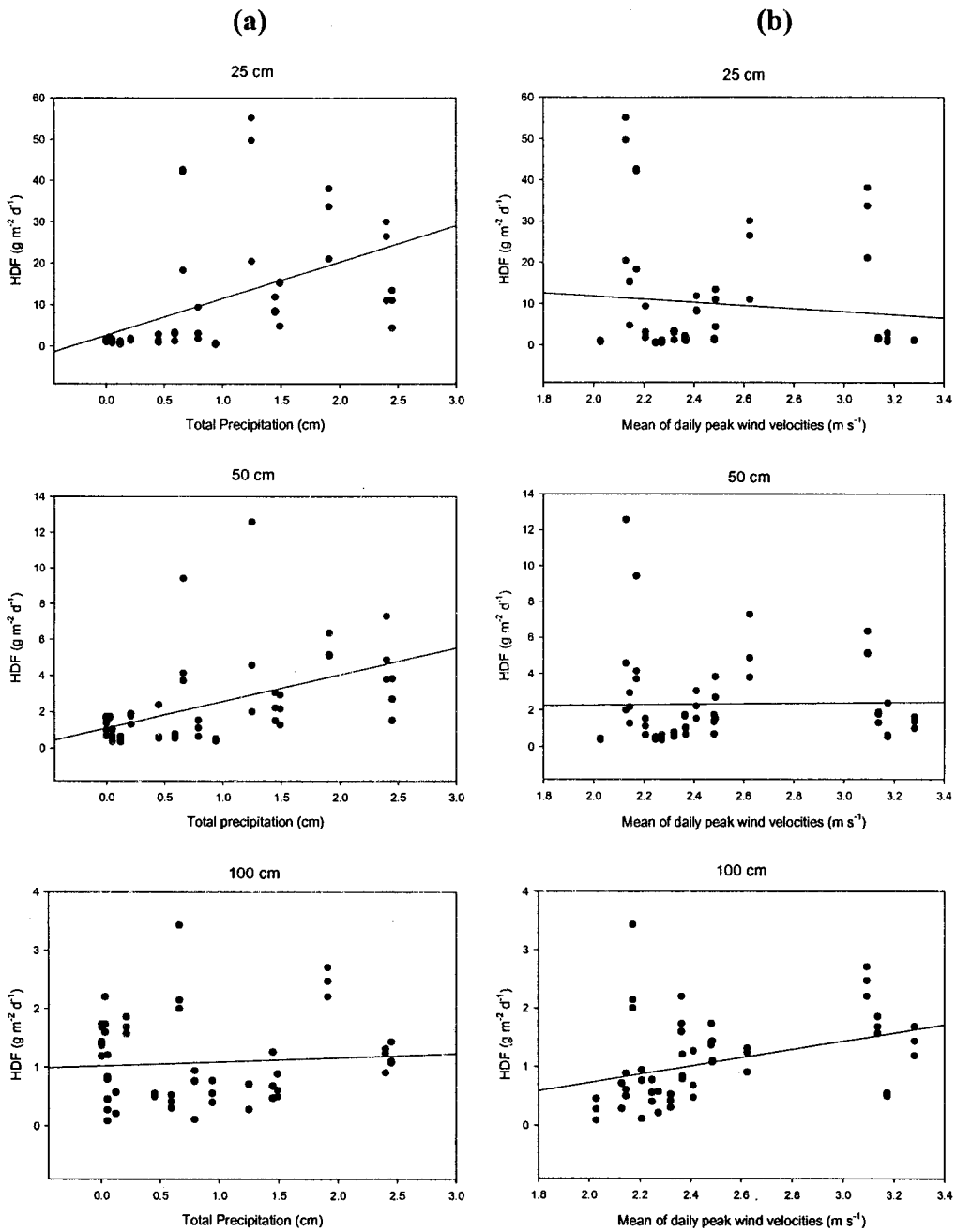

Figure 2.4. Relationship between the vertical flux measurements and the HDF measured at the TA-6 meteorological station.

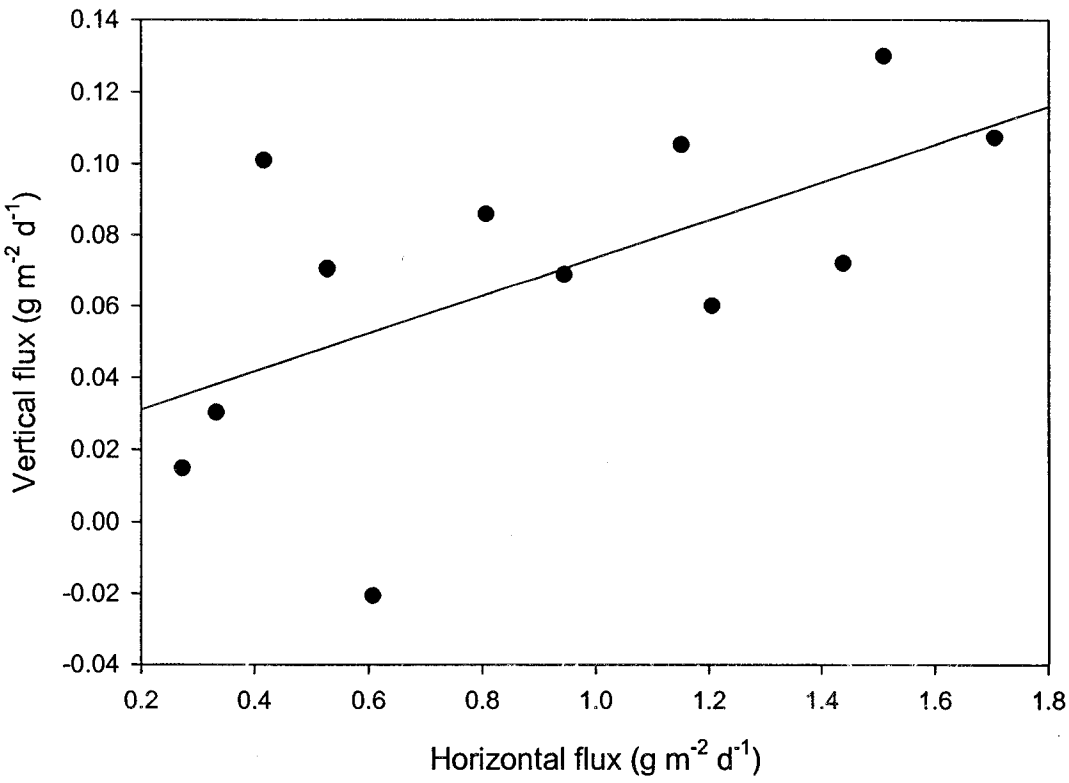

Chapter 3

Amplified Wind Erosion following Forest Thinning and Burning

3.0 Abstract

Impacts of tree thinning to reduce tree density in ponderosa pine forests on wind-driven horizontal dust flux were measured using passive dust collectors in thinned and burned ponderosa pine forest ecosystems near Los Alamos, New Mexico. Horizontal dust flux was measured at sampling heights of 0.25 m, 0.5 m, and 1m above the soil surface in two forest stands for each combination for thinning and fire history. Tree densities, canopy coverage, and ground cover were also measured in each stand. Median horizontal dust fluxes in unburned + unthinned plots ranged from 0.43 to 0.5 g m^{-2} d^{-1}, increased in range in the unburned + thinned plot (0.96 to 1.3 g m^{-2} d^{-1}) for the first year after thinning, and ranged from 0.75 to 1.0 g m^{-2} d^{-1} for the second year after thinning. In burned locations, median dust fluxes in the unthinned site ranged from 0.92 to 1.11 g m^{-2} d^{-1} compared to 1.49 to 2.18 g m^{-2} d^{-1} in the burned + thinned location. The results of the study show that wind erosion was significantly elevated in thinned and burned areas, and there were indications of reduced dust flux during the second year after thinning. There was no indication of a synergistic effect between burning and thinning. Finally, we found a significant relationship between tree and ground cover and dust flux. These results show that wind erosion is responsive to thinning and

burning and suggest that measurement of wind erosion may be an important metric for estimating ecosystem function.

3.1 Introduction

Soil is a key-integrating factor in forest ecosystems because of the strong coupling between soil quality and the biotic component in ecosystems that it supports (Fisher and Binkley 2000, Kimmins 2003, Wardle et al. 2004). Disturbed ecosystems that steadily lose soil and associated soil nutrients can become permanently degraded (Tongway and Ludwig 1997), and because of the contrasts between the slow rate of soil generation and potential for rapid loss through erosion, soil has been considered as one of the most important non-renewable resources (Pimental 2000; Toy et al. 2002, Lal et al. 2003). Therefore, management of forest ecosystems requires knowledge of the impacts of natural and managed disturbances forest soils.

Disturbances in forests ecosystems are ever-present and vary dramatically in spatial and temporal scale of impact (Rodgers 1996, Reice 2001, Kimmins 2004). One of the larger disturbances in a forest ecosystem is from wildfire. From a human perspective, each year wildfires burn millions of hectares of forests, cost billions of dollars to fight (National Fire Plan 2002), cost lives (both of firefighters and citizens), burn homes and structures, and result in significant post-fire soil erosion. To reduce the frequency and intensity of catastrophic wildfires in the ponderosa pine (*Pinus ponderosa*) forests in the southwestern United States (Friedrici 2003), forest management policies have turned toward forest thinning and prescribed burning to lower tree densities and fuel loads. Additionally, to reduce economic losses, salvaging of trees from burned areas has been frequently proposed.

Large-scale thinning of trees in forests can have significant, long-term impacts that can either enhance or degrade forest function partially through altered soil quality (Likens et al. 1978, Baker and Jemison 1991, Freedman 1995, Kimmins 2003, Selmants et al. 2003). Transport of soil and its associated nutrients and organic matter through wind and water erosion is one of the key mechanisms through which soil quality can be changed (Pye 1987, Baker and Jamison 1991, Lal et al. 1996, Sterk et al. 2001, Toy et al. 2002, Kaiser 2004), and soil erosion rates in have been shown to increase following disturbances to vegetation cover and the soil surface layer (Fryrear 1985, Zobeck et al. 1989, Belnap and Gillette 1998, Whicker et al. 2002). The impacts of these actions on potential water-induced erosion in forests are recognized (Freedman 1995) but potential wind-induced erosion impacts are poorly understood despite its potential importance (Breshears et al. 2003).

Wind transports soil material through several processes that include: 1) surface creep (soil particles > 500 μm), 2) saltation (soil particles ranging from 20 – 500 μm), and 3) suspension (soil particles < 20 μm) (Pye 1987, Toy et al. 2002). All of these processes redistribute soil, associated nutrients, and organic material throughout the forest at different spatial scales. On a local scale (scale < several meters), wind-driven surface creep and saltating particles dominate the mass movement of soil (Stout and Zobeck 1996, Gillette et al. 1997). In contrast, suspended particles are available for long-distance transport and redistribute soil and associated materials on regional, continental, and global scales.

Because soil nutrients and organic matter are often associated with smaller particles, the suspended aerosol can be relatively enriched in soil nutrients and organic

material. Thus, wind erosion has been found to preferentially remove the finer fraction of soil that is enriched in materials such as nitrogen, phosphorus, and organic material, all of which are critical to soil productivity (Sterk et al. 1996, 2001, Larney 1998, Goosens 2004). Conversely, deposition of aeolian dust in once disturbed areas then remediated to grassland or tree-covered patches has been shown to improve soil quality (Reeder et al. 1998, Shirato et al. 2004).

Soil erosion rates in an area depend on numerous factors and include vegetation cover (height and area coverage), soil characteristics such as texture, local meteorological conditions, and local topography (Toy et al. 2002). While the relationship between these variables and wind erosion has been extensively studied and successfully modeled for agricultural systems (Woodruff and Siddoway 1965, Hagen 1991, Skidmore 1994, Fryrear et al. 1998, Toy et al. 2002), there are little data on wind erosion and dust transport in forests, and there are even fewer measurements of wind erosion response to forest disturbances such as burning and thinning.

3.1.1 Historical context for the study and problem statements

The May 2000 Cerro Grande fire burned approximately 16,000 hectares of mostly ponderosa pine forest, including about 3000 hectares of land and some structures and facilities within Los Alamos National Laboratory (LANL 2000). To reduce the potential for future fire damage to nuclear facilities and to improve the forest "health" (Covington 2003, Mast 2003), approximately 4500 hectares of ponderosa pine forests was thinned on Los Alamos National Laboratory (LANL) property between 2000 and 2003 (LANL2001). Both unburned forest and moderately burned areas with surviving

trees were thinned. Because of the large amount of land needing thinning, mechanized techniques were used including the use of track-mounted feller bunchers (manufactured by Timbco), skidders, stroke delimbers, and logging trucks to haul off the lumber (Quam 2004). While the forest-thinning plan for LANL addressed concerns for water erosion (e.g., the areas thinned were restricted to slopes < 10%), little attention is given to wind erosion (LANL 2001). The potential for wind erosion was recognized for vehicle travel on roads, and some main roads were wetted to suppress dust. However, no moderating efforts were applied to soils disturbed by heavy equipment in the thinned areas. Because of the intrusive nature of the techniques and their impact on soil stability, it was important to measure the effect of the tree thinning operations on wind erosion. Further, removal of trees in burned forest has been proposed to salvage lumber, but Paine et al. (1998) and others have shown that multiple disturbances, including different disturbance types, can significantly affect the ecological trajectory of the recovery, possibly through alteration of soil quality.

This study was designed to address two problems associated with wind erosion and thinning. **First,** there are few measurements of wind erosion and dust transport in many ecosystems (disturbed or otherwise), and this may be particularly important in the semiarid ponderosa pine forest. **Second,** there are little data on the combined effects of ecosystem disturbances such as fire and thinning operations on wind erosion). Given the vast areas of the western United States that may be thinned, and may be thinned or salvaged following fire, there is a need to better understand the impact of thinning and salvaging on wind erosion and transport in forest ecosystems.

3.1.2 Study goals

The general goal of this study was to quantify the effects of tree thinning on wind erosion in both unburned and moderately burned disturbed ponderosa pine forests. A specific objective was to determine if thinning had a greater effect in burned than unburned forests. Measurements of wind-driven dust flux in thinned and unthinned areas in the unburned areas were also conducted over two years following tree thinning to indirectly assess forest recovery.

3.2 Methods

The study sites are located in the Jemez Mountains in North Central New Mexico (at general area coordinates of 35°52 N; 106°19' W) and elevations of about 2300 m within the boundaries of Los Alamos National Laboratory. Average annual precipitation in the area is about 500 mm (Bowen 1990). Woody vegetation is comprised mostly of ponderosa pine (*Pinus ponderosa* Laws. Var. Scopulorum Engelm.; nomenclature follows Martin and Hutchins, 1980) and gamble oak (*Quercus gambelii*). Ground vegetation consists of a variety of grasses and flowering plants (Foxx and Hoard 1995). The unburned sites had no recent history of fire with ground vegetation of perennial grasses and a litter cover of pine needles (Pinder et al. 2004).

The eastern flank of the Cerro Grande fire included forested areas within Los Alamos National Laboratory, and these areas were burned with varying severity (LANL 2000). The moderately burned areas had their ground vegetation and litter cover consumed in the fire with scorching, but not burning of pine needles. Scorching in

these areas extended up to 75% of the canopy, with the tree crown green. Scorched needles dropped in the years following the fire and formed a thin, partial cover over the bare soil surface. These moderately burned areas represent areas that are likely candidates for post-fire thinning to reduce subsequent fire hazards and for salvaging of dead trees for commercial purposes.

Primary factors in determining wind erosion rates in forested area include the amount of ground cover (Fryrear 1985), soil characteristics (Skidmore 1994), meteorological conditions, and tree structure in the forest, which can have a significant impact on wind velocity profiles in the forest (Stull 1988). Therefore, each of these factors was measured within each of the selected sampling plots.

3.2.1 Characterization of sampling sites

Sampling locations

Two stands were located in each of four forest site categories that included 1) unburned and unthinned, 2) unburned and thinned, 3) moderately burned and unthinned, and 4) burned and thinned. One stand was designated as a Primary site and the other was designated as a Secondary site. Primary sampling sites contained three dust-flux sampling stations and the Secondary sites had two dust-flux sampling stations. Dust flux samplers were arranged at 30 m intervals through the stand. Sampling sites were selected based on criteria including 1) relatively homogeneous tree structure and no roadways or disturbed areas within a 100-m radius (Baldocchi 1997) of the site, 2) selected sites were relatively flat (mostly with slopes less than 10%), and 3) the sites

should be fairly representative (soil and vegetation types and structure) of other locations in the region.

Thinning occurred in the study areas starting in the fall of 2001 (only the Primary unburned site was thinned at this time) with measurements of dust flux starting in March of 2002 and continuing through July 2003 at this location. The other sites were thinned during the fall of 2002 with measurements starting in March of 2003 and ending in July 2003.

Soil Characterization

To measure soil texture, surface soil (top 2 cm) was collected from five random locations in Primary site locations and three random locations in the Secondary sites. For each sampling location, twenty 38-mm diameter soil cores were obtained, composited, air-dried to a constant mass, and a 200 g aliquot was submitted to the Soil, Water, and Plant Testing Laboratory at Colorado State University for analyses of soil texture [% sand, % silt, and % clay (Miller and Gardiner 2001)] by a modified pipette method (Indorante et al., 1990).

Characterization of Tree Density and Canopy Cover

Tree density at unthinned sites was measured in March of 2002 in 5 100-m^2 plots within the Primary sites and in 4 100-m^2 plots within the Secondary sites, and measured in September of 2002 in 10 and 7 100-m^2 plots within the Primary and Secondary thinned sites, respectively. The number of trees and freshly cut tree stumps within a 100-m^2 area was determined at each location. The tree density was calculated

as the number of live trees divided by the sampled area. Tree density before thinning was determined by counting the sum of the remaining trees and the stumps of the recently cut trees, thus the percent reduction in tree density from thinning operation could also be calculated. Heights of standing trees were measured using a forester's altimeter (Avery and Burhart 1994). The percent canopy cover of live trees was estimated from measurements made in June 2001 using a spherical densiometer (Lemmon, 1956) that has a grid scratched into the surface of the mirror. Tree canopy measurements were made in 12 to 22 locations.

Ground cover

Ground cover was measured using 3.2 Mega pixel digital images of 1-m^2 plots of ground cover at randomly selected locations, with 10 plots at Primary sites and 7 plots in the smaller Secondary sites for a total of 17 plots areas within each of the four burn/thin site categories. Pictures of the ground cover within the 1-m^2 plots were taken before seasonal growth (early spring), at mid growth (summer), and at the end of the growing season (fall). The images were magnified ($\geq$ 2x) and the percent cover for each of the vegetation/cover plots was determined by visual examination of the picture using a computer generated grid consisting of 25 subgrids within the 1 m^2 sampling frame with lengths of 20 cm per subgrid side. The percent of live *vegetation cover* and *litter cover* in the plot was determined by averaging measures within the 25 subgrids. Vegetation and litter cover were separately evaluated, and a measure of the total cover was estimated from 81 points dispersed throughout the plot (Pinder et al. 2004).

3.2.2 Measurement methods for horizontal dust flux

Wind erosion rates were evaluated through measurement of horizontal dust flux (HDF), which is a direct measure of locally transported soils (Stout and Zobeck 1996, Breshears et al. 2003) and is significantly correlated with the vertical flux of suspended soil material that can be associated with erosion (Gillette et al. 1997, Whicker et al. 2005). The HDF was measured with Big Springs Number Eight (BSNE) dust samplers (Fryrear 1986, Zobeck et al. 2003). These samplers have a tail-fin and self-orient a small opening (10 cm^2) into the wind through which wind-driven dust particles enter. Once inside the sampler, the dust particles decelerate and deposit into a collection pan. The BSNE samplers have been shown to have good sampling efficiency for saltating particles, e.g., sizes > 50 μm, which make up a large fraction of the soil in the study area (Nyhan et al. 1978) and have been used extensively for field measurement of HDF (Fryrear 1986, Goosens and Offer 2000, Zobeck et al. 2003). The collected dust was sampled at intervals ranging from weekly during windy conditions (i.e., during the spring) to several weeks during less windy periods. To assess horizontal flux with height above the surface, BSNE samplers were positioned at sampling heights of 7 cm, 15 cm, 25 cm, 50 cm, and 100 cm.

The dust was collected in the field by washing out the collected dust using distilled water and then transferred into glass vials in the lab. The vials were placed into an oven and dried at 50° C to a constant mass, and the mass of the dried dust measured to the nearest mg. The HDF was calculated by using the mass of the dust collected and dividing the area of the sampler opening (10 cm^2) and the sampling period. The units of

HDF were g m^{-2} d^{-1}. This value represents the wind-driven mass of dust flowing horizontally along the earth surface at each sampling height.

3.2.3 Statistical analyses

Statistical comparisons of HDF among burned and unburned areas were performed using a mixed-model Analysis of Variance (ANOVA) where thinning, sampling periods and the interaction of burn severity and sampling dates were fixed-effects and sites and specific BSNE locations within sites were random-effects (Milliken and Johnson, 1984). Statistical computations were performed using the Type 3 option of PROC MIXED of the SAS System (Littell et al., 1996). Hypotheses of specific effects, such as 1) the effects of thinning and 2) changes in the effects of thinning among years, were tested using F ratios computed for Linear Contrasts of Means (Littell et al., 1996). Due to the differential effects of precipitation and wind speeds on HDF at different elevations (Whicker et al. 2005), separate analyses were performed for the 0.25, 0.5 and 1.0 m elevations, and separately for wet and dry sampling periods. Similar procedures were used to test for differences in tree densities, canopy cover, and ground cover among sites.

3.3 Results

3.3.1 Impact of thinning on tree densities, tree heights and canopy cover

Thinning reduced tree densities (Table 3.1) by 32% to 86 %. Mean tree densities on all thinned plots was $\geq$ 410 trees per ha before the thinning and $\leq$ 410 trees per ha after the thinning. Approximately 35 % of the trees on the burn plots before the

thinning had died from either the direct effects of the fire or the subsequent drought and bark beetle effects following the fire. These dead trees were included in the data in Table 3.1 to isolate the effects of thinning on tree density.

Although thinning in the burned areas reduced tree densities, tree densities on thinned sites in the burn areas were similar to those for the burned + unthinned sites. This lack of pronounced difference reflects significant variation among sites in tree densities, and 2) variation among sites in tree mortalities due to fire severity (Pinder et al., 2004).

Spherical densitometer measurements of tree canopy cover (Table 3.1) largely reflected the patterns of tree densities. Individual point measurements of canopy cover ranged from 0 to 96 %, and means for site ranged from 21.7 % to 77.9 %. Individual point measurements of 0 % only occurred on burned or thinned sites. Measurements within sites were often variable as indicated by the large ratios of standard deviations to means which were usually > 0.5. The similarities among sites in tree densities and the variability in individual densitometer measurements within sites complicated the comparison among burn and thinning treatments. Although there were significant differences in canopy cover measurements among sites within combinations of burning and thinning ($F = 5.17$; $df = 4, 116$; $P < 0.01$), there were no statistically significant effects ($P \geq 0.05$) of burning, thinning, or the interaction of burning and thinning.

Besides reducing densities, the thinning altered the distributions of tree heights. Because smaller trees were removed, the height distributions on thinned areas were skewed more toward taller trees in both the burned and unburned areas. Few trees $\leq$ 8-

m tall were present on the thinned sites, but > 20 % of the trees on the unthinned sites were ≤ 8-m tall.

3.3.2 Impact of thinning on forest ground cover

Table 3.2 shows the effects of thinning on ground cover (litter, live vegetation, and total cover). Thinning operation reduced the *litter cover* and exposed approximately 20% bare soil in both unburned (LCM $F = 21.1$; $df = 1, 83$; $P < 0.01$) and burned (LCM $F = 10.3$; $df = 1, 83$; $P < 0.01$) areas that were thinned. Although the litter cover in the burned areas was less than that in the unburned and was composed of a thinner layer of recently deposited pine needles (Pinder et al. 2004), there was no significant difference in the level of exposed soils between thinned sites in unburned and burned areas (LCM $F = 0.3$; $df = 1, 83$; $P \geq 0.10$). There was no measurable effect of thinning on *vegetation cover* because of variations in vegetation cover among sites within the same thin/burn category as discussed in Pinder et al. (2004). The results for *total cover* (Table 3.4), which includes both litter and vegetation, were similar to those for litter cover with significant decreases in total cover for thinned plots on 1) unburned (LCM $F = 12.7$; $df = 1, 83$; $P < 0.01$) and 2) burn areas (LCM $F = 16.8$; $df = 1, 83$; $P < 0.01$). These results indicate that any responses of vegetation cover were not sufficient to moderate the reductions in litter cover. There was no measurable recovery in total cover during the second year on the primary unburned and thinned site (LCM $F = 1.59$; $df = 1, 83$; $P \geq 0.10$).

The soils in the plots were characterized as silt loam soils with mean values of 41% sand, 47% silt and 12% clay across all sites. The percent of sand, silt, and clay in

the soils among the thinned and unthinned plots were not statistically different. Therefore, any difference in soil erosion between thinned and unthinned sites is not likely to be explained by differences in soil texture (Pinder et al. 2004).

3.3.3 Effects of thinning in burned and unburned forest on horizontal dust flux

Generally, HDF was significantly increased in the thinned and burned areas at the different sampling heights as shown for dry periods in Figure 3.1, with the summary statistics for these HDF measurements provided in Tables 3.3 (all data) and 3.4 (dry periods only). Further, statistical analysis showed the impact of thinning on horizontal dust flux generally decreased with elevation above the ground surface. At 0.25 m thinning resulted in statistically significant increases in dust flux for the unburned (LCM on logarithmic transformed data $F = 25.52$; $df = 1, 17$; $P < 0.001$) and the moderate burned areas (LCM on logarithmic transformed data $F = 14.78$; $df = 1, 17$; $P < 0.001$) with no significant difference in the degree of effect between unburned and burned areas (LCM on logarithmic transformed data $F = 0.16$; $df = 1, 17$; $P > 0.10$). The results at 0.50 m were similar to those at 0.25 m with statistically significant thinning effects for unburned (LCM on logarithmic transformed data $F = 6.74$; $df = 1, 17$; $P < 0.001$) and burned (LCM on logarithmic transformed data $F = 3.65$; $df = 1, 17$; $P < 0.001$) sites with no significant difference in degree of effect between unburned and burned areas (LCM on logarithmic transformed data $F = 2.80$; $df = 1, 17$; $P \geq 0.05$). At 1.00 m there was a statistically significant increase in dust flux on thinned unburned areas (LCM on logarithmic transformed data $F = 7.40$; $df = 1, 17$; $P < 0.05$) but not on burned areas (LCM on logarithmic transformed data $F = 0.0$; $df = 1, 17$; $P \geq 0.10$).

Figure 3.2 shows horizontal dust flux across time. There was a statistically significant decline in dust flux at 0.25 m on the primary thinned site between 2002 and 2003 (LCM on logarithmic transformed data $F = 5.82$; $df = 1, 17$; $P < 0.05$) where the mean dust flux declined by 40 % from 2002 to 2003. There was also a decline in dust flux from 2002 to 2003 on the primary thinned unburned site at 0.50 m (LCM on logarithmic transformed data $F = 12.26$; $df = 1, 17$; $P < 0.001$) similar to that observed at 0.25 m. There was no statistically significant decline in dust flux between years 2002 and 2003 on the primary thinned unburned site (LCM on logarithmic transformed data $F = 0.84$; $df = 1, 17$; $P \geq 0.10$). Although this two-year data set is limited to the primary unburned and primary unburned/thinned sites, it is suggestive of soil stabilization which may be indicative of the forest recovery.

HDF Analyses for Dry Periods

The above analyses were performed using only data from all sampling periods, and the results were similar to those obtained with data from dry sampling periods with no precipitation (Table 3.4). For dry sampling periods, we found that at 0.25 m that there were significant thinning effects in burned and unburned plots (LCM on logarithmic transformed data $F = 24.86$; $df = 1, 17$; $P \leq 0.001$) and no thinning + burn interactions (LCM on logarithmic transformed data $F = 1.00$; $df = 1, 17$; $P > 0.1$). At 0.5 m, we found significant overall thinning effects, but this difference was found only on the unburned plots (LCM on logarithmic transformed data $F = 3.98$; $df = 1, 17$; $P \leq 0.01$). There was also an interaction between the thinning and the fire effect (LCM on

logarithmic transformed data $F = 5.00$; $df = 1, 17$; $P \leq 0.05$) at the 0.5 m sampling height. Finally, the results at 1 m showed no significant thinning effects or interactions.

Regarding HDF measurements across time, we found mixed evidence of a decrease in HDF during the second year after the thinning. Specifically, there was a moderate but not significant reduction in HDF from 2002 to 2003 (LCM on logarithmic transformed data $F = 3.77$; $df = 1, 17$; $P < 0.1$) at the sampling height of 0.25 m. At 0.5 m, we found a significant reduction in dust flux in the second year at the primary unburned/thinned site (LCM on logarithmic transformed data $F = 7.88$; $df = 1, 17$; $P < 0.05$). There were no significant differences from 2002 to 2003 found at the 1-m sampling height.

3.3.4 Relationship between horizontal dust flux and vegetation cover

Combining data from this study and a companion study on the effects of wildfire severity on dust flux (Whicker et al. 2005), a relationship between ground and tree cover emerges. Figure 3.3 shows the horizontal dust flux as a function of percent ground and tree cover. There was a significant decrease in dust flux as the amount of ground and tree cover increased. These linear relationships, while significant, should not be extrapolated beyond the amount of cover measured in the study because others have shown erosion rates to have thresholds and to be non-linearly related to cover, especially at the lowest levels of ground cover (Bagnold 1941; Fryrear 1985; Davenport et al. 1998).

3.4 Discussion

Statistical analyses showed that thinning operations in unburned and moderately burned ponderosa pine forest significantly increased wind-driven dust transport, both during wet and dry sampling periods. The amount of this increase in dust flux in the thinned areas was equal at the burned and unburned locations. That is, we found little evidence of a synergistic interaction between the effects of thinning and moderate forest burning. Increases due to thinning were greatest at the lowest sampling heights, but much of the differences at these heights were related to the effects of rainsplash. This study also found evidence that dust fluxes decreased through two years post-thinning indicating soil stabilization. Finally, we found a significant relationship between HDF and tree and ground cover, which could prove to be extremely useful for establishing goals and procedures for tree thinning operations in forests that would minimize soil loss.

The effects of thinning on soil erosion can be compared to the increases in wind erosion from severely burned areas. In a companion study (Whicker et al. 2005), made similar measurements of horizontal dust flux in nearby severely burned forest stands at the same times as those in this study. Whicker et al. 2005 showed that wind erosion increased by a factor of about 3 in the severely burned areas, which may be slightly higher than that resulting from tree thinning. The data suggest that the severely burned areas were associated with the greatest wind erosion rates and the rates had not decreased even three years after the fire.

There are several ecological implications for these results. Given the tight link between forest structure, wind erosion of soil, and soil quality and productivity, it is

important to consider the long-term impact of disturbance in forests from thinning operations. Related, it is important to consider the impact of severe forest fires on wind erosion. While wind erosion increased in response to both of these forest disturbances, this data suggest the possibility that the forest management including thinning and moderate burns could result in lesser amounts soil loss through wind erosion. Wind erosion is just one impact of thinning though, as soil compaction can severely degrade soil productivity, lead to increase water erosion, and the effects can last for many years (Selmant et al 2003).

Thinning procedures vary in the scales of technologies applied and the effects of these variations may also be important factors in determining overall wind erosion. The procedures may involve cutting of mostly small trees with hand-held chain saws and the formation of small slash piles to be burned, or they can involve large-tracked vehicles with skidding and removal of large trees similar to the thinning at LANL. The spatial scale of the thinned areas can also vary in size and pattern. The extent of the thinning and the heavy equipment involved at LANL are near the upper end of the range. Thus, the damages and the impacts on erosion observed may also be on the upper end of the range.

There are very many different types of forest disturbance (Rodgers 1996, Kimmins 2003) that can affect forest soil quality. It would be important to study the combined impacts of multiple disturbances to the forest on soil erosion. For example, during this study, the forest was undergoing a drought that was accompanied by pine beetle attacks, and fire. Multiple disturbances have been shown to alter the ecological trajectory of the recovery of the affected ecosystem, and in severe cases, result in a

permanently altered end-state ecosystem. While this study does was not able to investigate the effects of different thinning strategies, or separate the effects of other forest disturbances (singularly or in combination in the case of multiple disturbances), these measurements in combination with other studies (Whicker et al. 2005) strongly suggest that horizontal flux measurements are a useful metric for measurement of soil stability, which is related to the ability of disturbed forest to conserve essential soils and nutrients required for ecosystem function (Tongway and Ludwig 1997).

This study also has implications for determining thinning strategies. To reduce the amount of soil erosion, the following suggestions are made. First, given the importance of vegetation and litter cover toward reducing wind erosion found in this study (Figure 3.3) and other studies (Fryrear 1985), thinning strategies that leave a layer of litter (e.g., pine needles and slash) on the soil surface may significantly reduce soil loss through wind erosion. This litter could also improve soil quality by conserving nutrients and soil organics. Successful plant recovery, either through residual plants or seeding, is also likely to also lesson wind erosion rates. Second, the increased HDF found in the thinned areas may be partially explained by significant disruptions to the soil surface by the tracked vehicles (Belnap and Gillette 1998; Grantham et al 2001). Techniques that minimize soil disruption and breaking of soil crusts would help conserve soil in the affected areas. For example, removal of trees during times when the soil is frozen or snow covered may result in less disruption to the soil surface and reduce wind erosion.

Finally, although this study was not designed to investigate the many potential impacts of different thinning strategies on wind erosion, proposed thinning procedures

might be evaluated against the relationship we found between HDF (related to soil stability) and targets for post-thin residual ground and tree cover.

3.5 Conclusions

This study is a unique evaluation of the effects of both thinning and burning on wind erosion measures and indicates that both produce significant increases in wind erosion and transport. Our results show 1) that wind erosion and transport are responsive to burning and thinning treatments in ponderosa pine forests, 2) increased HDF was temporary and evidence suggests that it declined within a year as ground cover increased, and 3) there was a direct relationship between tree and ground cover in forest and HDF that can be used to minimize soil loss resulting from thinning operations. More generally, our results, which build upon previous studies, indicate that measures of wind erosion and transport respond to ecosystem disturbances and should be considered as a metric for assessment of ecosystem function (Miller 2004).

3.6 References

Avery TE, Burhart HE. 1994. Forest measurements. McGraw-Hill Inc.: New York.

Bagnold RA. 1941. The physics of blown sand and desert dunes. Chapman and Hall Ltd., London.

Baker Jr., M.B., and R.L. Jemison. 1991. Soil loss- key to understanding site productivity. In: Proceedings of the 36th annual meeting of the Agencies and Science Working Together for the Future, New Mexico Water Research Institute, pp 71-76.

Baldocchi D. 1997. Flux footprints within and over forest canopies. Boundary-Layer Meteorology 85:273-292.

Belnap J, Gillette DA. 1998. Vulnerability of desert biological soil crusts to wind erosion: The influences of crust development, soil texture, and disturbance. J. Arid Environ. 39:133-142.

Breshears DD, Whicker JJ, Johansen MP, Pinder JE. 2003. Wind and water erosion and transport in semi-arid shrubland, grassland and forest ecosystems: quantifying dominance of horizontal wind-driven transport. Earth Surface Processes and Landforms 28:1189-1209.

Bowen BM. 1990. Los Alamos Climatology. Los Alamos National Laboratory LA-11735-MS; UC-902. National Technical Information Service, Springfield, VA.

Covington, W.W. 2003. The evolutionary and historical context. In: Friederici P. (ed), Ecological Restoration of Southwestern Ponderosa Pine Forests, Island Press: Washington, D.C., pp 26-47.

Davenport DW, Breshears DD, Wilcox BP, Allen CD. 1998. Viewpoint: Sustainability on piñon-juniper exosystems: a unifying perspective on soil erosion thresholds. Journal of Range Management 51:231-40.

Fisher RF, Binkley D. 2000. Ecology and the management of forest soils. John Wiley & Sons, Inc.: New York, New York.

Freedman B. 1995. Environmental ecology: the ecological effects of pollution, disturbance, and other stresses. Academic Press, San Diego, California.

Friederici P. 2003. Ecological Restoration of Southwestern Ponderosa Pine Forests, Island Press: Washington, D.C., pp 26-47.

Fryrear D.W. 1986. A field dust sampler. Journal Soil and Water Conservation 41:117-120.

Fryrear D.W. 1985. Soil cover and wind erosion. Transactions of the ASAE 28:781-784.

Fryrear DW, Saleh A, Bilbro JD, Schomberg HM, Stout JE, Zobeck TM. 1998. Revised wind erosion equation (RWEQ). Wind Erosion and Water Conservation Research Unit, USDA-ARS, Southern Plains Area Cropping Systems Research Laboratory. Technical Bulletin No. 1. http://www.csrl.ars.usda.gov/wewc/rweq.htm. [February 2005].

Foxx TS, Hoard D. 1995. Flowering plants of the Southwestern woodlands. Otowi Crossing Press: Los Alamos, NM.

Gillette, D.A., D.W. Fryrear, J.B. Xiao, P. Stockton, D. Ono, P.J. Helm, T.E. Gill, and T. Lee. 1997. Large-scale variability of wind erosion mass flux rates at Owens Lake: 1. Vertical profiles of horizontal mass fluxes of wind-eroded particles with diameter greater than 50 μm. Journal of Geophysical Research 102{D22):25,977-25,987.

Gillette DA, Fyrear DW, Gill TE, Ley T, Cahill TA, Gearhart EA. 1997. Relation of vertical flux of particles smaller than 10 μm to total aeolian horizontal mass flux at Owens Lake. Journal of Geophysical Research 102(D22):26009-26015.

Grantham WP, Redente EF, Bagley CF, Paschke MW. 2001. Tracked vehicle impacts to vegetation struture and soil erodibility. Journal of Range Management 54:711-716.

Griffin, D.W., C.A. Kellogg, and E.A. Shinn. 2001. Dust in the wind: long range transport of dust in the atmosphere and its implications for global public and ecosystem health. Global Change & Human Health 2(1):20-33.

Goossens, D., and Z.Y. Offer. 2000. Wind tunnel and field calibration of six aeolian dust samplers. Atmospheric Environment 34:1043-1057.

Goossens D. 2004. Net loss and transport of organic matter during wind erosion on loamy sandy soil. In: Wind Erosion and Dust Dynamics: Observations, Simulations, Modeling (Eds. D Goossens and M. Riksen). ESW Publications, Wageningen, 2004, pp. 81-102.

Hagen LJ. 1991. A wind erosion prediction system: concepts to meet user's needs. Journal of Soil and Water Conservation 46:106-111.

Indorante SJ, Follmer LR, Hammer RD, Koenig PG. 1990. Particle size analysis by a modified pipette procedure. Soil Science Society of America Journal 54:560-563.

Kaiser, J. 2004. Wounding earth's fragile skin. Science 304:1616-1618.

Kimmins JP. 2003. Forest ecology: a foundation for sustainable forest management and environmental ethics in forestry (3rd edition). Prentice Hall, Upper Saddle River, New Jersey, USA.

Lal R, Mokma D, Lowery B. 1996. Relation between soil quality and erosion. In: Lal R (ed), Soil Quality and Soil Erosion. CRC Press: Boca Raton, FL. pp: 237-258.

Lal R, Sobecki TM, Iivari T, Kimble JM. 2003. Soil degradation in the United States. Lewis Publishers, CRC Press: Boca Raton, FL.

LANL. 2000. A special edition of the SWEIS Yearbook: Wildfire 2000. Los Alamos National Laboratory Report LA-UR-00-3471.

LANL. 2001. Wildfire hazard reduction plan. Los Alamos National Laboratory Report LA-UR-01-2017.

Larney FJ, Bullock MS, Janzen HH, Ellert BH, Olson ECS. Wind erosion effects on nutrient redistribution and soil productivity. Journal of Soil and Water Conservation 53:133-140.

Lemmon, P.E. 1956. A spherical densitometer for estimating overstory density. Forest Science 2:314-320.

Likens GE, Bormann FH, Pierce RS, Reiners WA. 1978. Recovery of a deforested ecosytem. Science 492-496.

Littell, R. C., G. A. Milliken, W. W. Stroup, and R. D. Wolfinger. 1996. SAS System for Mixed Models. SAS Institute Inc., North Carolina.

Martin WC, Hutchins CR. 1980. A flora of New Mexico. J. Kramer, Germany. 2591 pages.

Mast JN. 2003. Tree health and forest structure. Pages 215-232 in P. Friederici, editor, Ecological Restoration of Southwestern Ponderosa Pine Forests, Island Press, Washington, D.C., USA.

Miller, M.E. 2004. The structure and functioning of dryland ecosystems- conceptual models to inform the vital-sign selection process. United States Geological Survey report, February Draft report.

Miller RW and Gardiner DT. 2001. Soils in our environment. Prentice Hall: Upper Saddle River, New Jersey.

Milliken, G. A., and D. E. Johnson. 1984. The Analysis of Messy Data. Volume I: Designed Experiments. Van Nostrand Reinhold Company, New York.

National Fire Plan. 2002. National fire plan web site www.fireplan.gov/index.cfm

Nyhan, J.W., L.W. Hacker, T.E. Calhoun, D.L. Young. 1978. Soil survey of Los Alamos County, New Mexico. Los Alamos Scientific Laboratory Report LA-6779-MS, Los Alamos, NM.

Nyhan, J.W., S.W. Koch, R.G. Balice, and S.R. Loftin. 2001. Estimation of soil erosion in burnt forest areas of the Cerro Grande fire in Los Alamos, New Mexico. Los Alamos National Laboratory report LA-UR-01-4658.

Paine, R.T., M.J. Tegner, and E.A. Johnson. 1998. Compound perturbations yield ecological surprises. Ecosystems 1:535-545.

Pickett STA, White PS. 1985. The ecology of natural disturbance and patch dynamics. Academic Press: San Diego, CA.

Pimental D. 2000. Soil as an endangered ecosystem. Bioscience 50:947.

Pinder JE, Whicker JJ, Breshears DD. 2004. Effects of the Cerro Grande fire on Ponderosa pine forests and recovery of the forest floor at LANL. Los Alamos National Laboratory report LA-UR-04-2495.

Pye K. 1987. Aeolian dust and dust deposits. Academic Press: London, UK.

Quam L. 2004. Personal communication.

Reeder JD, Schuman GE, Bowman RA. 1998. Soil C and N changes on conservation reserve program lands in the Central Great Plains. Soil and Tillage Research 47:339-349.

Reice SR. 2001. The silver lining: the benefits of natural disasters. Princeton University Press, Princeton, New Jersey, USA.

Rishel J, Johnson S, Holt D. 2003. Meteorological monitoring at Los Alamos. Los Alamos National Laboratory Report LA-UR-03-8097.

Rodgers P. 1996. Disturbance ecology and forest management: a review of the literature. United States Department of Agriculture, Forest Service, Intermountain Research Station, General Technical Report INT-GTR-339.

Selmants, P.C., A. Elseroad, and S.C. Hart. 2003. Soil and nutrients. In: Friederici P. (ed), Ecological Restoration of Southwestern Ponderosa Pine Forests. Island Press, Washington D.C..

Shao Y, McTainsh GH, Leys JF, Raupach MR. 1993. Efficiencies of sediment samplers for wind erosion measurement.Austrailian Journal of Soil Research 31: 519-532.

Shirato Y, Taniyama I, Zhang TH. 2004. Changes in soil properties after afforestation in Horqin sandy land, North China. Soil Sci. Plant Nutr. 50:537-543.

Skidmore EL. 1994. Wind erosion. In: R. Lal (ed.). Soil Erosion and Research Methods, 2nd Edition, pp. 265-293. Soil and Water Conservation Society and St. Lucie Press, Ankeny, IA.

Sterk G, Herrmann L, Bationo A. 1996. Wind-blown nutrient transport and soil productivity changes in southwest Niger. Land Degradation & Development 7:325-335.

Sterk G, Riksen M, Goossens D. 2001. Dryland degredation by wind erosion and its control. Annals of Arid Zone 41:351-367.

Stout, J.E., and T.M. Zobeck. 1996. The Wolfforth field experiment: a wind erosion study. Soil Science 161:616-632.

Stull RB. 1988. An introduction to boundary layer meteorology. Kluwer Academic Publishers: Dordrecht, The Netherlands.

Tongway, D.J., and J.A. Ludwig. 1997. The conservation of water and nutrients within landscapes, Chapter 2 In: Ludwig, J., Tongway, D., Freudenberger, D., Noble J. and Hodgkinson K. (eds), Landscape Function and Management: Principles from Austrailia's Rangelands. CSIRO Publishing, Melbourne, Austrailia, pp. 13-22.

Toy TJ, Foster GR, Renard KG. 2002. Soil erosion: process, prediction, measurement, and control. John Wiley & Sons: New York, NY.

Van Pelt RS, Zobeck TM. 2004. Chemical constituents of fugitive dust. UNPUBLISHED.

Wardle, D.A., R.D. Bardgett, J.N. Klironomos, H. Setälä, W.H. van der Putten, and D.H. Wall. 2004. Ecological linkages between aboveground and belowground biota. Science 304:1629-1633.

Whicker JJ, Breshears DD, Wasiolek PT, Kirchner TB, Tavani RA, Schoep DA, Rodgers JC. 2002. Temporal and spatial variation of episodic wind erosion in unburned and burned semiarid shrubland. Journal of Environmental Quality 31: 599-612.

Whicker JJ, Pinder JE, Breshears DD. 2005. Increased wind erosion from forest wildfire: implications for contaminant-related risks. Los Alamos National Laboratory Report LA-UR-05-0741.

Whitford, W.G., A.G. DeSoyza, J.W. Van Zee, J.E. Herrick, and K.M. Havstad. 1998. Vegetation, soil, and animal indicators of rangeland health. Environmental Monitoring and Assessment 51: 179-200.

Woodruff NP, Siddoway FH. 1965. A wind erosion equation. Soil Science Society of America Proceedings, 29:602-608.

Zobeck, T.M., D.W. Fryrear, and Pettit, R.D. 1989. Management effects on wind-eroded sediment and plant nutrients. Journal of Soil and Water Conservation, March-April:160-163.

Zobeck TM, Sterk G., Funk R, Rajot JL, Stout JE, Van Pelt RS. 2003. Measurement and analysis methods for field-scale wind erosion studies and model validation. Earth Surface Processes and Landforms 28:1163-1188.

Table 3.1. Results from measurements of tree densities and canopy cover in the various burn types.

Burn Type	Plot type	N plots	Unthinned Mean ± Std	Post-thin Mean ± Std	Unthinned Minimum	Thinned Minimum	Unthinned Maximum	Thinned Maximum
			Tree Densities (trees per ha)					
Unburned-control	Primary	5	1280 ± 455		700		1900	
	Secondary	4	50 ± 58		0		100	
Unburned-thinned	Primary	10	410 ± 623	110± 88	0	0	2100	300
	Secondary	7	1400 ± 719	200 ±129	200	0	2300	400
Burned-control	Primary	5	400 ± 255		200		800	
	Secondary	4	350 ± 129		200		500	
Burned-thinned	Primary	10	980 ± 394	410 ±288	400	0	1600	900
	Secondary	7	757 ± 435	243 ±140	100	100	1400	500
			Canopy Cover (percent)					
Unburned-control	Primary	15	77.9 ± 14.1		56		96	
	Secondary	12	46.0 ± 28.4		8		96	
Unburned-thinned	Primary	22		39.5 ± 21.6		0		76
	Secondary	14		33.1 ± 19.2		0		72
Burned-control	Primary	15	36.2 ± 29.6		0		88	
	Secondary	12	21.7 ± 17.1		0		48	
Burned-thinned	Primary	22		21.2 ± 17.6		0		56
	Secondary	14		29.1 ± 15.4		0		56

Table 3.2. Litter cover, vegetation cover and total cover (%) on the ground surface in thinned and unthinned sites in unburned and Moderate burn areas of Ponderosa pine forest. Data are means of measurements of 9 or 10 samplers at primary sites and 7 samplers at secondary sites. Samples collected during 2002 for the primary thinned unburned site and corresponding unthinned site and during 2003 for the secondary thinned unburned site, the primary thinned moderate burn site, the secondary thinned moderate burn site and corresponding unthinned sites

Ground Cover Type	Unburned				Moderate Burned			
	Unthinned		Thinned		Unthinned		Thinned	
	n	Mean±1 Std	n	Mean ±1 Std.	n	Mean±1 Std	n	Mean±1 Std
Litter	34	98.3 ± 3.6	17	77.1 ± 15.5	16	79.9 ± 18.0	17	61.6 ± 23.7
Vegetation	34	5.3 ± 5.8	17	11.5 ± 11.9	16	12.3 ± 11.4	17	6.3 ± 10.4
Total	34	98.2 ± 3.9	17	85.6 ± 11.0	16	82.4 ± 13.7	17	64.4 ± 19.2

Table 3.3. Summary statistics for measured horizontal mass flux (units of g m^{-2} d^{-1}) within thinning and burned treatments. This table is complimentary to Table 4, but statistics below are based on all sampling periods, including those periods with precipitation.

		Unburned						Burned					
		Primary			Secondary			Primary			Secondary		
		25cm	50cm	100cm	25cm	50cm	100cm	25cm	50cm	100cm	25cm	50cm	100cm
Unthinned	Median	0.50	0.55	0.50	0.86	0.94	0.94						
	Minimum	0.14	0.29	0.14	0.29	0.33	0.33						
	Maximum	2.15	1.91	1.63	1.46	1.46	1.62						
	Collection period: 3/26/02 to 7/5/02												
	Median	0.57	0.62	0.71	0.83	0.89	0.94	1.46	1.87	2.13	1.10	1.14	1.29
	Minimum	0.11	0.14	0.08	0.17	0.25	0.25	10.44	0.17	0.71	5.22	0.43	0.57
	Maximum	3.89	2.89	4.33	4.33	3.42	2.89	0.08	7.50	6.67	0.42	3.50	4.17
	Collection period: 3/26/03 to 7/5/03							Collection period: 3/26/03 to 7/5/03					
		25cm	50cm	100cm	25cm	50cm	100cm	25cm	50cm	100cm	25cm	50cm	100cm
Thinned	Median	1.33	1.33	0.94									
	Minimum	0.50	0.57	0.06									
	Maximum	4.38	2.14	1.76									
	Collection period: 3/26/02 to 7/5/02 (year 1 post-thin)												
	Median	0.96	1.00	1.00	1.29	1.07	0.85	3.23	2.29	1.77	2.08	1.78	1.75
	Minimum	0.17	0.14	0.17	0.43	0.29	0.29	0.57	0.42	0.42	0.75	0.57	0.57
	Maximum	4.22	3.83	111.80	60.00	6.33	6.78	76.89	15.22	35.00	25.22	7.00	4.33
	Collection period: 3/26/03 to 7/5/03 (year 2 post-thin)							Collection period: 3/26/03 to 7/5/03 (year 1 post-thin)					

Table 3.4. Summary statistics for measured horizontal mass flux (units of g m^{-2} d^{-1}) within thinning and burned treatments. Statistics are based on sampling periods with no precipitation.

		Unburned						Burned					
		Primary			Secondary			Primary			Secondary		
		25cm	50cm	100cm	25cm	50cm	100cm	25cm	50cm	100cm	25cm	50cm	100cm
Unthinned	Median	0.43	0.50	0.50	1.00	1.00	1.08						
	Minimum	0.14	0.28	0.14	0.50	0.57	0.71						
	Maximum	0.67	0.69	0.92	1.46	1.46	1.63						
	Collection period: 3/26/02 to 7/5/02												
	Median	0.47	0.44	0.50	0.73	0.79	0.73	1.31	1.69	1.88	0.92	1.00	1.11
	Minimum	0.11	0.29	0.14	0.29	0.29	0.43	0.71	1.00	0.71	0.43	0.57	0.57
	Maximum	0.83	0.71	0.83	1.29	1.00	1.14	3.00	3.67	4.56	1.29	2.00	1.86
	Collection period: 3/26/03 to 7/5/03							Collection period: 3/26/03 to 7/5/03					
		25cm	50cm	100cm	25cm	50cm	100cm	25cm	50cm	100cm	25cm	50cm	100cm
Thinned	Median	1.30	1.30	0.96									
	Minimum	0.50	0.57	0.06									
	Maximum	1.93	2.14	1.69									
	Collection period: 3/26/02 to 7/5/02 (year 1 post-thin)												
	Median	0.75	0.86	1.00	0.88	0.87	0.76	2.18	2.00	1.49	1.67	1.50	1.52
	Minimum	0.43	0.14	0.29	0.43	0.29	0.29	0.71	0.57	0.57	0.75	0.57	0.57
	Maximum	1.71	1.33	1.33	2.29	1.17	1.00	6.71	3.00	2.57	2.67	2.71	2.00
	Collection period: 3/26/03 to 7/5/03 (year 2 post-thin)							Collection period: 3/26/03 to 7/5/03 (year 1 post-thin)					

Figure 3.1. Box and whiskers plot of the horizontal mass flux categorized by thinning/burn category for each sampling height. Data shown is for dry periods only.

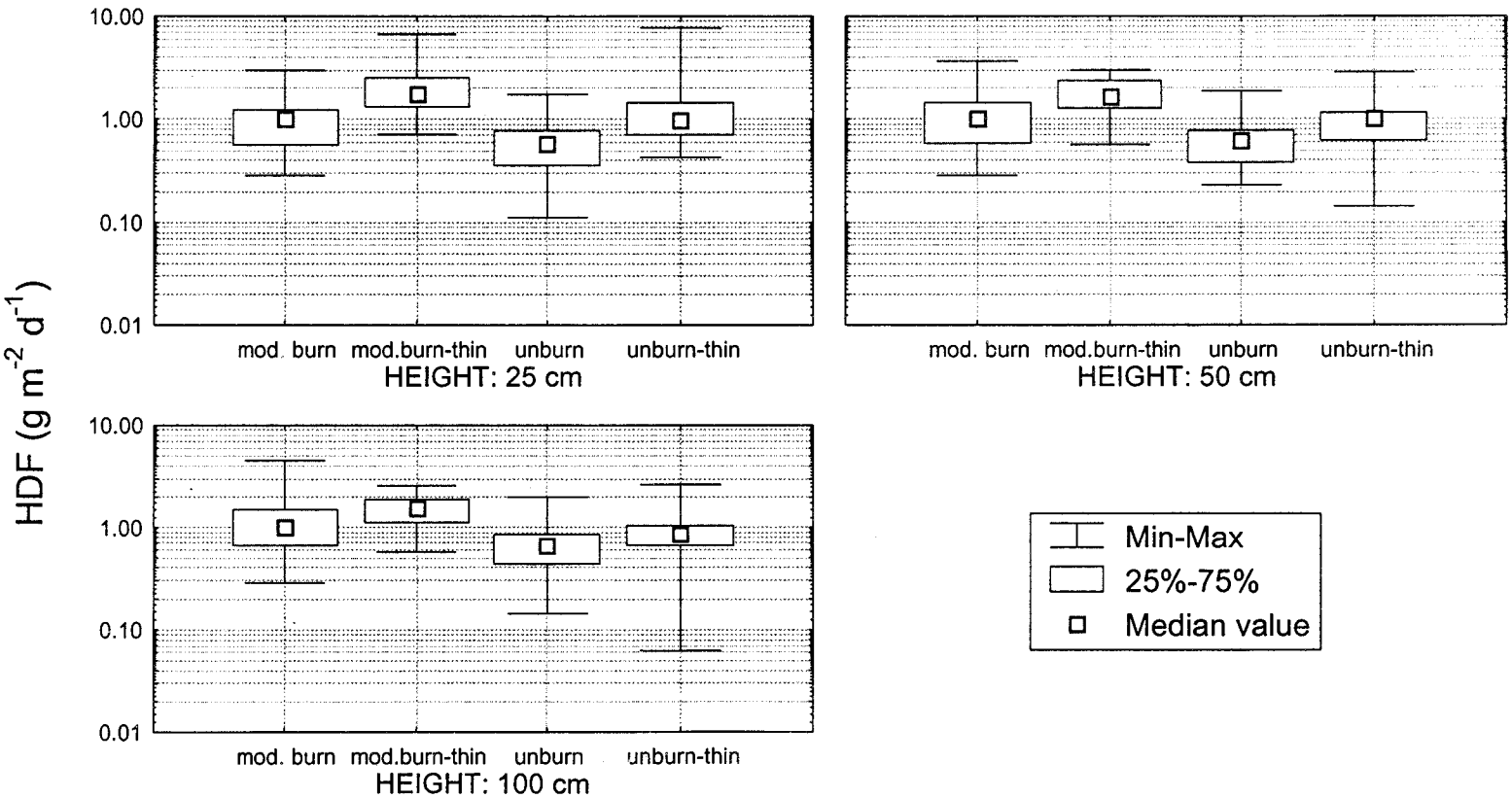

Figure 3.2. Mean horizontal dust flux in each of the burn/thin experimental categories through time during the years 2001-2002 (top) and 2003 (bottom). Data is from samplers at 1-m.

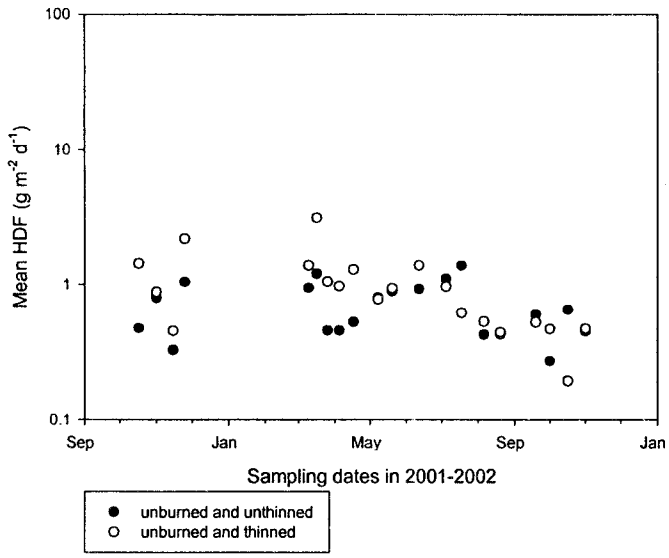

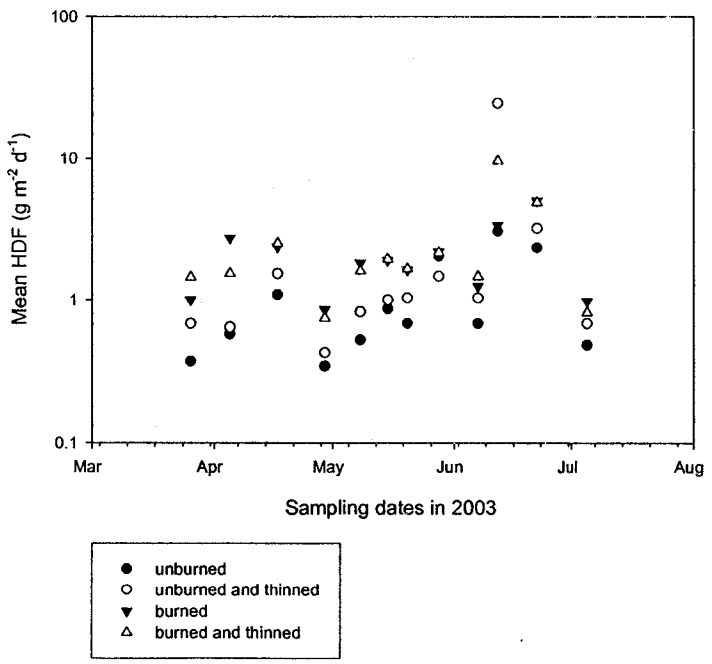

Figure 3.3. Mean horizontal dust flux at 1 m as a function of the percent cover of live tree and ground cover.

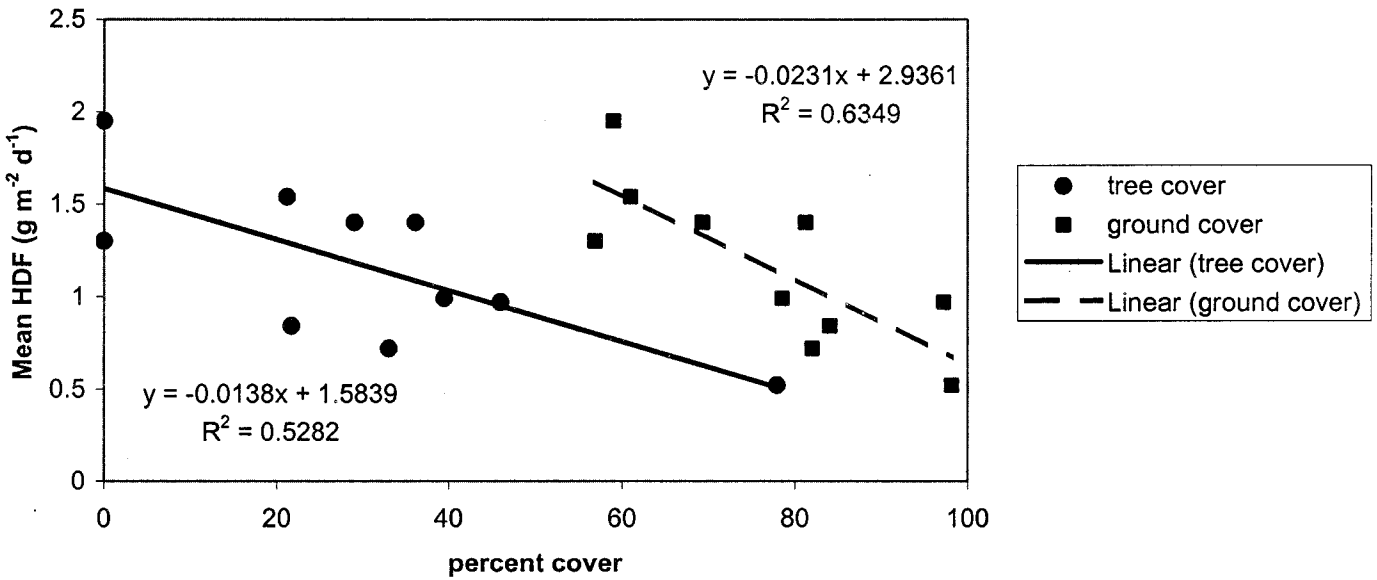

Chapter 4

Partition Coefficients (K_d) for Uranium in Size- Selected Surface Soils

4.0 Abstract

Fundamental to the environmental mobility of newly deposited depleted uranium (DU) is the biogeochemistry of DU in surface soil. Specifically, the rate a radionuclide is transported downward through surface soil determines its availability for transport through soil erosion. Further, DU can preferentially adsorb onto smaller soil particles, such as clays and soil organic material, which are most susceptible to wind erosion and airborne transport to off-site populations. Therefore, measurement of the partition coefficient (K_d) for uranium in soils from Los Alamos National Laboratory was done using an EPA-based protocol for both whole soil and the fine soil fraction (diameters < 45 μm). The 7-day K_d values, which are those specified in the EPA protocol, ranged from 276-508 mL g^{-1} for whole soil and from 615-2249 mL g^{-1} for the fine soil fraction. The 30-day values were twice the 7-day values. Rates of adsorption of ^{238}U to soil from solution were derived using a 2-component (FAST and SLOW) exponential loss model. Estimated loss rate constants for fine soil were generally faster relative to whole soil and varied across the two sampling sites, especially for the FAST component. The significant variation in soil-solution exchange kinetics among the soils promotes the use of site-specific data for estimates of environmental transport rates and

suggests possible differences in desorption rates from soil to solution (e.g., into groundwater or lung fluid) among the soils. Finally, we present evidence of generally unexplored relationships between wind erosion, soil characteristics, and K_d values.

4.1 Introduction

The Department of Energy (DOE) manages numerous sites that have large areas with low levels of radioactively contaminated soils (NAS 1989). One specific concern at the DOE managed Los Alamos National Laboratory (LANL) are soils contaminated with environmentally mobile depleted uranium (DU) that is produced by test explosions (Fresquez et al. 1998, LANL 2002). Explosions disperse DU across soil surfaces as larger shrapnel and smaller aerosol particles where they may constitute a potential ecological and human hazard, not only at LANL, but also across landscapes where there has been heavy use of DU munitions during war times (WHO 2001).

Deposited DU particles can remain on the soil surface where they are subject to wind and water erosion or they can be transported downward through the soil profile and become available for ground water transport or plant uptake (Breshears et al. 1993). Figure 4.1 shows these three possible and potentially competing pathways (Breshears et al 2003). For example, radionuclides that have low affinities for binding to soil particles remain in the soil water and have higher vertical migration rates. With sufficient water infiltration, these radionuclides quickly pass downward in the soil profile and become less available for transport through wind and water erosion (e.g., tritiated water), but are transported more readily into groundwater flows. Conversely, radionuclides that have a high affinity for binding to soil stay on or near the soil surface

and are more subject to transport by wind and water erosion (e.g., ^{137}Cs), especially in arid or ecologically disturbed locations where the vegetation cover is low (Shinn et al. 1989, Whicker et al. 2002a, Johansen et al. 2003, Whicker et al. 2004a, Whicker et al. 2005a).

A key parameter that describes the propensity for radionuclides such as DU to migrate downward with infiltrating water or remain on the soil surface is the soil partition coefficient (K_d). A large K_d implies rapid adsorption and retention of a radionuclilde onto soil particles with subsequent availability for erosional transport. A small K_d implies little retention by surface soils and more rapid downward leaching to ground water. Mathematically, the K_d equals the ratio of the concentration in the solid phase (such as soil) divided by the concentration in the liquid phase with units of mL g^{-1}. For the uranium isotopes of interest at LANL, studies have show that K_d values can range over several orders-of-magnitude and are highly dependent on important characteristics of the soil such as clay content and type, soil pH, and the amount of soil organic material (EPA 1999; Sheppard and Thibault 1990). These soil characteristics are highly variable in time and space and helps explain why K_d values for uranium can range over many orders-of-magnitude. The K_d values are also influenced by the initial chemical form of the uranium, including the oxidation state, and by laboratory protocol such as equilibrium time and whether the K_d measurement is based on adsorption (solution-to-soil) or desorption (soil-to-solution) (EPA 1999).

Beyond straightforward measurement and use of site-specific K_d values for radiological dose assessment, there remain questions regarding the complex relationships between the K_d, soil characteristics, physical processes such as erosion

that alter soils, the resuspension and transport of wind-driven soil, and the biokinetics of soil-bound radionuclides in the human lung. Perhaps because of the lack of information on these complex relationships, radiological dose assessments assume that the transport mechanisms in Figure 4.1 are primarily independent of each other and, in a sense, competing with each other for the transport of the radionuclide (Yu et al. 2001, Breshears et al. 2003). However, there are likely important feedbacks between each of these transport mechanisms, and they are not necessarily independent from each other.

For example, soil erosion, and specific to this study, wind erosion, have been shown to alter important soil characteristics that determine or influence the geochemistry of radionuclides. Wind erosion modifies the soil by preferentially removing soil fines such as those containing organic materials, clay and silt particles, and soil nutrients (Hennessy et al. 1986, Leys 2001, Toy et al. 2002, Lal et al. 2004). The amount of remaining soil fines can have a significant impact on the partitioning of the uranium in the soil. That is, one could expect that the vertical migration rate (as indicated by the K_d value) could be greater in eroded soils, which will be sandier, contain fewer organics and clays, and an altered pH (Toy et al. 2002, Lal et al. 2004). Also, disturbances to vegetation and soil surfaces dramatically increase mobility of radioactive and chemical contaminants through soil erosion (Larney et al. 1999, Johansen et al. 2003, Whicker et al. 2002a, Whicker et al. 2004a, Whicker et al. 2005b), but disturbance also can exacerbate degradation of soil (Toy et al. 2002, Lal et al. 2004) and further alter the rate of vertical migration in the soil. Few studies, if any, have linked these relationships together, even in a preliminary way.

Most measurements of K_d focus on the whole soil (EPA 1999), but it is also important to consider the fine fraction of soil (particles with physical diameter < 45 μm). Radionuclides can concentrate on these fine particles (Whicker and Schultz 1982) and these small soil particles are most available for long-distance transport through wind erosion and are directly inhalable. Therefore, there is a need to assess the adsorption kinetics of uranium to this fine soil fraction relative to the whole soil, and ultimately to relate these findings to wind transport and lung solubility.

Specific to this study, greater airborne concentrations of depleted uranium (DU) have been recently observed at Los Alamos National Laboratory (LANL), especially in areas near the firing sites (LANL 2002), and the timing of the increases corresponds to documented increases in wind erosion of soil in burned and recently thinned ponderosa pine forest areas (Whicker et al. 2002a, 2003, 2004b). Because of the potential for DU exposures to workers and the public, there was a need to measure the K_d values for total soil and for the fine fraction of soil, which is most susceptible to wind erosion, long-distance transport, and inhalation.

4.2 Methods

4.2.1 General characteristics of forest sampling sites

The study sites are located in the Jemez Mountains in North Central New Mexico (at general area coordinates of 35°52 N; 106°21' W) and at an elevation of about 2300 m. These areas are along the western edge of Los Alamos National Laboratory, and located about 10 km southwest of Los Alamos, NM. Average annual precipitation in the area is about 500 mm (Bowen 1990). Woody vegetation is

comprised mostly of ponderosa pine (Pinus ponderosa Laws. Var. Scopulorum Engelm.; nomenclature follows Martin and Hutchins, 1980) and gamble oak (*Quercus gambelii*). Ground vegetation consists of a variety of grasses and flowering plants (Foxx and Hoard 1995).

Because of restricted access to the explosives testing areas, which contain soils contaminated with depleted uranium, uncontaminated soils were collected at two representative LANL locations, both about five km north of the testing areas. The two sampling sites (Site 1 and Site 2) were separated by about 750 m, and the selected locations were generally similar to the firing sites in terms of dominant vegetation, elevation, topography, and meteorological conditions. The two sites differed in that the Site 1 soil occurred near the bottom of a long, gentle slope and had greater vegetation cover, which could lead to an enrichment in fine material such as silts and clays through fluvial and aeolian sedimentation. Site 2 soils occurred on a ridge top where the fine soil materials were more likely to be lost through erosion.

4.2.2 Soil collection methods

Because one of the goals of this and companion studies was to investigate the mobility of depleted uranium in the surface soils, only the top 2 cm of the soil profile was collected. The surface soil was collected from 5 randomly located plots at the Site 1 location and from three randomly selected plots at the Site 2 location. Twenty soil cores of 38 mm diameter were obtained at each sampling location, air dried, then composited.

4.2.3 Sample preparation and K_d measurements

The soil was air-dried and a 200 g sample from each sampling location was submitted to the Soil, Water, and Plant Testing Laboratory at Colorado State University for characterization. Analysis of soil texture was performed using a hydrometer method (Gee and Bauder 1986) and reported as the percent by mass of sand, silt, and clay (Miller and Gardiner 2001). Particle sizing was also performed to determine the percent of the particles that would be suspendable and respirable (i.e., those with aerodynamic diameters <10 μm) using a modified pipette method (Indorante et al., 1990). The soil pH was measured by creating a soil paste by saturating the soil with deionized water, waiting 24 hours, then measuring the pH of the paste. The content of organic matter in the soil was measured using the Modified Walkely Black Method (Workman et al 1988). Sub samples of the fine fraction of the soil (< 45 μm in physical diameter) were separated from each of the Site 1 and 2 soils using a mechanical sieve to study the partitioning dynamics for the smaller soil particles that provide most of the available surface area for adsorption. Clay mineralogy was also investigated using x-ray diffraction techniques because of the varying cation exchange capacity between different clay types.

Measurement of the Kd

K_d measurements were made according to EPA protocol (EPA 1999) with ^{238}U in uranyl nitrate solution in the +VI oxidation state. The +VI form would be expected

from slow oxidation of DU on particle surfaces over time, but some of the larger DU particles may not have fully oxidized and would be in the +IV oxidations state, which is less soluble than the +VI form (EPA 1999). The assumption that the DU in soil is in the +VI state should result in estimates of greater solubility, lower K_d values, and faster infiltration through the soil profile with water flow relative to +IV form.

One-gram soil samples were placed into 50 mL plastic test tubes and combined with 30 mL of a 165,000 ppm ^{238}U solution of UNO_3 at a pH of 5.5. The soil-solution mixtures were agitated using a mixing wheel and the solutions sampled at intervals of 0.17 d (4hrs), 1 d, 2d, 7 d, 10 d, 15d, 20 d, and 30 d. Two tubes of Site 1 and two tubes of Site 2 soil were sampled at each interval. Soil and solution were separated by centrifugation and the supernatant tested for pH, passed through a 0.45 μm filter, and submitted for ICP-MS analysis. The amount of ^{238}U in the soil was calculated as difference in the total ^{238}U in the original spike (165,000 ppm) minus the amount of ^{238}U measured in the solution for each time period. Blanks and spiked solutions were submitted for laboratory analysis to assess laboratory procedures. Results for blanks were < 0.002% of the spike amount and the measurements for the spiked solutions were < 0.3% of the spike.

The partition coefficient values for each measurement time ($K_d(t)$) were calculated using the formula:

$$K_d(t) = \frac{^{238}U(t)_{soil}}{^{238}U(t)_{solution}}, \qquad (1)$$

where $^{238}U(t)_{soil}$ is the uranium concentration in the soil at time t, and $^{238}U(t)_{solution}$ is the uranium concentration in the solution at time t. The results are reported in the units of mL g^{-1}.

4.3 Results

4.3.1 Soil characteristics

Characteristics of the soils from the two sites are given in Table 4.1. The table shows that the soils from the two sites are different, with Site 1 having greater pH, percent soil organic material, and fine soil fraction (as shown by greater clay and silt percentages). The distributions of clay particles and inhalable particles (< 10 μm) at the two sites are shown in Figure 4.2 and were statistically different by a Mann-Whitney test ($P \leq 0.05$) (StatSoft 1994). The differences are consistent with the expectation from field observations that Site 1 could be a place where fine materials accumulate and Site 2 a place where fine materials could be eroding away.

4.3.2 K_d measurement results

The results generally show that 1) the K_d values for the fine fraction of soil were higher in almost all cases than the whole soil, 2) K_d values for Site 1 location were higher than the Site 2 location for the fine soil fraction and for the whole soils through about day 15, after which the K_d values for the whole soil were approximately equal, and 3) that the K_d value may not have been reached full equilibrium after 30 days (Table 4.2 and Figure 4.3).

Equilibrium levels of adsorption of ^{238}U to whole soil, as indicated by the 30-d K_d mean value, were statistically equal at values of 1057 ± 180 mL g^{-1} and 1074 ± 2 mL g^{-1} for the Site 1 and Site 2 soils, respectively. However, the EPA prescribed day-7 values showed higher K_d values of 493 ± 21 mL g^{-1}at Site 1 relative to those at Site 2 at 318 ± 59 mL g^{-1}. These 7-day K_d values are consistent, but on the low end of those reported for other soils where the pH in the K_d measurement tubes was 5.5 (EPA 1999).

As with the results for the whole soil, the measured K_d values for the fine fraction increased rapidly during the first 10 days but the rate of increase slowed dramatically after 15 days. The 30-d equilibrium K_d value for U in the fine fraction of LANL soils was 3318 ± 66 mL g^{-1} for the Site 1 location and 795 ± 3 mL g^{-1} for the Site 2 location. The average single-point estimates of the EPA 7-day K_d values were approximately 2249 mL g^{-1} and 615 mL g^{-1} for the Site 1 and 2 locations, respectively.

4.3.3 Adsorption model results

The dramatic change in K_d values with time (Figure 4.3) is important for predicting uranium transport in the environment following a release. Figure 4.4 shows a time-series plot of natural log of the ^{238}U concentration in solution for the Site 1 and 2 locations in whole soil (Figure 4.4a) and the fine fraction (Figure 4.4b). These plots suggest that there is a very rapid adsorption that occurs in the first hours and then a more moderate adsorption rate after the first day.

The adsorption rates were modeled as a simple two-component exponential with a "FAST" and a "SLOW" phases, though more phases could be determined through more intensive sampling, especially in the earliest phases. The adsorption rate constant

for the FAST phase was calculated using measurements in the first day only (t = 0, 0.17, and 1 day), and the adsorption rate for the SLOW phase was calculated for measurements made after the first day. Table 4.3 shows the calculated loss rate constants categorized by sampling location (Sites 1 and 2) and soil type (whole or fine). As reflected in the K_d values, the results suggest that 1) the rate constants are higher for the FAST component in the fine soil relative to the whole soil, 2) adsorption rates for the FAST phase is roughly between 1 and 2 orders-of-magnitude higher than the SLOW phase, and 3) the rate constants for the FAST phase are higher at Site 1 relative to Site 2. Experimental limitations precluded multiple measurements, which would have allowed for more definitive statistical comparisons in adsorption rates.

4.4 Discussion

First, this study quantified K_d values for ^{238}U in surface soils collected from areas roughly similar in location, elevation, vegetation, geology and topography to those LANL sites with DU contamination. The K_d values were within the range of those reported by the EPA (EPA 1999) for pHs between 4 and 5, though the range of reported values is quite large (0.4 up to 160,000). The K_d values were high enough to suggest that deposited DU would remain on the soil surface and generally be available for transport through erosion processes for long periods. Second, the results document the temporal variation in K_d measurements. The measured K_d values increased quickly through about day 10 to 15, then the rate of increase in K_d slowed through day 30. The 7-day K_d values were less than the 30-day values by factors of 2.2 to 3.4 in the whole soil and 1.3 to 2.4 in the fine soil fraction. In some cases, the data showed that the K_d

may not have reached full equilibrium even after 30 days, so this must be considered when using reported K_d values in dose assessments. **Third**, the net adsorption rates of ^{238}U were modeled. The adsorption data suggested a two-component model with FAST and SLOW phases, and the loss rate constants for each phase estimated. The modeling suggested faster adsorption in the fine soil fraction relative to the whole soil, especially in the FAST phase. The presence of fast and slow rates indicates the different adsorption phases with the soils. Each phase probably involves multiple binding sits for uranium. More numerous sampling periods and longer duration measures of K_d may identify more phases and slower binding sites, but the current number of sampling periods and durations is sufficient to indicate rapid and appreciable adsorption and retention in surface soils. **Fourth**, we generally found substantially higher K_d values for the fine fraction of soil compared to the whole soil. This finding was expected because of the much larger available surface area per gram of material for adsorption in the fine fraction of the soil, and the larger amounts of clay and organic material in the fine soil fraction. An exception to this trend is found in the Site 2 soils where the K_d for whole soil appears greater than that for fine soil by day 30. The higher Kd values on day 30 for the Site 2 whole soil which drive this discrepancy in the data suggests that equilibrium in this soil may be slow to reach. **Finally**, we found differences in measured K_d values between Sites 1 and 2; however, it was not possible to identify the specific cause (such as clay content) because the two soils differed in several parameters. These findings have several important implications for health physicists and environmental scientists.

4.4.1 Implications for dose assessment and site-specific measurement of K_d

Key to the accuracy and credibility of the dose assessment is new knowledge of the kinetics of the DU in the local soils (EPA 1999) as well as the solubility of the soil-bound DU in the lung (Eidson 1989, 1994; NCRP 1997). The differential partitioning of uranium between the solid and liquid phases in fine and whole soil found in this study is an important consideration for dose assessments from inhaled uranium because 1) the uranium may concentrated in fine fraction of the soil, 2) the fine soil fraction will be preferentially resuspended by wind and transported to off-site populations, and 3) the solubility of soil-bound uranium in lung fluid is uncertain.

The lung solubility of the soil-bound uranium resuspended from a site could be very different from values reported in other studies that used uranium in other chemical and physical forms (NCRP 1997). Therefore, it is important to measure the solubility of the soil-bound uranium in lung fluid for estimating dose. Further, differences in soil characteristics among sites also suggest the possibility of differential lung solubility across sites. Specific to this study, the differences in adsorption rates of the FAST and SLOW phases in the fine soil fraction of soils collected at the Site 1 and 2 locations imply the possibility of differences in desorption rates into lung fluid. For example, the slower adsorption rate of the resuspendable fine soil fraction from the Site 2 location suggests greater lung solubility for these soils relative to Site 1. Note that these predicted differences are directly inferred from the modeled kinetics of the phases and not the simple estimate of K_d.

Though not generally explored, the variability soil characteristics and related K_d measurements between Sites 1 and 2 argues for performing K_d measurements with soils

taken at multiple locations to assess this variability at relevant spatial scales. There are several possible explanations for the difference in K_d across the two sites including pH, soil size, and organic content (EPA 1999), and each of these factors can be altered through erosion (Hennessy et al. 1968, Toy et al. 2002, Lal et al. 2004). Although the specific causative factor cannot be identified, the relative magnitudes of the K_d are consistent with the assessment that Site 1 may be an area of fluvial and aeolian accumulation while Site 2 could be an area of potential erosion of fine materials. This idea is supported by measurements of wind-driven horizontal dust flux (HDF)(Whicker et al. 2005a), which shows a consistently higher HDF at Site 2 relative to Site 1 (Figure 4.5). This may account for the differences in whole soil K_d but cannot directly explain the large differences in K_d for the < 45 μm soil fractions. These differences imply that the composition of the fine particles had impacts on the uranium K_d that were not obvious from soil measures or clay mineralogy.

4.4.2 Implications for cleanup of depleted urainum contaminated sites

This relatively large K_d values measured in this study suggest that DU at LANL will largely remain in surface soils for long periods if the soil is undisturbed. Regarding decisions concerning cleanup strategies for DU contaminated sites, it is important to ask not simply how to clean them up, but rather whether or not to clean them up at all (Breshears et al. 1993, Whicker et al. 2004). One of the major clean-up options to be considered—physical removal of the soils—is extremely costly and requires virtual destruction of the contaminated ecosystem and the availability of a new site approved to dispose of the contaminated materials that are removed. Soil substrate removal only

translocates the problem, may add significant health risks to the clean-up workers, and may actually enhance the dispersion of contamination in the process (Shinn et al. 1989; Whicker et al. 2004). In contrast, if the long-term risks from DU in surface soils of the environment are sufficiently low, contaminants may be left in place, providing that soil stability, even during extreme events, is adequately demonstrated (Whicker et al. 2005b). For exposure assessment to DU, a thorough understanding of its kinetics in the soils and the variability of such are required, as well as an assessment of lung solubility of the DU under the specific conditions of exposure.

4.5 Conclusions

Adsorption K_d values were measured through time for whole and fine surface soils collected at several sites within LANL. Results suggest 1) rapid adsorption onto soils during the first day, 2) increasing K_d values through time with a 30-day K_d value about twice the 7-day value, 3) generally greater K_d values for the fine soils that are susceptible to resuspension and inhalation, and 4) differences between adsorption kinetics among two sampling sites whose soil characteristics differed, possibly due to impacts of soil erosion.

4.6 References

Bowen BM. Los Alamos climatology. Los Alamos National Laboratory LA-11735-MS; UC-902. National Technical Information Service, Springfield, VA; 1990.

Breshears DD, Whicker JJ, Johansen MP, Pinder JE. Wind and water erosion and transport in semi-arid shrubland, grassland and forest ecosystems: quantifying dominance of horizontal wind-driven transport. Earth Surface Processes and Landforms 28:1189-1209; 2003.

Breshears DD, Whicker FW, Hakonson TE. Orchestrating environmental research and assessment for remediation. Ecological Applications 3: 590-594; 1993.

Eidson AF. The effect of solubility on inhaled uranium compound clearance: a review. Health Phys 67:1-14; 1994.

Eidson AF, Damon EG, Hahn FF, GriffithWC. The utility of invitro solubility testing in assessment of uranium exposure. Radiation Protection Dosimetry 26:69-74; 1989.

Environmental Protection Agency (EPA). Understanding variation in partition coefficient, K_d, values. EPA 402-R-99-004A; 1999.

Foxx TS, Hoard D. Flowering plants of the southwestern woodlands. Los Alamos, NM: Otowi Crossing Press; 1995.

Fresquez PR, Armstrong DR, and Mullen MA. Radionuclides in soils collected from within and around Los Alamos National Laboratory; 1974-1996. Journal of Environmental Science and Health, A33: 263-278; 1998.

Gee GW, Bauder JW. Particle size analysis. In: Klute (ed.) Chapter 15: Methods of Soil Analysis Part 1: Physical and Mineralogical Methods, pgs 383-411. Madison, WI: American Society of Agronomy Inc., Soil Science Society of America Corporation; 1986.

Hennessy JT, Kies B, Gibbens RP, Tomble JM. Soil sorting by forty-five years of wind erosion on a southern New Mexico range. Soil Science Society of America Journal 50:391-394; 1986.

Indorante SJ, Follmer LR, Hammer RD, Koenig PG. 1990. Particle size analysis by a modified pipette procedure. Soil Science Society of America Journal 54:560-563.

Johansen MP, Hakonson TE, Whicker FW, Simanton RJ, Stone JJ. 2003. Pulsed redistribution of a contaminant following forest fire: Cs-137 in runoff. Journal of Environmental Quality 32:2150-2157; 2003.

Lal R, Sobecki TM, Iivari T, Kimble JM. Soil degradation in the United States: extent, severity, and trends. Boca Raton, FL: Lewis Publishers; 2004.

Los Alamos National Laboratory. Environmental surveillance at Los Alamos during 2002. Los Alamos National Laboratory Report LA-14085-ENV;2002

Martin WC, Hutchins CR. A flora of New Mexico. J. Kramer, Germany; 1980.

Miller RW, Gardiner DT. Soils in our environment. Upper Saddle River, NJ: Prentice Hall; 2001.

NAS (Committee to Provide Interim Oversight of the DOE Nuclear Weapons Complex). Nuclear weapons complex: management for health, safety and the environment. Washington, D.C.: National Academies Press; 1989.

NCRP-National Commission on Radiation Protection. Deposition, retention and dosimetry of inhaled radioactive substances. NCRP Report No. 125; 1997.

Shepppard MI, Thibault DH. Default Soil Solid/Liquid Partition Coefficients, K_ds, for four major soil types : a compendium. Health Physics 59: 471-482; 1990.

Shinn JH, Essington EH, Miller FL, O'Farrell TP, Orcutt JA, Romney EM, Shugart JW, Sorom ER. Results of a cleanup and treatment test at the Nevada Test Site: evaluation of vacuum removal of Pu-contaminated soil. Health Physics 57: 771-779; 1989.

StatSoft. 1994. STATISTICA for Windows Volume 1: General conventions and statistics I. StatSoft Release 5.0. Tulsa, OK.

Toy TJ, Foster GR, Renard KG. Soil erosion: processes, prediction, measurement, and control. New York: John Wiley & Sons; 2002.

Whicker FW, Hinton TG, MacDonell MM, Pinder JE, Habegger LJ. 2004a. Avoiding destructive remediation at DOE sites. Science 303:1615-1616; 2004a.

Whicker FW, Schultz V. Radioecology: nuclear energy and the environment. Boca Raton, FL: CRC Press; 1982.

Whicker JJ, Breshears DD, Wasiolek PT, Kirchner TB, Tavani RA, Schoop D, Rodgers JC. Temporal and spatial variation of episodic wind erosion in unburned and burned shrubland. Journal of Environmental Quality 31:599-612; 2002a.

Whicker JJ, Breshears DD, Pinder JE, Mack KN. Wildfire effects on contaminant transport through wind erosion: preliminary results. Proceeding of the 2002 Health Physics Society Midyear Meeting, Orlando, FL; 2002b.

Whicker JJ, Pinder JE, Breshears DD. Increased wind erosion from forest wildfire: implications for contaminant-related risks. Los Alamos National Laboratory Report LA-UR-0741; 2005a.

Whicker JJ, Pinder JE, Breshears DD, Eberhart C. Estimates of increased exposure to contaminated dust following wildfire. Los Alamos National Laboratory Report LA-UR-0742; 2005b.

Whicker JJ, Pinder JE, Breshears DD, Mack KN. Increased contaminant transport through wind erosion following wildfire. Health Physics 84:S206; 2003.

Whicker JJ, Pinder JE; Breshears DD; Baker KN. Secondary effects of thinning in ponderosa pine forests: wind erosion as an ecosystem health metric. Proceedings of the Eighth Symposium on Biological Research in the Jemez Mountains, New Mexico. Santa Fe, NM; 2004b.

Workman SM, Soltanpour PM, Follett RH. Soil testing method used at Colorado State University for the evaluation of fertility, salinity, and trace element toxicity. Agricultural Experiment Station, Department of Agronomy Soil Testing Laboratory and Coopertive Extension. Technical Bulletin LTB88-2; 1988.

World Health Organization (WHO). Depleted uranium: sources, exposure and health effects. Department of Protection of the Human Environment WHO/SDE/PHE/01.1: 2001.

Yu C, Zielen AJ, Cheng J-J, LePoire DJ Gnanapragasam E, Kamboj S, Arnish J, Wallo III A, Williams WA, Peterson H. User's manual for RESRAD Version 6. Argonne National Laboratory report ANL/EAD-4; 2001.

Table 4.1. Characteristics of soil for the Site 1 and Site 2 sampling locations.

	pH	% SOM	% Sand	% Silt	% Clay[a]	Texture class
Site 1	4.8 ± 0	10.2 ± 0.2	34.0 ± 2.1	53.6 ± 1.5	12.4 ± 1.1	Silt loam
Site 2	4.2 ± 0	9.5 ± 1.8	51.3 ± 5.0	39.3 ± 6.7	9.3 ± 2.5	Loam/Sandy loam

[a] X-ray diffraction results show that the dominant clay types were quartz, illite and mica

Table 4.2. Measurement results for K_d values (units mL g^{-1}) through time categorized by soil type and LANL sampling location. Results from multiple measurements are separated by a comma.

	Whole soil		Fine soil	
Day	**Site 1**	**Site 2**	**Site 1**	**Site 2**
0.17	228, 233	136, 138	640, 782	238, 231
1	345, 336	185, 188	1181, 1166	475, 479
2	403, 398	218, 229	1274	521
3			1281	558
7	478, 508	359, 276	2249	615
10	554	657	2757, 2639	663, 683
15	636, 561	562, 572	3151	730
20	1049	769	3137	735
30	929, 1184	1075, 1072	3271, 3365	793, 797

Table 4.3. Calculated loss rate constants for adsorption rates of ^{238}U to LANL soils in units of d^{-1}. The correlation coefficient (r^2) is in parentheses. Estimates are based on a two-compartment model using least-square exponential fits of the concentration of ^{238}U in solution over time.

	Whole soil		Fine soil	
	FAST	**SLOW**	**FAST**	**SLOW**
Site 1	-1.4 (0.44)	-0.03 (0.89)	-2.1 (0.43)	-0.03 (0.65)
Site 2	-1.1 (0.43)	-0.05 (0.89)	-1.8 (0.55)	-0.01 (0.86)

Figure 4.1 Transport processes for soil-bound contaminants.

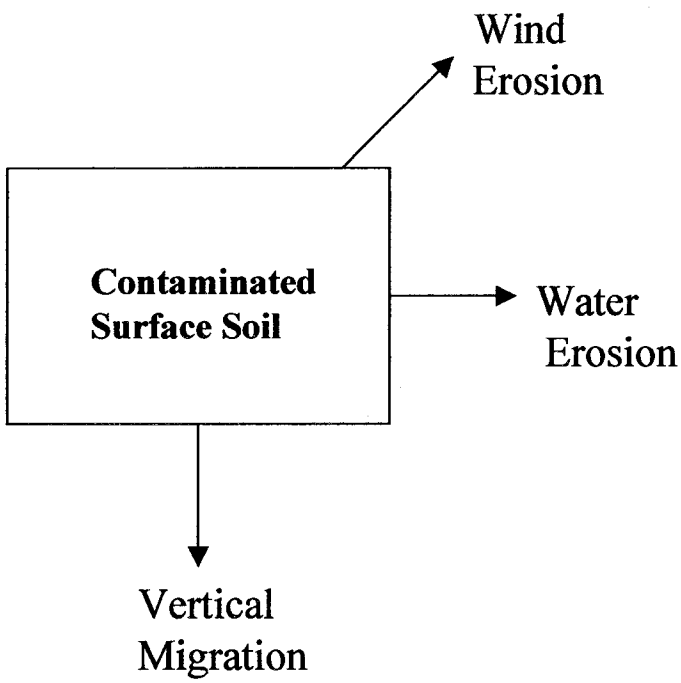

Figure 4.2. Distribution of particle sizes for soils from Sites 1 and 2. Box represents the 25th and 75th percentiles and the solid line represents the median.

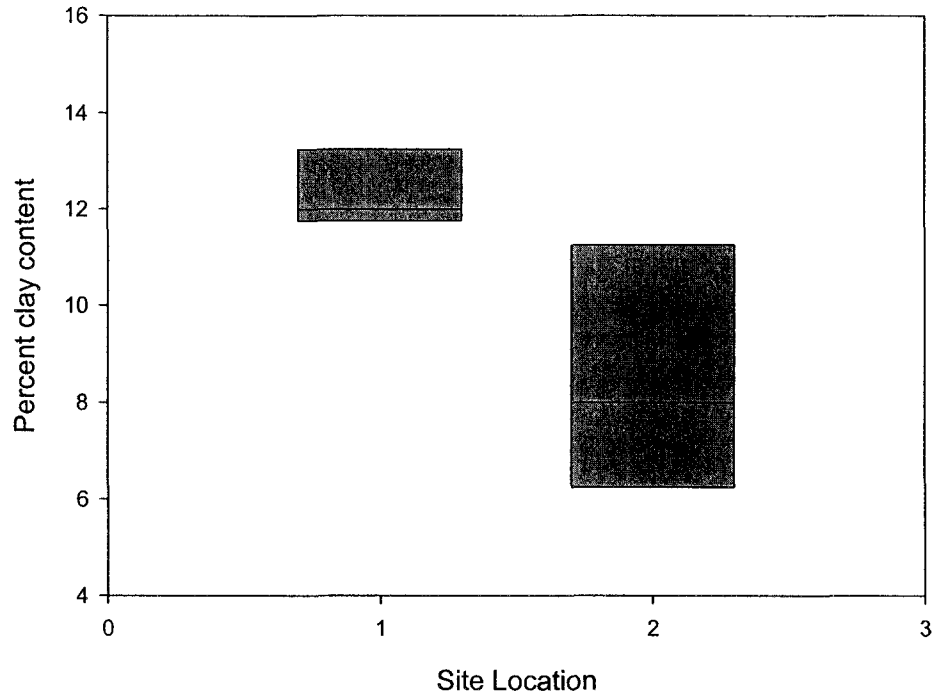

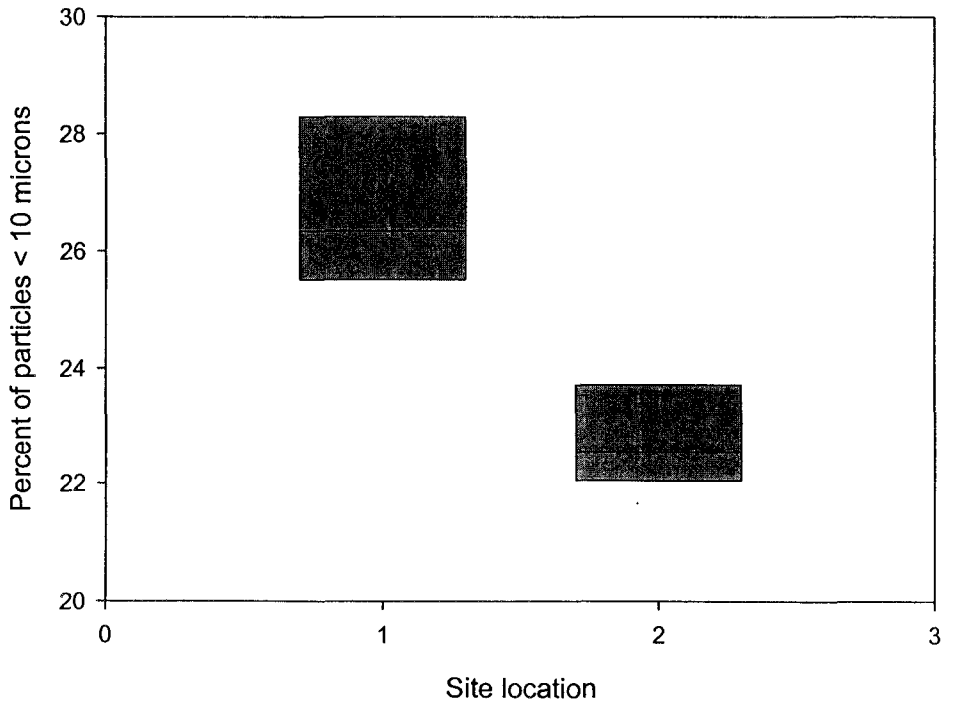

Figure 4.3. Time series of K_d values categorized by sampling location and by whole or fine soil.

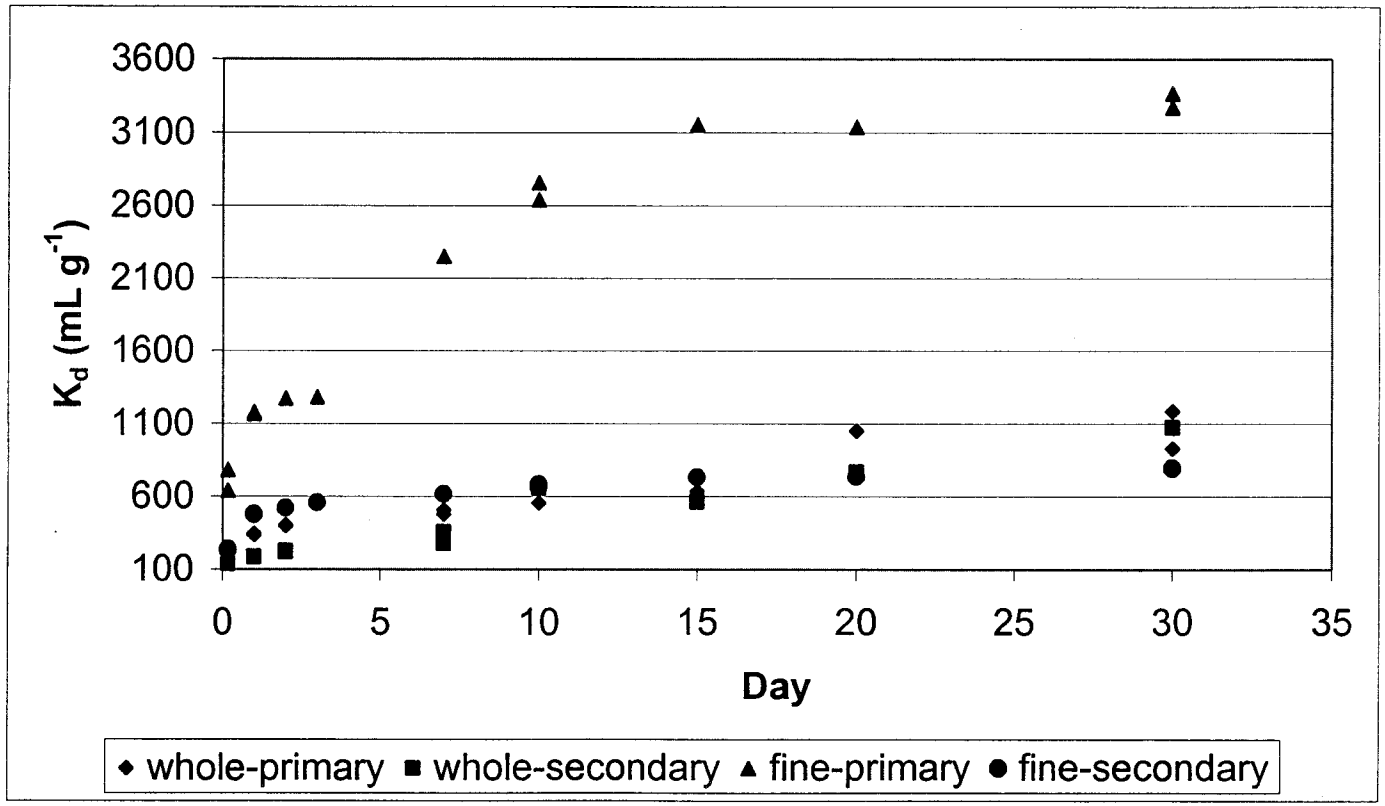

Figure 4.4. Time series of the natural log-transformed concentration of natU in solution for the LANL Primary and Secondary sampling sites for whole soil (a) and for the fine fraction (b).

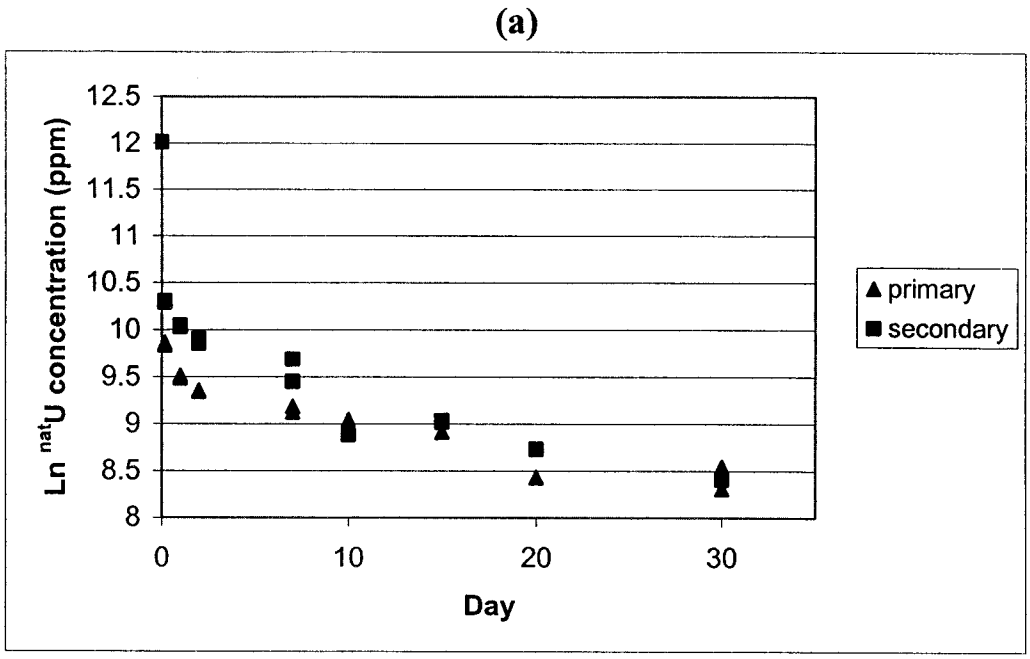

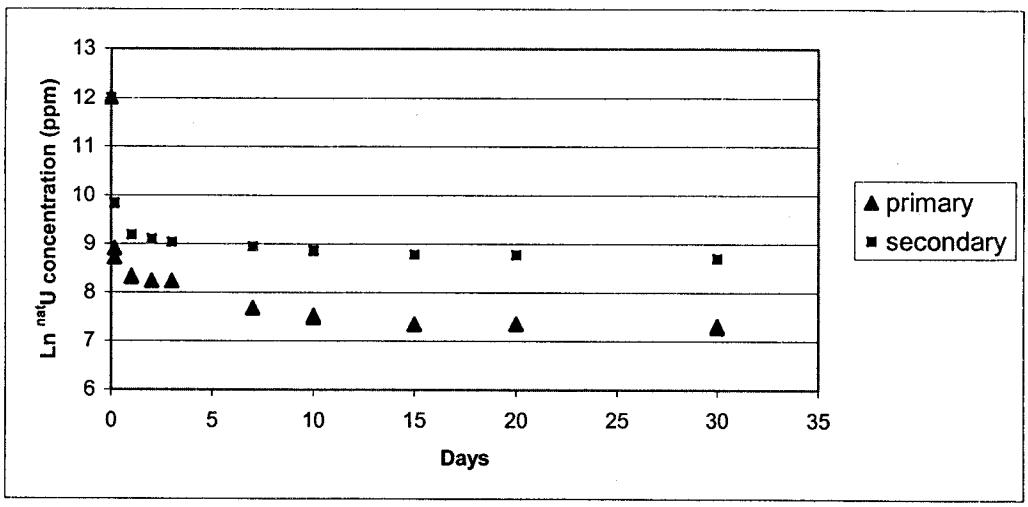

Figure 4.5. Comparison of distributions of horizontal wind-driven dust flux measurements made at Site 1 and 2 sampling locations during dry periods. The box represents the 25th and 75th percentiles, whiskers represent the 10th and 90th percentiles, the solid line represents the median, and the 5th and 95th percentiles are shown as dots.

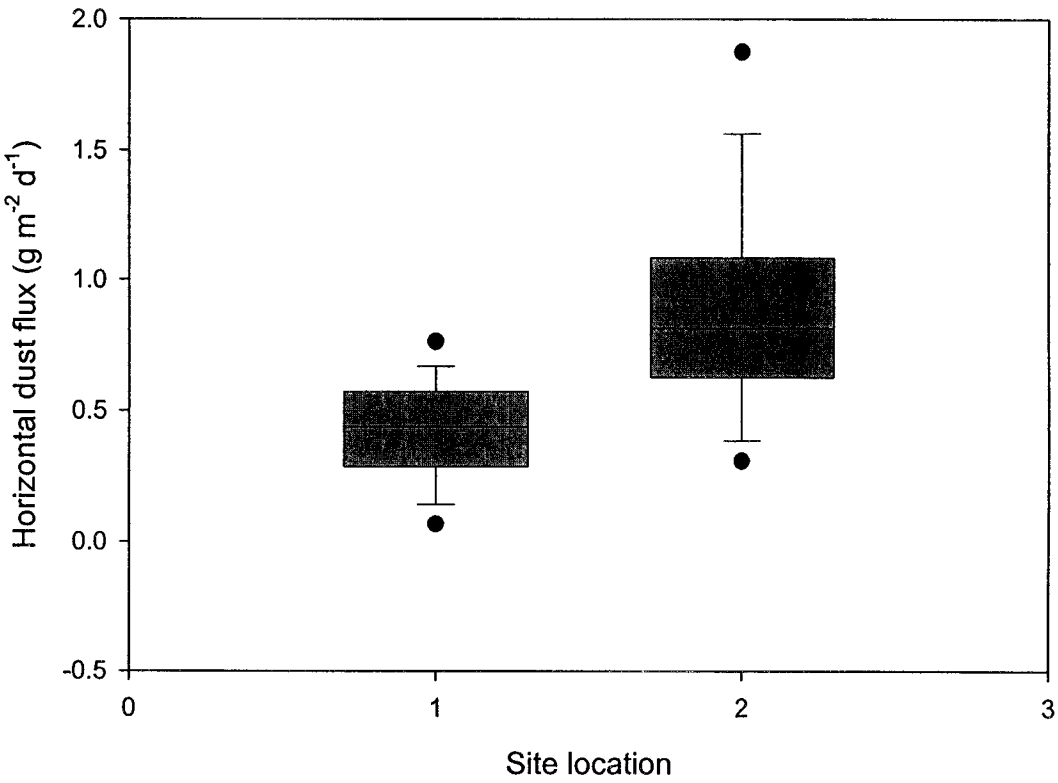

Chapter 5

Estimates of Increased Exposure to Contaminated Dust Following Wildfire

5.0 Abstract

In May of 2000, the Cerro Grande fire burned over roughly 30% of Los Alamos National Laboratory (LANL), mostly in ponderosa pine forest along the western edge of LANL. Some burned areas included soils that contained a variety of contaminants, including depleted uranium (DU). The rapid and dramatic removal of vegetation and litter cover exposed the contaminated soil, thus increasing their environmental mobility through wind and water erosion. Wind erosion is of particular concern because of potential increased inhalation, and is a special concern for LANL workers who work in or near these burned areas. This study used measurements of wind-driven dust flux in severely burned, moderately burned, and unburned areas using passive dust collectors to assess possible increased respirable dust (aerosol with particles less than 10 μm in aerodynamic diameter or PM-10) emissions and associated inhalation doses to LANL workers. Using 1) statistical relationships between dust flux and PM-10 measurements, and 2) the relative amounts of severely burned, moderately burned, and unburned areas, we calculate relative increase of about 1-4% in PM-10 dust emission across the entire LANL resulting from the fire. Calculations of relative inhalation dose from DU suggest a high-end estimate of a 26% increase for LANL workers on severely burned areas.

The suggested increase in worker dose is confirmed by increased DU air concentrations measured at locations within and at the border of LANL. Despite the potential increased doses, the estimated annual dose was < 1 μSv, which is far below the dose limits for occupational or public exposures. These results point out the importance of ecosystem disturbance in increasing mobility of soil-bound contaminants, which ultimately can increase exposure. It is important to investigate the magnitude of the increases when deciding appropriate strategies for long-term stewardship of contaminated lands.

5.1 Introduction

The Cerro Grande fire in May of 2000 burned over 19,000 hectares of forest, including about 3000 hectares within the boundaries of Los Alamos National Laboratory (LANL 2000). Beyond the immediate effects of the fire, there were significant concerns regarding the impact of the fire on increased mobility of radioactive and chemical contaminated LANL soils primarily through wind and water transport. Wind transport of contaminated soils can be of particular concern because wind may carry soil-bound contaminants to neighboring areas where they present an inhalation risk and may enter the food pathway through deposition on plant surfaces (Whicker and Schultz 1982).

Recent measures suggest that concentrations of some radioactive elements in air have increased, both within and outside LANL boundaries since the fire (LANL 2002). While the radioactive air concentrations in the neighboring communities are well-within safe limits (Kraig et al. 2002), there were still unanswered questions regarding the impact of the fire on wind-driven resuspension of radioactive and chemical

contaminants and the potential effects of these increases on exposure levels to LANL workers whose job sites may be near the sources of airborne contaminated dust. In addition, most of these workers are not qualified as being "Radiation Workers" because their estimated annual doses are below the 100 mrem threshold (DOE 1993), therefore, are not part of a bioassay program which would directly assess exposure to the radioactive dusts.

Moreover, the measurements of atmospheric radionuclides are generally made along the perimeter of LANL property and are 1) designed for assessments of public exposures, 2) determined before the fire, 3) more than a km from the heavily burned areas on LANL property, and 4) not always positioned downwind of burned areas. Therefore, additional onsite information on post-fire resuspension rates of soils was needed to better assess the impacts of the fire on dust emissions and subsequent onsite and offsite radiation exposures.

Increases in wind-driven transport of LANL soils resulting from the dramatic reductions in vegetation cover from the fire are not easily estimated from other studies on fire effects. There have few studies on the effects of fire on wind erosion, and these studies have mainly focused on other ecosystems such as rangelands in Texas (Zobeck et al. 1989) and shrublands in Southern New Mexico (Whicker et al. 2002) where disturbance responses may differ markedly from the LANL forests. These studies showed that fire significantly increased wind erosion, but the results of these studies may underestimate those at LANL where the mass and vertical structure of the forest vegetation has a greater effect on wind velocities and soil litter cover. It is also important to consider the possible moderating effect of the remediation done on LANL

severely burned and thinned areas, but the level of effectiveness of these efforts to stabilize the soil remains unknown. Knowledge and consideration of the effects of fire, and follow-up remediation efforts on wind erosion is essential for more accurate assessment of human and ecological risk.

Thus, there was a need for comparisons of wind-driven dust in burned and unburned locations within the LANL areas (Whicker et al. 2005). Further, there is interest in the concentrations of a wide variety of dispersed chemical and radioactive contaminants in the airborne dust (LANL 2002, Fresquez et al. 1998), but it is prohibitively costly to analyze the airborne dust for each contaminant at every potential release location within LANL. Therefore, a generic methodology was needed which could be used to quantitatively assess the potential amount of increases in worker human exposure to any contaminant of concern. Because 1) the fire burned over firings sites with documented DU soil contamination, and 2) increases in depleted uranium air concentrations were measured after the Cerro Grande fire (LANL 2002), the methodology will be demonstrated for DU, with a specific focus on exposures to LANL workers. Depleted uranium is both a radiological and chemical hazard whose hazard level varies substantially based on the mode of intake and the solubility of the material. Detailed information on characteristics, biokinetics, and environmental behavior of depleted uranium in provided in Appendix B.

Comparative measurements of wind-driven dust flux were made for several years following the fire in burned and unburned areas (Whicker et al. 2005), but these measurements only document the increases in dust flux in the burned areas. They do not provide a quantitative assessment of potential increases in exposures resulting from

increased dust inhalation. The goal of this study was to develop a methodology to combine dust flux measurements made in burned areas at LANL with measurements of airborne concentrations of particulate matter with aerodynamic diameters less than 10 μm (hereafter called PM-10) to quantify potential increases in resuspension and inhalation of contaminants of concern.

5.2 Methods

5.2.1 Site description

The location of the study was along the western edge of LANL property located to south of Los Alamos, NM, USA (35° 52' N and 106° 19' W) at an elevation of about 2400 m. The pre-fire vegetation was dominated by *Pinus poderosa* Douglas ex P.&C. Lawson var. *scopulorum* Englem (ponderosa pine). Because of access restrictions, the areas used in this study did not contain notable levels of any contaminants, but the study sites were within a few km of LANL ponderosa pine sites that do contain contaminated soils, and the vegetation, soil, topography, and geology of the study sites are generally representative of the contaminated sites.

During the course of the study, measurements of dust flux were made at sites in three categories of burn severity, which were established to assess dust flux along a burn gradient. The results of these measurements were reported by Whicker et al. (2005). First, severely burned sites were characterized as having ground vegetation and litter cover consumed in the fire and all portions of the pine trees burned, including the crown (tree top). Second, moderately burned sites included areas where the fire was primarily a ground fire that consumed the vegetation and litter cover but did not reach

the top crown of the pine trees. Most trees in the moderately burned areas contained green needles in at least the top third of the tree. The third forest sites were unburned and used as comparison sites.

5.2.2 Assessing the spatial extent of severely and moderately burned forests

The amount of burned and unburned forest area was needed to estimate the increase in fugitive dust across the LANL site as a result of the fire. Because the classifications of fire severity as severe and moderate can vary among agencies and individuals, the extent of the Severe and Moderate burn categories as used in this study were estimated by comparing pre-fire and post-fire Thematic Mapper (hereafter, TM) satellite images. These TM images contain 6 bands of reflected electromagnetic radiation in the visible and infrared bands that are recorded from 30-m by 30-m areas termed pixels (Lillesand and Kiefer, 1994). Pre-fire and post-fire images were obtained for the dates of March 13, 2000 and April 1, 2001, respectively, and rectified to NAD-27 Universal Transverse Mercator coordinates (Lillesand and Kiefer, 1994). These late-winter and early-spring images were used to 1) insure the absence of snow cover, whose highly-reflective surface can complicate the interpretation of vegetation patterns, and 2) predate the onset of seasonal, herbaceous plant growth. Extensive herbaceous growth promoted by post-fire remediation efforts could complicate the assessment of damage to pine tree canopies.

To assess damage to pine canopies, the data in the TM images were converted to Normalized Difference Vegetation Indices (hereafter, NDVI; Lillesand and Kiefer, 1994), which is a measure of chlorophyll abundance based on ratios of infrared to

visible reflectance. A reduction in NDVI between the pre-fire and post-fire images for a pixel is an indication of chlorophyll loss and fire damage to the canopy within that pixel. The degree of this difference for pixels was scaled to be representative of that for plots of Severe and Moderate fire severity. Pixels were scored as Severe burn when there were pine canopies present before the fire but no evidence of live trees after the fire. Pixels were scored as Moderate burn when there was at least some evidence of live trees after the fire. Pixels where there was little difference between pre- and post-fire NDVI were scored as unburned. However, low intensity ground fires that caused little scorching or mortality of large pines would 1) not have caused a measurable change in NDVI and 2) would not be detected by this procedure.

Because the pre-fire, late-winter image was unsuitable for mapping land cover types, land cover maps developed in the Multiple Resolution Land Cover program (Vogelmann et al., 1998) were used to show the extent of ponderosa pines, piñon/juniper, shrubland and grassland vegetation on LANL.

5.2.3 Measurements of horizontal dust flux and PM-10 concentrations

Horizontal dust flux (HDF) was measured using Big Spring Number Eight (BSNE) samplers (Fryrear 1986). These passive samplers self-orient a 10 cm^2 opening into the wind through which airborne dust is carried into, decelerated, and deposited into a collection pan. These BSNE field dust collectors have been extensively tested and show good sampling efficiency for soils with higher fractions of sand and silt (Fryrear 1986; Goossens and Offer 2000) such as those that are abundant at LANL (Nyhan et al. 1978). The HDF was calculated as the collected mass divided by the

product of the sampler opening (10 cm^2) and the sampling period and is expressed in units of g m^{-2} d^{-1}.

Within each of the three burn categories, two sampling plots, a primary and secondary site, were selected to assess variability within burn category. A line transect was established in each of the sampling areas along which the dust sampling stations were positioned every 30 m. This dust sampling transect consisted of three dust sampling stations in the primary sampling sites and two in the secondary sampling sites. In addition to sampling locations across a burn severity gradient, dust flux samplers were also set up at a fourth site that was adjacent the TA-6 meteorological tower operated by LANL. This meteorological tower was within several km of all the sampling sites and had the electrical power necessary to power sampling pumps for air sampling.

To establish relationships between HDF measurements and exposure-related metrics, the correlation between HDF and PM-10 (particulate matter less than 10 μm in aerodynamic diameter) concentration measurements made at 1-m above the soil surfaces were needed. A TEOM (Tapered Element Oscillating Microbalance) Series 1400a Ambient Particulate Monitor was used to continuously measure PM-10 concentrations in 0.5 hr increments. The sampler is manufactured by Ruprecht & Pataschnick Co., Inc of Albany, New York. It has been designated as a U.S. EPA equivalent method for the determination of 24-hour average PM-10 concentrations in ambient air. A size selective inlet uses impaction to achieve a 50% particle collection cut point of about 10 μm at a flow rate of 1.67 x 10^{-2} m^3 min^{-1}. A portion of this flow, 3 x 10^{-3} m^3 min^{-1}, goes through a filter that is fixed to the free end of a tapered oscillating

"finger" or element. Mass changes on the filter, measured by changes in the vibration frequency, are used to calculate air concentrations.

TEOM measurements were conducted from 28 June 2001 to 23 July 2002 at the TA-6 meteorological station. Though some data were lost due to disruptions in electrical power, approximately 14,350 30-minute mass concentration means were recorded. Some of these data were discarded due to low flow rates and pronounced negative values < -2 $\mu g\ m^{-3}$ were discarded. A total of 14,007 measures from 313 days were obtained.

Daily means were computed by averaging the 30-minute means, and daily means were retained in the data when ≥ 36 30-minute intervals were available for a given day. Daily means were available for 290 days with 97% of these days having measures from > 44 30-minute intervals. Averages of TEOM daily means were computed for sampling intervals of the BSNE data collected from the TA-6 meteorological location and compared to mean HDF measures at 1-m for the same interval. Because of the considerable day-to-day variability observed in TEOM data, only those intervals of longer than 10 days where TEOM data were available from > 50% of the days were involved in these comparison.

5.2.4 Calculations

A linear-least squares regression was performed with the PM-10 concentrations from TEOM measurements ($C_{PM\text{-}10}$) as the dependent variable and the mean of the 1-m HDF measurements made at the adjacent BSNE sampler locations (HDF_{1m}) as the

independent variable. The general form of this linear model of this relationship was simply:

$$C_{PM\text{-}10} = (HDF_{1m})(m) + b \qquad (1)$$

where m and b are the best fit slope and intercept of the equation, respectively. The slope, m, represents the effectiveness of saltating particles to suspend PM-10 particles and the intercept, b, represents an average "background" PM-10 concentration.

An important assumption is that the relationship in equation 1 holds in other sampling locations. Because of limitations in access to electrical power, we were not able to fully test this relationship at all sites. Fundamentally though, BSNE samplers almost exclusively measure wind-blown saltating soil particles (Fryrear 1986), and the impaction of the saltating particles onto the soil surface is the main mechanism for suspension of smaller soil particles (Bagnold 1941). Therefore, for these calculations, we assume a similar relationship between HDF and PM-10 concentrations at other sites, though recognizing the uncertainty. We expect that this relationship, because it was made in an open grassy area of forest, would be steeper than one in a forested area with greater ground cover because the measured HDF in the unburned forests would reflect more background dust relative to saltating particles (Whicker et al. 2005).

Given the relationship in equation 1, the relative effects of the forest fire severity on increasing PM-10 concentrations can be estimated from the HDF measurements. The relative increase in PM-10 concentrations above the "background" concentration can be calculated by dividing both sides of equation 1 by the intercept (b), yielding the following equation:

$$\frac{C_{PM\text{-}10}}{b} = \frac{(HDF_{1m})(m)}{b} + 1 \qquad (2)$$

Equation 2 was used to estimate fractional increases in PM-10 concentrations above the "background" level in each of the burned and unburned locations. Then, the effect of the fire on increasing PM-10 concentrations was estimated by dividing the relative increases above background in the severely and moderately burned areas by that obtained for the unburned plots. This calculation also provides some estimate of the relative increase in inhalation of a contaminant due to the fire.

Calculating relative increase avoids numerous assumptions in exposure scenarios such as exposure times, inhalation parameters, and particle size and solubility characteristics of the inhaled contaminants. However, it can be very useful to estimate the range of possible doses for evaluation against safety standards, so conservative exposure assumptions are made that allow calculation of average and upper-bound doses from inhalation of the contaminated soil aerosol.

5.2.5 Calculation of average and upper-bound dose for occupational workers from soils contaminated with depleted uranium

Because of the focus on LANL workers, the following dose calculations are based on exposure parameters for occupational workers and use generally conservative assumptions to estimate an average and an upper bound of potential dose. The dose estimates are based on the empirical model describing the relationship between the mean HDF in each of the burned and unburned areas and the PM-10 concentration and

the following assumptions: 1) average and upper limit of contaminant concentration in LANL soils (LANL 2002), 2) a 5 time enrichment of contaminant concentration in the PM-10 aerosol relative to the soil (Shinn et al. 1997, Van Pelt and Zobeck 2005), 3) workers either work at all burn locations equally through the year or at a single burned site, and 4) the workers spend their entire work year outdoors (no shelter) in the location(s). The actual values of the assumption are detailed below.

5.3 Results

The average 1-m HDF measurement at the TA-6 location was 1.05 g m^{-2} d^{-1} (median = 0.74 g m^{-2} d^{-1}) with a standard deviation of 0.75 g m^{-2} d^{-1} (range from 0.27 g m^{-2} d^{-1} up to 2.46 g m^{-2} d^{-1}). The average PM-10 concentration was 13.1 μg m^{-3} (median = 11.9 μg m^{-3}) with a standard deviation of 3.7 μg $m^{-3}$and a range of 7.94 μg m^{-3} up to a maximum of 20.6 μg m^{-3}. The average 1-m HDF measurements made in the burned and unburned locations were provided in Whicker et al. 2005 and listed in the first row in Table 5.1.

Using the measurements from the TA-6 location, we found a significant correlation between the HDF measurements made at 1 m and PM-10 mean concentrations (C_{PM10}) measured by a TEOM (Figure 5.1). The C_{PM10} measures increased in a statistically significant ($F = 32.1$; $df = 1, 8$; $r^2 = 0.80$; $P < 0.001$) linear fashion with increasing mean HDF at 1-m elevations (n=10). The regression equation of C_{PM10} measures on HDF measures at 1-m has intercept (± SE) and slope (± SE) of 8.4 (± 1.0) and 4.4 (± 0.8), respectively.

$$C_{PM10} = \overline{HDF}(4.4) + 8.4 \qquad (3)$$

An analogous regression procedure using the individual daily means of C_{PM10} data rather than the interval mean also indicated a statistically significant relationship of C_{PM10} to HDF ($F = 63.8$; $df = 1, 178$; $P < 0.001$) with no significant residual relationship due to the sampling intervals (Lack of Fit F-test = 1.45; $df = 8, 170$; $P > 0.05$). The intercepts and slopes of this procedure were similar to those in equation 3.

The fire increased the mean HDF by 60% and 243% in the moderately and severely burned areas, respectively. Next, the empirical relationship shown in Figure 5.1 was used to estimate mean C_{PM10} for each of the burned areas using the HDF measurements from the burned and unburned areas. The relative increase in PM-10 levels above background (equation 2) increased with burn severity (Table 5.1). The burn/unburn ratio provides the best indicator of the relative effects of the fire toward increasing PM-10 concentrations. We estimated an 11% increase in PM-10 concentration in the moderately burned areas and a 27% increase in the severely burned areas.

5.3.1 Extent of severe and moderate burn areas on LANL

The comparison of pre-fire and post-fire NDVIs estimated that severe burns occurred on 127 ha of ponderosa pine and piñon/juniper woodlands and 746 ha of moderate burns occurred on these woodlands. Most of these burns, especially the severe burns, occurred on that portion of LANL south of Los Alamos and in ponderosa pine forests.

The estimate of 873 ha for both Severe and Moderate burns is greater than the 393 ha of "Cerro Grande Fire High-burn severity" estimated from post-fire TM data by McKown et al. (2003). Because the McKnown et al. (2003) study used only post-fire images, their separation between "High-burn severity" and unburned forests probably overlaps the Moderate category used in this study. For example, some areas of moderate burn were not apparent in the April 1, 2000 data and were only identified by comparison of their NDVI to the pre-fire image.

Neither the 873 ha of burned forest estimate or the 393 ha of McKown et al. (2003) are consistent with a previous estimate of 3061 ha of burned area on LANL (LANL 2001). The 3061 ha estimate includes nonforest areas that burned and forest areas where the fire severity was less than the Moderate burn used here and resulted in too little damage to the pine canopy to be detected from TM data. Low-intensity fires, which consume only a part of the forest floor, can have little effect on the canopies of large trees (Gaines et al., 1958; Davis et al., 1968).

For the purposes of these calculations, we used the NDVI analyses and assumed that of the total 11,694 ha of LANL property a total of 521 ha burned (124 ha was severely burned and the rest, 397 ha, was moderately burned). This gives 3.4 % of LANL in the Moderate burned severity class and 1.1 % in the Severely burned class. Finally, the last row in Table 5.1 shows the calculation for an estimated 1% increase of PM-10 concentration across LANL as a result of the fire. This value is calculated as the average of increased PM-10 concentrations in the burned areas weighted by the fraction of LANL burned and unburned areas in each of the three burn severity categories. For comparison, we also calculated the increase in PM-10 concentrations using the burn

estimates from LANL (2001) which estimated 2724 + 842 ha of low- to moderate-burn intensity (these were added together into the moderate burn PM-10 category) and 30 ha of severe burn area. These values give an estimated increase of PM-10 aerosol across LANL of about 4% (Table 5.1).

5.3.2 Estimated post-fire dose from soils contaminated with depleted uranium

Using the empirical model shown in equation 3, PM-10 concentrations in the burned and unburned areas can be predicted, and it becomes possible to examine levels of potential increases in inhalation doses from resuspended soils that are contaminated. While this methodology could be used for any contaminant of concern, the initial concern was for depleted uranium because of the increased concentrations of DU found in air samples made as part of the routine environmental surveillance program, and also many of the areas burned over during the fire were contaminated with DU from explosives testing.

The first step in this dose assessment is to convert the PM-10 concentrations to an activity concentration in units of Bq m^{-3}. However, simply multiplying the PM-10 concentration measured in units of $\mu g\ m^{-3}$ by the local activity concentration of DU in the local soil (units of Bq μg^{-1}) ignores the potential enrichment of uranium in aerosol due to the preferential occurrence of uranium on smaller soil particles and the greater effect of wind on suspending smaller soil particles (Van Pelt and Zobeck 2005). The types of measurements needed to accurately assess the enrichment ratio (concentration of a contaminant in the aerosol to that in the soil) in LANL soils were beyond the scope of this study and are not found in the literature for PM-10 concentrations. Therefore,

we used a conservative enrichment ratio of 5. This is generally larger (more than a factor of 2 greater) than what other studies have found for other radionuclides (Shinn et al. 1997), and is slightly larger than that found by Van Pelt and Zobeck (2005) for uranium in Texas soils. Finally, we used average and maximum concentrations of uranium that were measured in the top 5 cm of soil on LANL property. The average onsite DU concentration value (C_{DU}) was 3.6 μg of uranium per gram of surface soil and an upper-bound concentration (2 standard deviations above the mean) of roughly 5.6 μg of uranium per gram of soil (LANL 2002). We further assume that all the uranium in the soil is DU from LANL operations with a specific activity of 14 Bq mg^{-1} (Guilmette et al. 2004). The resulting estimates for average and upper bound DU concentrations in PM-10 aerosol are defined as:

$$C_{DU-PM10}\frac{Bq_{DU}}{g_{PM10}} = C_{PM10} \times C_{soil} \times ER \times 1.4E4\frac{Bq_{DU}}{g_{DU}}, \qquad (4)$$

where C_{PM10} = the PM-10 concentration in g m^{-3}, C_{soil} is concentration of DU in soil in unit of g_{DU} per g of soil, ER is the enrichment ratio of 5 $g_{DU\text{-}PM10}$ per $g_{DU\text{-}soil}$ in soil over 1g_{PM10} per g_{soil}, and the specific activity of DU is 1.4 x 10^4 Bq g^{-1}. This value can then be multiplied with calculated PM-10 concentrations to estimate the PM-10 concentrations of DU. The PM-10 concentrations are derived using the empirical relationship from equation 3 and are given in Table 5.1. Multiplying the PM-10 concentrations by $C_{DU\text{-}PM10}$ (equation 4) gives estimated PM-10 concentrations of DU (Table 5.2). The estimates in Table 5.2 are 2 to 27 times greater than the measured DU air concentrations at Los Alamos that range from 1.85 x 10^{-7} Bq m^{-3} up to 1.1 x 10^{-6} Bq

m^{-3} (LANL 2002). This comparison shows the approach above is giving conservative but reasonable values for air concentrations.

Next, the link between HDF and PM-10 concentrations were used to estimate potential increases in doses from inhaled DU. The doses to workers are calculated using Derived Air Concentrations (DAC) listed in DOE (1993). The DAC values represent air concentrations that if inhaled by a worker for 40 hours per week, 50 weeks of the year (for a total respired volume of 2400 m^3) the worker would receive a 50 mSv committed effective dose equivalent (CEDE), or the DOE occupational dose limit (DOE 1993). The DAC value for ^{238}U is listed as 0.6 Bq m^{-3}. The estimated doses then becomes:

$$Dose = C_{DU-PM10} \times \frac{50mSv}{0.6\frac{Bq}{m^3}} . \qquad (4)$$

The summary for these calculations and the upper-bound occupational doses for DU are provided in Table 5.2. These calculations show that the fire potentially increased the doses up to 26% in the severely burned areas, but that the doses were <<1% of the 50 mSv annual dose limit.

In addition, one should consider that most of the LANL forest was not severely burned, but either unburned or moderately burned. To account for this exposure scenario, an average soil concentration is used and the worker is assumed to move randomly throughout LANL spending time in each area in exact proportion to the amount of burned/unburned area (i.e., 96% in unburned areas, 3% in moderately burned areas, and 1 % in severely burned areas determined from the NDVI analysis). The weighted average concentrations is then equal to:

$$2.62E-6\frac{Bq}{m^3} = (0.96*2.61E-6)\frac{Bq}{m^3} + (0.03*2.89E-6)\frac{Bq}{m^3} + (0.01*3.30E-6)\frac{Bq}{m^3}.$$

(5)

This area weighted-average concentration gives an expected annual dose of about 0.22 μSv, again far below the occupational dose limit. For comparison, the LANL (2001) burn area estimates (Table 5.1) give a comparable annual dose of 0.23 μSv.

5.4 Discussion

Results of previous studies have shown that horizontal dust flux increased with the severity of burn effects from the Cerro Grande fire. This study provides a direct link between the increases in horizontal dust flux and PM-10 concentrations. This link is important because the increased HDF at 1 m in the burned areas suggests the possibility of increased production of respirable particles in burned areas, and some of these burned areas contain soils that are contaminated.

The maximum estimated inhalation dose from exposure was very small, < 1 μSv yr^{-1}. Operationally, this provides justification to keep the LANL workers generally classified as non "radiation workers." Specific jobs that are particularly dusty or in highly contaminated areas still may require evaluation on an individual basis. While these calculations were performed for DU, the same approach can be taken for other radioactive and chemical constituents in the soil as well. For example, using upper soil values of 0.009 Bq g^{-1} of ^{239}Pu (LANL 2002), one can calculate an upper-bound annual

dose estimate of 0.37 μSv, assuming 100% of a worker's time is spent in the severely burned area. A total estimated committed effective dose equivalent can also be calculated by summing over doses from all radioactive constituents in the soil. This approach certainly has its limitations due to uncertainty in selection of exposure parameters, but choice of conservative values for dose assessment allows for an initial screening, which if high, would provide the motivation to perform a more thorough evaluation.

The methodology outlined also provides an approach to evaluate the effects of future fires at LANL. Before 1890, there were numerous fires (about 1 every 10 years) in this area, but these were grass fires of low intensity. In contrast, in the past 50 years there have been 5 major fires near LANL that were spectacular crown fires and resulted in the death of the vegetation from the ground up and over extensive tracts of land (LANL 2000). In coming years to decades LANL will face continuing threats from fire. Because the results of the time-weighted dose calculations are dependent on the amount of area burned and the severity of the burn, hypothetical dose calculations can easily be performed to assess risk consequences from future fires and their burn severity.

5.4.1 Implications for long-term stewardship of contaminated lands

LANL and DOE are faced with decisions regarding cleanup strategies for contaminated sites. One important question to ask about these sites is not how to clean them up, but rather whether or not to clean them up at all (Breshears et al. 1993, Whicker et al. 2004). One of the major clean-up options to be considered—physical removal of the soils—is extremely costly and requires virtual destruction of the

contaminated ecosystem and the availability of a new site approved to dispose of the contaminated materials that are removed. Soil substrate removal only translocates the problem, may add significant health risks to the clean-up workers, and may actually enhance the dispersion of contamination in the process (Whicker et al. 2004). In contrast, if the long-term risks from actinides in surface soils of the environment are sufficiently low, contaminants may be left in place, providing that soil stability, even during extreme events, is adequately demonstrated.

5.5 Conclusions

This study, in combinations with others, provided estimates of the flux of respirable particles from existing sites to the atmosphere under unburned and worst-case burned scenarios and estimates of the level of increased dose as a result of the Cerro Grande fire. Post-fire estimates of radiation dose from inhalation of radioactive soils are far below existing safety standards and document the absence of significant inhalation risk.

5.6 References

Bagnold, R.A., 1941. The physics of blown sand and desert dunes. London:Chapman and Hall Ltd.

Breshears, D.D.; Whicker, F.W.; Hakonson, T.E. 1993. Orchestrating environmental research and assessment for remediation. *Ecological Applications* 3(4): 590-594.

Davis, J. R.; Ffolliott, P.F.; Clary, W.P.. 1968. A fire prescription for consuming ponderosa pine duff. USDA Forest Research Note RM-115.

DOE (Department of Energy). 1993. Occupational radiation protection; final rule. Code of Federal Regulations, 10CFR 835.

Fresquez, P.R., D.R. Armstrong, and M.A. Mullen. 1998. Radionuclides in soils collected from within and around Los Alamos National Laboratory. J. Environ. Sci. Health A33(2):263-278.

Fryrear, D.W. 1986. A field dust sampler. Journal Soil and Water Conservation 41:117-120.

Gaines, E. M., Kallendar, H.R.; Wagner, J.A. 1958. Control burning in southwestern ponderosa pines: Results from the Blue Mountain plots, Fort Apache Indian Reservation. Journal of Forestry, 56:323-327.

Goossens, D., and Z.Y. Offer. 2000. Wind tunnel and field calibration of six aeolian dust samplers. Atmospheric Environment 34:1043-1057.

Gonzales, G.J., P.R. Fresquez, and C.M. Bare. 2001. Contaminant concentrations in conifer tree bark and wood following the Cerro Grande fire. Los Alamos National Laboratory Report LA-UR-01-6157.

Guilmette, R.A.; Parkhurst, M.A.; Miller, G.; Hahn, F.F.; Roszell, L.E.; Daxon, E.G.; Little, T.T.; Whicker, J.J.; Cheng, Y.S.; Traub, R.J.; Lodde, G.M.; Szrom, F.; Bihl, D.E.; Creek, K.L. 2004. Human health risk assessment of Capstone Depleted Uranium aerosols. Battelle report PNWD-3442.

LANL (Los Alamos National Laboratory). 2000. A special edition of the SWEIS yearbook: wildfire 2000. Los Alamos National Laboratory Report LA-UR-00-3471.

LANL (Los Alamos National Laboratory). 2001. Wildfire hazard reduction project plan. Los Alamos National Laboratory Report LA-UR-2017.

LANL (Los Alamos National Laboratory). 2002. Environmental surveillance at Los Alamos during 2002. Los Alamos National Laboratory Report LA-14086-ENV.

Lillesand, T. M.; Kiefer, R.W. 1994. Remote Sensing and Image Interpretation, Third Edition. John Wiley and Sons, Inc., New York.750 pp.

McKown, B.; Koch, S.W.; Balice, R.G.; Neville, P.. 2003. Land Cover map for the Eastern Jemez Region. Los Alamos National Laboratory Report LA-14029. 84 pp.

Nyhan, J.W., L.W. Hacker, T.E. Calhoun, D.L. Young. 1978. Soil survey of Los Alamos County, New Mexico. Los Alamos Scientific Laboratory Report LA-6779-MS.

Shinn, J.H., E.H. Essington, F.L. Miller, T.P. O'Farrell, J.A. Orcutt, E.M. Romney, J.W. Shugart, and E.R. Sorom. 1989. Results of a cleanup and treatment test at the Nevada Test Site: evaluation of vacuum removal of Pu-contaminated soil. Health Physics 57(5): 771-779.

Shinn, J.H., Homan, D.N.; Robinson, W.L. 1997. Resuspension studies in the Marshall Islands. Health Physics 73:248-257,

Whicker, J.J., D.D. Breshears, P.T. Wasiolek, T.B. Kirchner, R.A. Tavani, D.A. Schoep, and J.C. Rodgers. 2002. Temporal and spatial variation of episodic wind erosion in unburned and burned semiarid shrubland. J. Env. Qual. 31(2): 599-612.

Whicker, J.J.; Pinder, J.E.; Breshears, D.D. 2005. Increased wind erosion from wildfire: implications for contaminant-related risks. Los Alamos National Laboratory Report LA-UR-05-0741.

Whicker, F.W., T.G. Hinton, M.M. MacDonell, J.E. Pinder III, and L.J. Habegger. 2004. Avoiding destructive remediation at DOE sites. Science 303: 1615-1616.

Whicker, F.W., and V. Shultz. 1982. Radioecology: nuclear energy and the environment. CRC Press, Boca Raton.

Van Pelt, R.S.; Zobeck, T.M. 2005. Chemical constituents in fugitive dust. Unpublished data.

Vogelmann, J. E.; Sohl, T.; Howard, S.M.. 1998. Regional characterization of land cover using multiple sources of data. Photogrammetric Engineering and Remore Sensing, 64:45-57.

Zobeck, T.M., D.W. Fryrear, and Pettit, R.D. 1989. Management effects on wind-eroded sediment and plant nutrients. Journal of Soil and Water Conservation, March-April:160-163.

Table 5.1. Summary of results and calculations for increases in PM-10 concentrations in each of the burn/unburn categories.

	Unburned	Moderately Burned	Severely Burned
Mean HDF ($g\ m^{-2}\ d^{-1}$)	0.44	0.70	1.07
PM-10 concentration ($\mu g\ m^{-3}$)	10.34	11.48	13.11
Relative to PM-10 in burned forests relative to unburned	1.00	1.11	1.27
Est. Fraction of burned/unburned areas LANL			
NDVI data	0.96	0.03	0.01
LANL (2001) data (Low burn=Mod. burn)	0.69	0.30	0.01
Overall weighted average increase in PM-10 from fire			
NDVI data	1.00(0.96) + 1.11(0.03) + 1.27(0.01) = 1.01		
LANL (2001) data (Low burn=Mod. burn)	1.00 (0.69) + 1.11(0.30) + 1.27 (0.01) = 1.04		

Table 5.2. Summary of calculation values of for estimating doses to occupationally exposed workers from DU contaminated soils.

	Unburned	Moderately burned	Severely burned
Estimated PM-10 concentration ($\mu g\ m^{-3}$)	10.34	11.48	13.11
Estimated DU concentration ($Bq\ m^{-3}$)			
Mean	2.6×10^{-6}	2.9×10^{-6}	3.3×10^{-6}
Upper-bound	4.1×10^{-6}	4.5×10^{-6}	5.1×10^{-6}
Estimated dose ($\mu Sv\ yr^{-1}$)			
Mean	0.22	0.24	0.28
Upper-bound	0.34	0.38	0.43
Net increase above unburned locations ($\mu Sv\ yr^{-1}$)			
Mean		0.02	0.06
Upper-bound		0.04	0.09
Relative increase in dose			
Mean		9%	27%
Upper-bound		12%	26%

Figure 5.1. PM-10 concentrations as related to HDF measurements. The estimated intercept for the regression is 8.4 ± 1.0 with a slope of 4.4 ± 0.8. The correlation coefficient is 0.80.

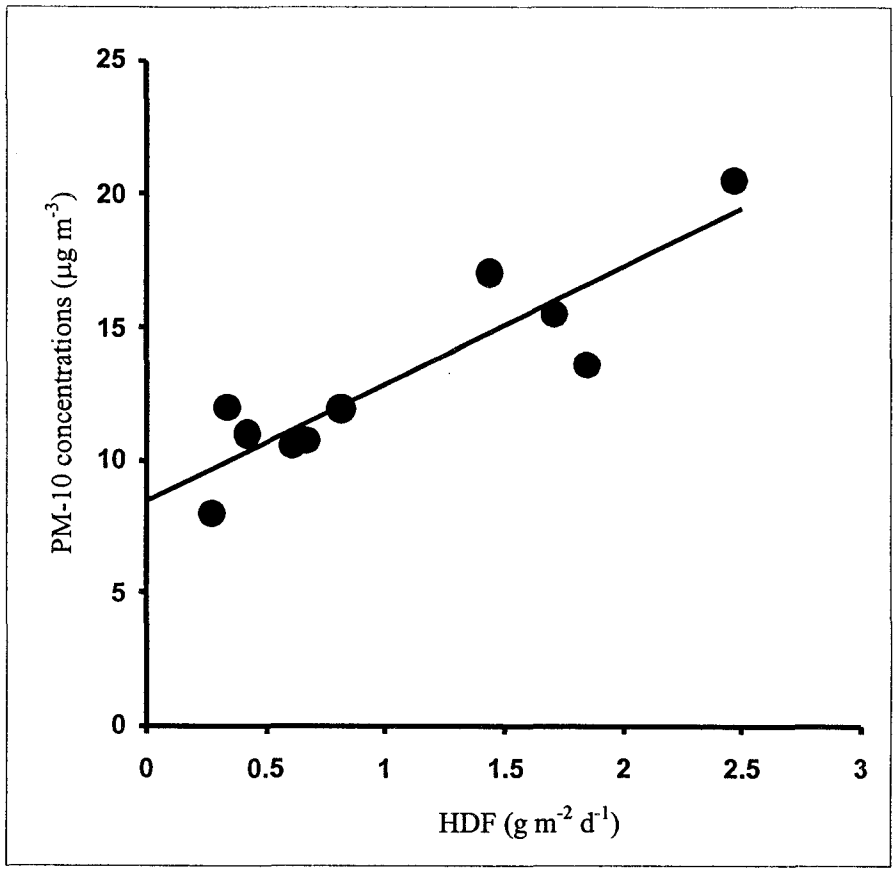

Chapter 6

Summary and Integration of Findings

6.0 General Summary

The Department of Energy (DOE) has the responsibility to manage its contaminated areas in a manner that protects its workers and the public from undue health risk. Assessments are performed to estimate potential health risks over long periods of time, but these often do not include the effects of low-probability, high-impact disturbances, which have the potential to significantly increase contaminant transport and consequent human and ecological risk. For forested areas of Los Alamos National Laboratory (LANL), two important disturbances that have the potential to increase transport of contaminants include forest fire and tree thinning. Forest wildfire threatens LANL and much of the Western United States, due to historic grazing and fire suppression, and can be triggered by drought, which could increase in intensity and frequency from global climate change. Further, land management strategies in forested DOE sites over the years could include tree thinning, which is another high impact disturbance in forests. The transport of contaminated soils through wind and water erosion following forest disturbances such as fire or thinning could be significantly increased and these transport rates should be investigated as to their impact on human and ecological risk. Assessments of contaminant-related human and ecological risk require estimation of transport rates, but relative to water transport, data for estimating

wind-driven transport rates in non-agricultural settings are few and responses to ecosystem disturbances such as forest wildfire and thinning are almost entirely lacking.

6.1 Integration of findings

Forest fire and thinning operations at LANL increased wind transport of soil and increased potential exposure to the public and some LANL workers to contaminated dust from the disturbed forest areas. The potential for increased exposure to contaminated dust was suggested by our finding that wind-driven dust flux was significantly greater in both types of burned areas relative to unburned areas, by more than one order-of-magnitude initially and by 2-3 times a year after the fire. Unexpectedly, the elevated dust fluxes did not decrease during the second and third years in burned areas, possibly because an ongoing drought delayed post-fire recovery. Further, the results of the tree thinning study showed that wind erosion was significantly elevated in thinned and burned areas, though there were indications of reduced dust flux during the second year after thinning. There was no indication of a synergistic effect between burning and thinning. Finally, we found a significant relationship between tree and ground cover and dust flux.

The finding of increased wind erosion in these disturbed forest areas, combined with a finding of higher concentrations of depleted uranium (DU) in the air around LANL, prompted us to assess whether (DU), one of the contaminants of concern, would remain on soil surfaces and thus be susceptible to wind erosion. Therefore, measurement of the partition coefficient (K_d) for uranium in soils from Los Alamos National Laboratory was done using an EPA-based protocol for both whole soil and the

fine soil fraction (diameters < 45 μm). The 7-day K_d values, which are those specified in the EPA protocol, ranged from 276-508 mL g^{-1} for whole soil and from 615-2249 mL g^{-1} for the fine soil fraction. These relatively large K_d values suggest that a large fraction of deposited DU will quickly and preferentially attached to smaller particles and remain on soil surfaces. This soil-bound DU would be available for transport through wind erosion for long periods of time.

Finally a post-fire assessment of the relative increase of LANL PM-10 emissions was done, and from this data we estimated the increase in potential dose to onsite workers. Measurements of wind-driven dust flux in burned areas using passive dust collectors combined with measurement of PM-10 measurements were used to assess the potential for increased respirable dust emissions and associated inhalation doses to LANL workers. From statistical relationships between dust flux and PM-10 measurements and the relative amounts of burned and unburned areas, we calculated a relative increase of about 1-4% in PM-10 dust emission across the entire LANL resulting from the fire. Calculations of relative inhalation dose from DU suggest a high-end estimate of a 26% increase for LANL workers on severely burned areas. Despite the potential increased doses, the estimated annual dose was < 1 μSv, which is far below the dose limits for occupational or public exposures.

Combined, these results show that wind erosion is responsive to disturbances in ponderosa pine forests. While most studies on the effects of forest disturbances on soil erosion have focused on water erosion, our results highlight the importance of considering wind- as well as water-driven transport and erosion, particularly following

disturbance, for ecosystem biogeochemistry in general and human and ecological risk assessment in particular.

6.2 Future work

Below are a list of topics that our data suggest are candidates for additional study. **First,** we developed an empirically-based method to calculate respirable dust concentrations for any contaminant of concern. In this study we focused on DU, but other contaminants should be looked at as well. The list of other soil-bound contaminants could include plutonium, chemical compounds from explosives testing, and beryllium. **Second**, the relationship between horizontal dust flux and PM-10 concentrations used to calculate airborne concentrations of contaminants was measured in a large opening in the forest and may not apply to other forest landscapes, especially those with more trees. However, because the relationship was in a more open area, the relationship should over predict PM-10 concentrations and therefore provide conservative estimates for airborne concentrations of the contaminants. **Third**, measurements of the vertical flux in the forest canopies would provide important information to determine if forested areas are areas where dust is deposited rather that eroded. This would be important information on the role of trees in filtering and concentrating contaminants and other important soil nutrients and organic matter. **Fourth**, comparison of vertical dust flux measurements (a measure of soil and soil nutrient conservation) among undisturbed, thinned, and burned areas can be used to assess potential costs and benefits associated with various land management strategies and used for optimization of soil conservation. **Fifth,** it would be very interesting to

measure the chemical constituents of the airborne dust. This would allow for measurement of specific atmospheric fluxes of materials into and out of these forest areas and provide important information toward a better understanding of the biogeochemical cycling in the forest. **Sixth,** specific measurements of particle size and of solubility of the contaminants in lung fluid would provide for more accurate dose assessment. **Seventh,** measurements of enrichment ratios, and how they might be impacted by soil disturbance, would provide needed data to help in exposure assessments. **Finally,** there are few measurements of wind erosion and dust transport in many ecosystems, and fewer investigate the role of disturbance on dust production and transport. Measurements, such as those in this study, provide important information that could help us to better understand, thus manage, these important ecosystems in a manner that preserves ecosystem function and maintains public and worker health.

Appendix A

Methods for Measurements of Dust Flux and Aerosols

A1.0 Horizontal dust flux

Horizontal dust flux (HDF) is a metric of material transport associated with wind erosion (Breshears et al. 2003) and was measured using Big Spring Number Eight (BSNE) samplers (Fryrear 1986). A tail fin attached to each BSNE sampler orients their 10-cm^2 opening into the wind where airborne dust enters and is deposited onto a collection pan as winds decelerated through wider portions of the sampler. BSNE field dust collectors have been extensively tested and have good sampling efficiency for soils with higher fractions of sand and silt (Fryrear 1986; Goossens and Offer 2000) such as those that are abundant at LANL (Nyhan et al. 1978). The HDF was calculated by using the mass of the dust collected and dividing the area of the sampler opening (10 cm^2) and the sampling period. The units of HDF were then expressed as g m^{-2} d^{-1}. This value represents a measure of the wind-driven mass of dust flowing horizontally along the earth surface at a particular height. Multiple samplers may be mounted at different heights to measure gradients in HDF with increasing distance above the soil surface. Lack of time-resolved data on particle size and wind velocity in all the sampling areas precluded corrections for collection efficiency, so a collection efficiency of 100% was assumed. Sampling efficiencies of the BSNE samplers measured by Goossens and

Offer (2000) and Fryrear (1986) were less than 100%, so our estimates of HDF will be biased low, but only maybe by a factor of two or less according to these studies.

A BSNE sampling station consisted of at least three BSNE samplers at heights of 0.25 m, 0.5 m, and 1 m. About 99% of the wind-driven dust mass occurs with 0-1 m interval (Stout and Zobeck 1996). The BSNE samplers thus provide measures of integrated wind erosion collected over sampling intervals of normally one to two weeks at multiple heights above the ground.

Dust samples were washed into plastic bags with distilled water, transferred into 22 mL glass vials, dried at 50° to a constant mass, and weighed with a sensitivity of 0.001 g. Horizontal mass flux was calculated as the mass of the dust deposited in the sampler and divided by the product of the sampling period and the area of the opening (10 cm^2). Tap water was used for sample washings for some of the initial samples, and these data corrected for the residual mineral mass.

Measurements of HDF were collected beginning in May of 2001 and extended through July of 2003. Samples were collected generally at intervals of weekly to biweekly in 2001 from June through November, in 2002 from January through November, and from March through July in 2003.

Relationships between the HDF and meteorological conditions were established using 1-m wind and precipitation data from the Davis meteorological station and HDF measurements from 3 nearby BSNE sampling stations. These HDF measurements were made from May 2001 to September 2002 in an open, unforested area. The BSNE, Davis and TA-6 measuring points were arranged in a triangular pattern with approximately 200 m per side.

A1.1 Vertical dust Flux Measurements

We measured vertical soil flux (F) using the gradient method (Stull, 1988, Blackadar 1997, Whicker et al. 2002), for which it is determined as the product of the eddy diffusivity coefficient (K_z) and the mass concentration (χ) gradient with height (z):

$$F = K_z * \frac{d\chi}{dz} \quad . \qquad [1]$$

The eddy diffusivity coefficient itself is a function of the friction velocity (u_*):

$$K_z = k_v z u_* \quad , \qquad [2]$$

where: k_v = von Karman dimensionless constant (approximately 0.4), and z = height of the measurement. The friction velocity, a measure of the boundary shear created as winds pass over vegetation and soils, can be estimated for a given terrain and wind velocity by measuring the wind velocity profile with height (Bagnold, 1941), or by using high-frequency, three-dimensional measurements of wind velocities (Stull, 1988):

$$u_*^2 = \left[\overline{u'w'}^2 + \overline{v'w'}^2\right]^{\frac{1}{2}} \quad , \qquad [3]$$

where u′, v′, w′ are the instantaneous wind velocity components in both horizontal (x and y) and vertical (z) directions. We used the later approach and measured the instantaneous wind velocity components using a factory-calibrated sonic anemometer at the TA-6 meteorological tower (Rishel et al. 2003). Friction velocity measurements

used were made between August 2000 and August 2001, and a subset of friction velocity measurements, those made at night (more likely to be neutral atmospheric stability), was used in these calculations.

Total suspended particulate (TSP) samples were generally collected weekly from samplers positioned at two heights (1 m and 3 m) to determine the concentration gradient with height ($d\chi/dz$). We collected TSP air samples using a sampling inlet (Figure A-1) that was based on the PM-10 inlet design of Liu and Pui (1981). The inlet is not directionally dependent, and it provides accurate sampling for predominant particle sizes measured at our study sites and for intermediate wind velocities. Aspiration efficiencies for particles of aerodynamic diameters of 8.5 and 11 μm was 100% ± 10% at wind speeds up to 2.8 m s^{-1} (Liu and Pui, 1981). We modified this inlet to collect all airborne particulate rather than just particles less than 10 μm. These modifications included placing the filter close to the bottom plate and adding a coarse wire screen to keep insects and larger debris out of the filter. To supplement the Liu and Pui (1981) study, tests of the modified sampling inlet at high-wind velocities of 12, 15, and 17 m s^{-1} indicated that collection efficiencies were ~120% (an over sampling of 20%) for 5 μm particles and ~50% for both 10 μm and 30 μm particles (Rogers et al., 2000). The results of this study suggested that collection efficiencies at these high-wind velocities were affected by particle size but not by wind velocity in the range tested.

The vertical flux measurements were correlated to HDF measurement made from the BSNE samplers also located near the TA-6 meteorological tower over 15 overlapping time periods. Investigation of potential links between HDF (saltating particles that are locally redistributed) and vertical flux is important for many reasons,

but importantly because the vertically transported aerosol is mostly smaller dust particles that are transport longer distances and present a potential inhalation risk if contaminated.

A1.2 PM-10 concentrations

To establish relationships between HDF measurements and exposure-related metrics, the correlation between HDF and PM-10 (particulate matter less that 10 μm in aerodynamic diameter) concentration measurements made at 1-m above the soil surfaces were needed. A TEOM (Tapered Element Oscillating Microbalance) Series 1400a Ambient Particulate Monitor was used to continuously measure PM-10 concentrations in 0.5 hr increments. The sampler is manufactured by Ruprecht & Pataschnick Co., Inc of Albany, New York. It has been designated as a U.S. EPA equivalent method for the determination of 24-hour average PM-10 concentrations in ambient air. A size selective inlet uses impaction to achieve a 50% particle collection cut point of about 10 μm at a flow rate of 1.67×10^{-2} m^3 min^{-1}. A portion of this flow, 3×10^{-3} m^3 min^{-1}, goes through a filter that is fixed to the free end of a tapered oscillating "finger" or element. Mass changes on the filter, measured by changes in the vibration frequency, are used to calculate air concentrations.

TEOM measurements were conducted from 28 June 2001 to 23 July 2002 at the TA-6 meteorological station. Though some data were lost due to disruptions in electrical power, approximately 14,350 30-minute mass concentration means were recorded. Some of these data were discarded due to low flow rates and pronounced

negative values < -2 $\mu g\ m^{-3}$ were discarded. A total of 14,007 measures from 313 days were obtained.

A1.3 Locations of samplers

Within each of the three burn and two thinning categories, two sampling plots, a primary and secondary site, were selected to assess variability within each category. A line transect was established in each of the sampling areas along which the dust sampling stations were positioned every 30 m. This dust sampling transect consisted of three dust sampling stations in the primary sampling sites and two in the secondary sampling sites. In addition to sampling locations across a burn severity gradient and in thinned areas, dust flux samplers were also set up at a fourth site that was adjacent the TA-6 meteorological tower operated by LANL. This meteorological tower was within several km of all the sampling sites and had the electrical power necessary to power sampling pumps for air sampling. Figure A-2 is an aerial photograph of the study area with the approximate locations of each of the sampling areas.

A2.0 References

Blackadar, A.K. 1997. Turbulence and diffusion in the atmosphere. New York: Springer.

Fryrear, D.W. 1986. A field dust sampler. J. Soil Water Conserv. 41:117-120.

Goossens, D., and Z.Y. Offer. 1997. Aeolian dust erosion on different types of hills in a rocky desert: wind tunnel simulations and field measurements. J. Arid Environ. 37:209-229.

Liu, B.Y.H., and Y.H. Pui. 1981. Aerosol sampling inlets and inhalable particles. Atmos. Environ. 15:589-600.

Nyhan, J.W., L.W. Hacker, T.E. Calhoun, D.L. Young. 1978. Soil survey of Los Alamos County, New Mexico. Los Alamos Scientific Laboratory Report LA-6779-MS.

Rodgers, J.C., P.T. Wasiolek, J.J. Whicker, C. Eberhart, K. Saxton, and D. Chandler. 2000. Performance evaluation of LANL environmental radiological air monitoring inlets at high wind velocities associated with resuspension. Los Alamos National Laboratory Report LA-UR-00-3091.

Rishel, J.; S. Johnson, and D. Holt. 2003. Meteorological monitoring at Los Alamos. Los Alamos National Laboratory Report LA-UR-03-8097.

Stout, J.E., and T.M. Zobeck. 1996. The Wolfforth field experiment: a wind erosion study. Soil Science 161:616-632.

Stull, R.B. 1988. An introduction to boundary layer meteorology. Kluwer Academic Publishers, The Netherlands.

Whicker, J.J., D.D. Breshears, P.T. Wasiolek, T.B. Kirchner, R.A. Tavani, D.A. Schoep, and J.C. Rodgers. 2002. Temporal and spatial variation of episodic wind erosion in unburned and burned semiarid shrubland. J. Env. Qual. 31(2): 599-612.

Figure A1. Schematic of sampling inlet used to measure the total suspended particulate concentrations, which were used in vertical flux calculations.

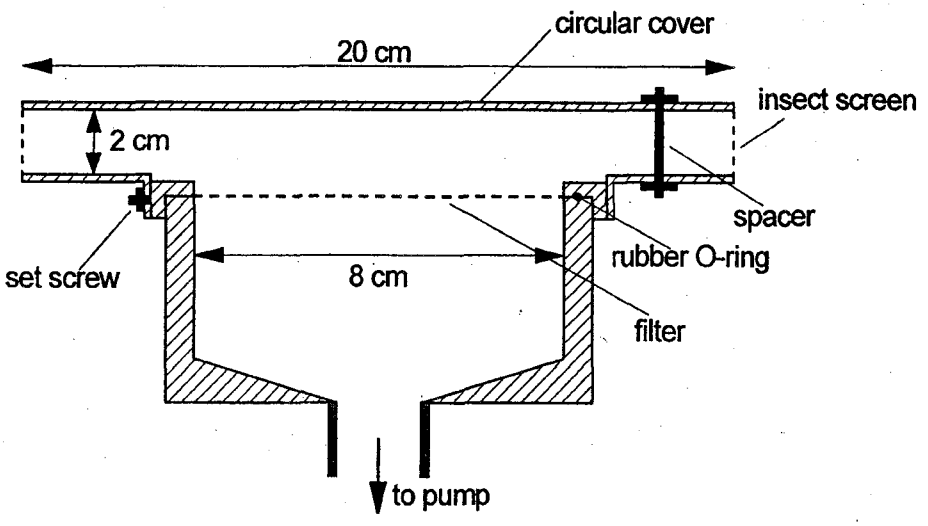

Figure A-2. Arial photograph taken in May 1991 showing the approximate locations of each of the sampling plots.

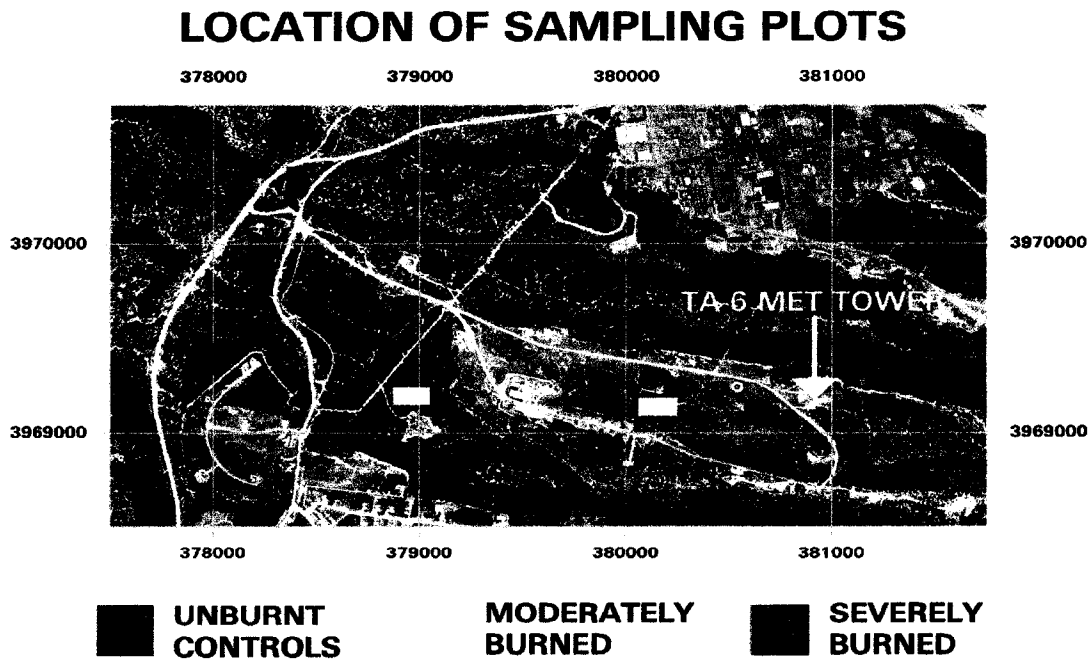

Appendix B

General Characteristics, Biokinetics, and Environmental Behavior of Depleted Uranium

B1.0 General characteristic of uranium

Uranium is ubiquitous in the abiotic and biotic components of the environment and is found in the earths crust at an average concentration of about 2 mg of ^{nat}U per kg of the earth's crust. Uranium tends to concentrate in silica-rich minerals and thus can preferentially concentrate in igneous rocks such as granites. The element of uranium has an atomic number 92 with an atomic mass of 238.0289 g/mol. The density of uranium metal is 19 g/cm^3. The Radiological Health Handbook (USDHEW 1970) lists 14 isotopes of uranium, but the isotopes of uranium found in nature are ^{234}U, ^{235}U, and ^{238}U, with respective half-lives of 2.4 x 10^5 yr, 7.1 x 10^8 yr and 4.5 x 10^9 yr. Also, ^{235}U is a particularly important uranium isotope because of its relatively high capture and fission cross-sections, which are 101 and 577 barns, respectively. Combined, these properties allow uranium to be used for numerous applications ranging from counter weights in airplanes to nuclear power and weapons.

B1.1 Isotopic composition of uranium forms

The isotopic composition of the terms used to describe the relative abundances of the main radioisotopes of uranium in the various forms Table B-1.

Table B-1. Percent abundances of uranium isotopes in several important forms of uranium.

Uranium Form	^{234}U %	^{235}U %	^{238}U %
Natural[1]	0.0054	0.72	99.2746
Depleted[1]	0.0006	0.2	99.8
Enriched (Reactor grade)[2]	_	3-4	≈97
Enriched (weapons grade)[2]	_	>90 %	< 10 %

[1]World Health Organization (WHO) 2001
[2] Whicker and Shultz 1982

B1.2 Primary chemical characteristics of uranium

Uranium is in the actinide series and each isotope of uranium, while radiologically different, is chemically identical and shows similar chemical behavior in the environment and in the body (WHO 2001). The chemical characteristics of uranium in the environment can vary dramatically based on the composition of the uranium chemical compound and the environmental conditions (e.g., oxidation state of the U, pH, etc.). The oxidation states of uranium are +3, +4, +5, and +6, but the +4 and +6 states the most common in the environment. U(VI) species tend to dominate in oxidizing environments while U(IV) species dominate in reducing environments, and both U(IV) and U(VI) exist in a number of minerals forms (EPA 1999). U(IV) in

solution can adsorb strongly onto mineral surfaces and onto organic matter (EPA 1999) which, as described below, can effect its environmental transport.

B2.0 General biokinetics of depleted uranium in humans

Internally deposited DU is potentially both a radiological and chemical hazard with primary target organs being lungs, kidneys, liver, and bone surfaces. Uranium can be taken into the body through either inhalation or ingestion. For this project, where the exposure to the DU would be from working in areas with contaminated soils, the primary mechanism for intake is likely through inhalation, but there will also could be some intake from ingestion of soils through dust deposition in the upper respiratory tract and mouth that is subsequently swallowed. Once in the body, the biokinetics of the uranium will depend largely on its solubility in the lungs for inhaled uranium, or in the gut if ingested. Table B-1 shows the ICRP solubility class for typical uranium compounds.

Table B-1. Typical compounds of uranium and their respective ICRP-based solubility class (WHO 2001).

ICRP solubility class	Typical compounds
F	UF_6, UO_2F, $UO_2(NO_3)_2$
M	UO_3, UF_6, UCl_4, U_3O_8
S	UO_2

Radiologically, DU and its decay progeny emit both alpha and beta particles, and because of its close proximity to viable cells, the deposited energy has the potential

to cause damage to these cells. However, the very long half-life of ^{238}U (4.5×10^9 years) dictates that it is less of a radiological hazard relative to other alpha emitting actinides with shorter half-lives, such as plutonium. With regards to chemical toxicity, long-term studies have shown that high levels of exposure to uranium can result in impairment of kidney function (WHO 2001).

Following an intake, most of the DU is eliminated from the body in feces or urine. For example, the fractional uptake value, f_1, for ingestion of ^{238}U is only 2% for class F and 0.2% for class M. The f_1 values for inhalation are similar and are 2% for class F and M, but 0.2% for class S. The uranium that goes to blood is then distributed through the body, with peak concentrations in the kidney 1 day following the intake, and later systemic burdens found mostly in the skeleton, liver, and kidneys at ratios of 63:2.8:1 (WHO 2001).

To determine dose limits for DU, one then has to consider both its radiological and chemical toxicity. Regarding chemical toxicity, the ACGIH (2000) recommends an exposure limit of 0.2 mg m^{-3} for both soluble and insoluble forms of DU, which translates to an intake of about 2 mg d^{-1}. A worker who has an intake rate of 2 mg d^{-1} for 50 work-weeks per year (5 days per week) could potentially have an annual intake of 500 mg of DU. This annual intake limit is a more restrictive than those for radiological dose for the soluble forms of DU, but not for the insoluble forms, as shown in the table B-2 (ICRP-68). For comparison, the effective dose coefficient for ingestion is several orders-of-magnitude less than those for inhalation (4.4×10^{-8} Sv Bq^{-1} for class F and 7.6×10^{-9} Sv Bq^{-1} for classes F). This analysis point out the importance of

considering both chemical and radiological toxicity when evaluating health effects and safety restrictions.

Table B-2. Dose coefficients and annual intake limits for natural and depleted uranium categorized by ICRP solubility class (WHO 2001).

Isotopic Composition	Natural Uranium	Depleted Uranium
ICRP-Type F compound		
Dose Coefficient (Sv/Bq)	6.15×10^{-7}	5.92×10^{-7}
Annual Intake Limits(Bq, mg)	3.25×10^{4}, 1290	3.38×10^{4}, 2270
ICRP-Type F compound		
Dose Coefficient (Sv/Bq)	1.85×10^{-6}	1.68×10^{-6}
Annual Intake Limits(Bq, mg)	1.08×10^{4}, 430	1.19×10^{4}, 800
ICRP-Type F compound		
Dose Coefficient (Sv/Bq)	6.29×10^{-6}	5.92×10^{-6}
Annual Intake Limits(Bq, mg)	3.18×10^{3}, 130	3.38×10^{3}, 230

B3.0 General environmental behavior of uranium

Human dietary intakes of uranium range from 1-2 μg/d but can be as high as 300 μg/d in locations with areas containing high levels in the water (WHO 2001). The primary sources of uranium in the environment are rock and the soil. The plant uptake of uranium from soil is generally low to moderate and uranium concentrations generally diminish with trophic level, but it can concentrate in marine biota (Whicker and Shultz 1982).

Environmental transport rates of uranium are dependent on the solubility of the uranium in water, which in turn is highly dependent on the chemical compounds of the uranium. For example, uranium carbonates readily dissolve in water and are of importance in typical ground and surface waters (EPA 1999). Uranium carbonate complexes are highly mobile in soils as well. Also, uranium can form organic complexes as well and become fixed in areas with high organic compounds (WHO

2001). As a local example, the uranium concentration in LANL soils correlate well with the amount of organic matter in the soil (Longmire et al. 1996). In summary, mobility of U in soil is largely dependent on proximity to ground water, soil and water pH, soil organic carbon content and the amount of clay in the soil.

B3.1 Description of the K_d value

A key factor in determining the environmental mobility and bioavailability of a radionuclide is its solubility in solutions such as water. The K_d value (or partition coefficient) is a measure of this solubility and is calculated as the ratio of the concentration of the uranium in the solid soil divided by the uranium concentration in the solution.

$$K_d = \frac{C_{solid}}{C_{liquid}} \qquad (1)$$

where K_d is the partition coefficient (L/kg), C_{solid} is the concentration of a radionuclide in the solid phase such as soil (Bq/kg), and C_{liquid} is the concentration of the radionuclide in the liquid phase. Equation 1 shows that more soluble radionuclides will have lower K_d values and radionuclides with higher K_d values will be relatively insoluble. The K_d value can then be useful in predicting the concentration in a drinking water source (eqn. 2) or it can be used to determine the leach rate of a radionuclide in ground water movement (eqn. 3).

$$C_{drinkingwater} = \frac{C_{soil}}{K_d} \qquad (2)$$

$$k_{leach} = \frac{P + I - E - R}{d\left(1 + \frac{\rho K_d}{\theta}\right)} \qquad (3)$$

where k_{leach} is the leach rate constant (yr^{-1}), P is the precipitation rate and I is the irrigation rate (cm/yr), E is the evapotranspiration rate (cm/yr), R is the surface runoff rate (cm/yr), d equals the soil depth to the next layer, ρ is the soil bulk density (g/cm^3), K_d is the partition coefficient from eqn.1 (mL/g), and θ is the soil water content (mL/cm^3).

The values of K_d for uranium vary depending on numerous environmental variables, but primarily on the pH of the soil/solution and the type of soil. Table B-3 shows the variation of K_d for uranium as related to soil pH and Table B-4 shows the variation of the uranium K_d for different soil types.

Table B-3. Kd values as related to soil pH (EPA 1999).

Solution pH	**K_d range**
3	<1 - 32
4	0.4 - 5000
5	25 - 160,000
6	100 – 1,000,000
7	63 – 630,000
8	0.4 – 250,000
9	<1 – 7,900
10	<1 - 5

Table B-4. The geometric mean of the K_d as related to soil type (Sheppard and Thibault 1990).

Soil Type	Geometric Mean Kd
Sand	35
Loam	15
Clay	1600
Organic	410

Table B-3 illustrates that the highest K_d values are for near neutral pH conditions with increasing solubility as the solution becomes more acidic or alkaline. Table B-4 shows that the highest Kd values are for clay soils. High Kd values are often associated with clay soils of because clay has a relatively large surface area per gram of soil compared to the other soil types and they can have a high affinity for cations.

Dose assessment requires an assessment of all exposure pathways and the K_d is important for both the inhalation and ingestion pathways. The inhalation pathway includes radionuclide emitted from nuclear buildings, but the source of much of the intakes is from wind-driven resuspended soils. The K_d values are important for resuspension-derived intakes because the depth profile of a radionuclide is highly dependent on the solubility of the radionuclide in the soil. Radionuclides with high K_d values largely remain in the top layers of soil where they are available to wind and water erosion. Radionuclides with smaller K_d values are more mobile in environmental transport processes that are based on water movement, such root uptake of a plant, as described by the Concentration Ratio.

B3.2 Concentration ratios for uranium

The concentration ratio (or concentration factors) describes the fraction of a radionuclide in the soil that is taken into a plant. Equation 4 shows how the concentration ratio is calculated.

$$CR = \frac{C_{Veg}}{C_{soil}} \qquad (4)$$

where CR is the concentration ratio (dimensionless), C_{veg} is the concentration in the vegetation (Bg/g), and C_{soil} is the concentration in the soil (Bg/g). Table B-5 shows the range of concentration ratios for uranium in different plant types.

Table B-5. Range of Concentration Ratios for uranium in different plant types (WHO 2001).

Plant type	Range of Concentration Ratios
Leafy vegetables	$1.2 \times 10^{-4} - 1.0 \times 10^{-2}$
Root vegetables	$2.0 \times 10^{-4} - 3.0 \times 10^{-2}$
Fruits	$4.0 \times 10^{-4} - 4.0$
Grains and Cereals	$2.0 \times 10^{-4} - 1.3 \times 10^{-3}$

The ranges of the concentration ratios are up to a couple of orders-of-magnitude and are dependent on soil pH, organic content, and measurement technique (e.g., include the surficial dust or not, dry or wet mass), etc. (WHO 2001). This large variation in CR (also for the K_d values) makes it difficult to select a CR without site-specific measurements, but RESRAD uses 2.5×10^{-3} as a reasonable estimate of the uranium CR for vegetables (Yu et al. 2001). RESRAD also uses the vegetable wet weight and soil dry weight in their calculation for CR whereas others use dry weights

only (Whicker and Schultz 1982). As a relative comparison, the CR used in RESRAD for uranium is 2.5 times larger than that for plutonium, but the dose conversion factor (mrem/pCi) for uranium is about 10 times lower than plutonium.

The CR can be time dependent, especially if the surficial dust on the plant is included in the calculation and the radionuclide is deposited onto the plant from the atmosphere. In this case the time dependency can be estimated by equation 5.

$$C_{veg} = C_{veg}(o)e^{-k_w t} \qquad (5)$$

where $C_{veg}(o)$ is the concentration following atmospheric deposition (t = 0), and k_w is the weathering rate constant (d^{-1}), and t is time (d). Finally, the CR can also be used to estimate the rate of uptake in a plant as shown in equation 6.

$$R_{up} = C_{soil} CR\left(\frac{dB}{dt}\right) \qquad (6)$$

where R_{up} is the rate of root uptake (Bq/d-m^2) and dB/dt is the derivative of the plant biomass with respect to time (g/d-m^2).

B3.3 Other important environmental transport factors for uranium

RESRAD lists a number of transfer factors for uranium that are specifically used for dose assessment for the ingestion pathway. The ingestion pathway for dose assessment requires other transfer factors such as that from cattle ingested fodder/water/soil-to-meat and ingested fodder/water/soil-to-milk. RESRAD uses the

transfer factors of 3.4×10^{-4} (d/kg) and 6.0×10^{-4} (d/kg) for fodder/water/soil-to-beef and fodder/water/soil-to-milk, respectively (Yu et al. 2001). Both of these transfer factors are higher than that for plutonium, suggesting that uranium is more mobile into foodstuffs than plutonium. For aquatic foods, RESRAD lists the bioaccumulation factors for fish and crustacea and mullosks (Yu et al. 2001). The bioaccumulation factor for fish is 10 (L/kg) and 60 (L/kg) for crustacea and mullosks.

B4.0 References

American Conference of Governmental Hygienists (ACGIH). 2000. Threshold limiting values for chemical substances and physical agents and Biological exposure indicies. Cincinnati, OH: ACGIH.

EPA. 1999. Understanding variation in partition coefficient, Kd, values. United States Environmental Protection Agency, Office of Air and Radiation, EPA-402-R-99-004A.

International Commission on Radiological Protection (ICRP). 1994. Dose coefficients for intakes of radionclides by workers. ICRP Publication 68.

Longmire PA, Reneau SL, Watt PM, McFadden LD, Gardner JN, Duffy CJ, Ryti RT. Natural background geochemistry, geomorphology, and pedogenesis of selected soil profiles and Bandelier Tuff Los Alamos, New Mexico. Los Alamos National Laboratory LA-12913-MS.

Sheppard SC, Thibault DH. 1990. Default soil solid/liquid partition coefficients, Kds, for four major soil types: a compendium. Health Physics 59:471-482.

USDHEW. 1970. Radiological Health Handbook. United States Department of Health, Education, and Welfare, Public Health Service, Food and Drug Administration.

Whicker FW, Shultz V. 1982. Radioecology: nuclear energy and the environment. Boca Raton, FL: CRC Press.

WHO. 2001. Depleted uranium: sources, exposure, and health effects. World Health Organization, Department of Protection of the Human Environment, WHO/SDE/PHE/01.1.

Yu C, Zielen AJ, Cheng J-J, LePoire DJ, Gnanapragasam E, Kamboj S, Arnish J, Wallo A, Williams WA, Peterson H. 2001. Users manual for RESRAD Version 6. Argonne National Laboratory ANL/EAD-4.